

Klinik und Poliklinik für Herzchirurgie an der Universitätsmedizin Rostock

Direktor: Prof. Dr. med. Gustav Steinhoff

**MikroRNA-basierte Stammzellmodifikationen mittels  
magnetischer Transfektionskomplexe –  
Ein nicht-viraler Ansatz für die kardiale Regeneration**

Inauguraldissertation

zur

Erlangung des akademischen Grades

Doktor der Medizinwissenschaften (Dr. rer. hum.)

der Universitätsmedizin Rostock



vorgelegt von

Anna Schade (geborene Sponholz), geb. am 17.02.1987 in Rostock

aus Rostock

Rostock, 18. Juni 2015

**Gutachter:**

1. Gutachter: Prof. Dr. med. Gustav Steinhoff, Klinik und Poliklinik für Herzchirurgie, Universitätsmedizin Rostock
2. Gutachter: Prof. Dr. med. Dr. rer. nat. Brigitte M. Pützer, Institut für Experimentelle Gentherapie und Tumorforschung, Universitätsmedizin Rostock
3. Gutachter: PD Dr. med. Stefan Brunner, Medizinische Klinik und Poliklinik I, Universität München

**Datum der Einreichung:** 19. Juni 2015

**Datum der Verteidigung:** 02. Dezember 2015

Department of Cardiac Surgery at the University of Rostock

Director: Prof. Dr. med. Gustav Steinhoff

**MicroRNA-based Stem Cell Modifications using Magnetic  
Transfection Complexes –  
A Non-Viral Approach towards Cardiac Regeneration**

Dissertation

to obtain

the academic degree

doctor rerum humanarum, (Dr. rer. hum.)

at the Medical Faculty, University of Rostock



submitted by:

Anna Schade (nee Sponholz), born 17.02.1987 in Rostock

from Rostock,

Rostock, 18. June 2015

**Reviewer:**

1. Reviewer: Prof. Dr. med. Gustav Steinhoff, Department of Cardiac Surgery,  
University of Rostock
2. Reviewer: Prof. Dr. med. Dr. rer. nat. Brigitte M. Pützer, Institute of Experimental  
Gene Therapy and Cancer Research, University of Rostock
3. Reviewer: PD Dr. med. Stefan Brunner, Medical Clinic and Policlinic I, University of  
Munich

**Date of submission:** 19. June 2015

**Date of defense:** 02. December 2015

Gewidmet meinen Kindern

## Zusammenfassung

Herz-Kreislauf-Erkrankungen sind weltweit die häufigste Todesursache. In den letzten Jahren haben besonders zellbasierte Therapien mit dem Ziel Herztransplantationen zu vermeiden breite Aufmerksamkeit erregt. Im Besonderen aus Knochenmark isolierte humane mesenchymale Stammzellen (hMSZ) konnten durch ihr großes therapeutisches Potential in der regenerativen Medizin überzeugen. Die meisten klinischen und präklinischen Studien wurden jedoch mit expandierten hMSZ durchgeführt, die das Risiko von Verunreinigungen und des Verlusts der Stammzeleigenschaften bergen. Daher sind frisch isolierte Zellen trotz niedrigerer Erträge für klinische Anwendungen zu bevorzugen. Es ist bewiesen, dass das Regenerationspotential von hMSZ durch genetische Modifikationen mittels mikroRNAs (miRs) verbessert werden kann. Darüber hinaus sind DNA-freie Transfektionsmethoden weniger riskant für die klinische Anwendung im Menschen. Dennoch sind bis heute keine sicheren und klinisch relevanten miR Transfermethoden entwickelt worden. In vorangegangenen Studien unserer Arbeitsgruppe gelang es, einen magnetischen nicht-viralen Vektor, bestehend aus dem kationischen Polymer Polyethylenimin (PEI), das über Biotin-Streptavidin Binding an magnetische Eisenoxidnanopartikel (MNP) gebunden ist, zu entwickeln und damit DNA effizient in expandierte hMSZ einzubringen. Außerdem bieten MNP-haltige Komplexe zusätzliche Vorteile: sie ermöglichen eine verbesserte Selektivität und Sicherheit der Transfektionsvektoren und geringere Nebenwirkungen *in vivo*. Daher war es das Ziel, diesen Ansatz für den effizienten Transfer von miRs in frisch isolierte hMSZ zu übertragen. Zusätzlich sollte überprüft werden, ob die magnetisch veränderten Stammzellen mit Hilfe eines externen Magnetfeldes *in vitro* zielgerichtet gelenkt werden können. Initial wurde eine optimale Zusammensetzung des Transfektionskomplexes entwickelt zur effizienten Modifikation von expandierten hMSZ. Neben höchsten miR Transfektionsraten zeigte der optimierte magnetische Vektor eine bessere und länger andauernde Wirksamkeit im Vergleich zur PEI-basierten Transfektion. Aufbauend auf den gewonnen Erkenntnissen gelang es, mit dem magnetischen, nicht-viralen Vektor miR effizient in frisch isolierte hMSZs (~ 70% Aufnahmeeffizienz) einzubringen. Im Vergleich zu kommerziell erhältlichen, magnetischen Transfektionsreagenzien, die für den effizienten DNA-Transfer getestet sind, konnte der neuentwickelte magnetische Vektor gleiche Aufnahmeeffizienzen erzielen. Es wurde gezeigt, dass alle untersuchten magnetischen Transfektionskomplexe für einen potenziellen Einsatz zur Modulation von Stammzellen mit miRs geeignet sind. Zusätzlich

wurde der Nachweis erbracht, dass sowohl frisch isolierte als auch expandierte hMSZ nach Transfektion mit den entsprechenden miR/PEI/MNP Komplexen spezifisch durch ein von außen angelegtes Magnetfeld gelenkt werden konnten. Dies soll ein verbessertes Anwachsen des Stammzelltransplantates *in vivo* unterstützen und damit das Regenerationspotenzial der Stammzellen erhöhen. Im Rahmen dieser Dissertation konnte somit ein magnetischer, nicht-viraler Vektor entwickelt werden, der nachweislich miR effizient in frisch isolierte Stammzellen einschleust mit dem Ziel die Stammzeleigenschaften gezielt zu steuern. Zusätzlich besteht die Möglichkeit die modifizierten Stammzellen durch ein externes Magnetfeld präzise *in vivo* zu lenken. Damit können die Ergebnisse als Grundlage für die Entwicklung innovativer Strategien zur Regeneration des geschädigten Herzens dienen.

**Schlagwörter:** mesenchymale Stammzellen, CD105; nicht-viraler Gentransfer, mikroRNA; magnetische Nanopartikel, Polyethylenimin; Magnetofektion

## Summary

Cardiovascular diseases (CVDs) are the leading cause of morbidity and mortality worldwide. During the last years, cell-based therapies gained huge attention for regeneration of the injured heart aiming to avoid heart transplantation. In particular, bone marrow derived human mesenchymal stem cells (hMSCs) have been shown great therapeutic potential in regenerative medicine. However, most trials were using culture expanded hMSCs that bear the risk of contaminations and loss of their stem cell character. Thus, freshly isolated cells might be preferable for clinical applications. In recent years, it was shown that the regenerative properties of hMSCs can be enhanced by genetic modifications using microRNAs (miRs). Moreover, DNA-free transfection methods bear less safety risks. However, safe and effective miR delivery methods suitable for clinical applications have not been developed, yet. Previously, our group succeeded to efficiently deliver DNA into expanded hMSCs using a magnetic non-viral vector consisting of cationic polymer polyethylenimine (PEI) bound to iron oxide magnetic nanoparticles (MNPs). Moreover, MNP-containing complexes enable improved selectivity and safety of delivery and reduced side effects *in vivo*. Thus, the aim of this thesis was to adopt this approach for efficient miR delivery in freshly isolated hMSCs using miR/PEI/MNP complexes and to show proof-of-concept for magnetic targeting of transfected cells *in vitro*. Initially, the optimal complex formulation was determined for efficient modification of expanded hMSCs. Moreover, we assessed transfection efficiencies of MNP-based complexes and found a better long term performance compared to polyplex transfection, which might be beneficial considering clinical use. Afterwards, we succeeded to transfer our magnetic non-viral approach for efficient miR delivery to freshly isolated hMSCs (~ 70% uptake efficiency). Additionally, MNP-based transfection was compared to magnetic transfection reagents commonly used for DNA delivery. Interestingly, our MNP-containing complexes yielded similar uptake rates. Hence, all investigated magnetic transfection reagents have the potency to deliver miRs in hMSCs. Moreover, it was demonstrated that freshly isolated and expanded hMSCs could be specifically guided by an externally applied magnetic field after transfection with the corresponding miR/PEI/MNP complexes contributing to enhanced cell retention and engraftment of transplanted cells *in vivo*. Conclusively, in this thesis a magnetic non-viral carrier for efficient miR delivery in freshly isolated stem cells was developed allowing specific control of stem cell properties as well as precise magnetic



targeting of transfected cells *in vivo*. Therefore, we expect that our approach will serve as a basis for innovative strategies to regenerate the injured heart.

**Keywords:** mesenchymal stem cells; CD105; non-viral carrier; microRNA; magnetic nanoparticles; polyethylenimine; magnetofection

## List of Contents

<b>Zusammenfassung .....</b>	<b>I</b>
<b>Summary .....</b>	<b>III</b>
<b>1 Introduction .....</b>	<b>1</b>
1.1 Prospective Stem Cell Resources for Cardiac Regeneration .....	1
1.1.1 Human Embryonic Stem Cells .....	2
1.1.2 Induced Pluripotent Stem Cells .....	2
1.1.3 Human Mesenchymal Stem Cells.....	3
1.2 Modifications of Mesenchymal Stem Cells for Cardiac Regeneration .....	5
1.2.1 Pretreatment of Mesenchymal Stem Cells.....	5
1.2.2 Preconditioning of Mesenchymal Stem Cells .....	5
1.2.3 Genetic Modification of Mesenchymal Stem Cells.....	6
1.3 Different Nucleic Acid Species for Gene Therapy .....	7
1.3.1 DNA-based Gene Therapy .....	7
1.3.2 RNA-based Gene Therapy.....	8
1.4 Small RNA-Based Delivery Methods .....	13
1.4.1 Non-Viral Delivery Methods.....	14
1.4.2 Magnetic Gene Targeting Strategies .....	16
1.5 Aim of the Thesis.....	19
<b>2 Materials and Methods.....</b>	<b>20</b>
2.1 List of Chemicals.....	20
2.2 List of Solutions.....	22
2.3 hMSC Isolation and Culture .....	23
2.3.1 Isolation of Mononuclear Cells .....	23
2.3.2 Isolation of hMSCs by Plastic Adherence .....	23
2.3.3 Isolation of hMSCs by Magnetic Cell Separation .....	24
2.4 Immunophenotyping of hMSCs .....	24
2.5 Functional Differentiation Assay.....	25
2.5.1 Adipogenic Differentiation of hMSCs.....	26
2.5.2 Osteogenic Differentiation of hMSCs .....	26
2.6 Preparation of Transfection Complexes .....	27

2.6.1	Preparation of Polyplex-based Transfection Complexes.....	27
2.6.1.1	Preparation of miR/PEI Complexes.....	27
2.6.1.2	Preparation of miR/PEI/MNP Complexes.....	28
2.6.1.3	Preparation of miR/PEI/CombiMag Complexes .....	29
2.6.2	Preparation of Lipoplex-based Transfection Complexes .....	29
2.6.2.1	Preparation of miR/Magnetofectamine <sup>®</sup> Complexes .....	29
2.7	Characterization of miR/PEI and miR/PEI/MNP Complexes.....	30
2.7.1	Condensation Assay.....	30
2.7.2	Particle Size and Zeta Potential Measurement .....	30
2.8	Transfection Experiments.....	30
2.9	Uptake Efficiency and Cytotoxicity .....	31
2.10	Intracellular Visualization of miR/PEI/MNP Transfection Complexes .....	31
2.10.1	Fluorescent Labeling of miR/PEI/MNP Transfection Complexes .....	31
2.10.2	Confocal Laser Scanning Microscopy.....	32
2.11	Real-Time PCR.....	33
2.11.1	RNA Isolation of Cultured hMSCs.....	33
2.11.2	RNA Isolation of Freshly Isolated hMSCs.....	33
2.11.3	Real-Time PCR of miRs.....	34
2.11.4	Real-Time PCR of Target Genes.....	36
2.12	Migration Assay.....	37
2.13	Magnetic Targeting of MNPs .....	38
2.14	<i>In Vitro</i> Magnetic Targeting of hMSCs.....	38
2.15	Statistical Analysis.....	38
<b>3</b>	<b>Results.....</b>	<b>39</b>
3.1	Characterization of Freshly Isolated and Expanded CD105 <sup>+</sup> hMSCs.....	39
3.1.1	Evaluation of Cell Morphology .....	39
3.1.2	Determination of Differentiation Capacity .....	40
3.1.3	Evaluation of the hMSC-Immunophenotype.....	41
3.2	Optimization of Transfection Complexes in Cultured hMSCs .....	43
3.2.1	Optimization of miR Amounts .....	43
3.2.2	Optimization of PEI Amounts .....	44
3.2.3	Optimization of MNP Amounts .....	45
3.3	Characterization of Transfection Complexes .....	47

3.3.1	Condensation Assay.....	47
3.3.2	Determination of Particle Size and Zeta Potential.....	47
3.4	Evaluation of miR Processing in Cultured hMSCs over Time.....	49
3.4.1	Investigation of Mature miR Expression Levels .....	49
3.4.2	Microscopic Observations of Transfection Complexes.....	51
3.4.3	Evaluation of Target Genes Expression .....	53
3.4.4	Analysis of Migratory Potential.....	54
3.5	Optimization of Transfection Complexes in Freshly Isolated hMSCs.....	55
3.5.1	Optimization of miR Amount.....	55
3.5.2	Optimization of PEI Amount.....	57
3.5.3	Optimization of MNP Amount .....	58
3.6	Evaluation of miR Processing in Freshly Isolated hMSCs.....	60
3.7	Evaluation of MNP-mediated Transfection in Comparison to Established Magnetic Transfection Reagents in Freshly Isolated hMSCs.....	61
3.8	<i>In Vitro</i> Magnetic Targeting of hMSCs.....	63
<b>4</b>	<b>Discussion .....</b>	<b>65</b>
4.1	Comparison of Freshly Isolated and Expanded CD105 <sup>+</sup> hMSCs.....	65
4.2	Establishment of a Standardized miR Transfection Protocol in Expanded hMSCs .....	66
4.3	Physicochemical Characterization of Transfection Complexes .....	69
4.4	Intracellular Transfection Performance of miR/PEI/MNP Complexes in Expanded hMSCs .....	70
4.5	Optimization of MNP-Mediated Transfection in Freshly Isolated hMSCs.....	74
4.6	Comparison of Different Magnetic miR Carrier Systems in Freshly Isolated hMSCs .....	77
4.7	<i>In Vitro</i> Targeting of Magnetically Modified hMSCs.....	78
<b>5</b>	<b>Conclusion .....</b>	<b>80</b>
<b>6</b>	<b>References.....</b>	<b>81</b>
<b>7</b>	<b>Appendix.....</b>	<b>i</b>
	List of Abbreviations .....	i
	List of Figures.....	v
	List of Tables .....	vi

## List of Contents

---

List of Equations.....	vi
Curriculum Vitae .....	vii
Acknowledgement .....	x
Selbständigkeitserklärung.....	xi

## **1 Introduction**

### **1.1 Prospective Stem Cell Resources for Cardiac Regeneration**

Cardiovascular diseases (CVDs) are the leading cause of death worldwide according to the statistics of the World Health Organization (WHO). In 2008, approximately 17.3 million deaths were caused by CVDs. Forecasts predict a further global increase of cardiovascular deaths to 23.3 million in 2030 [1]. Among them, ischemic heart diseases are the most common causes of death (~ 7.3 million) [2]. Ischemic heart failures are caused by a sudden occlusion of the coronary arteries following a limited myocardial perfusion. Consequently, cardiomyocytes die due to oxygen deprivation which initiates, for example (e.g.) the formation of a non-contractile scar, ventricular wall thinning up to the formation of sustained heart failure and under certain circumstances death [3]. So far, preventive strategies, drug therapies and surgical or interventional reperfusion methods are available to treat cardiovascular diseases by ensuring coronary perfusion, prevention of cardiac arrhythmias and improving the efficiency of the remaining cardiac function [4, 5]. After the establishment of a chronic heart failure in the end-stage, heart transplantation remains the only therapeutic option [6]. However, due to the restricted access of donor hearts and risks in the subsequent immunosuppressive therapy only a limited amount of patients can be treated. According to the statistics from Eurotransplant, about 590 hearts were transplanted in Europe in 2013. However, more than twice as many donor organs would be required [7].

Therefore, targeted causal and curative therapies for the regeneration of the heart or the replacement of damaged cardiomyocytes have to be developed. For these reasons, the attention has turned to cell-based therapies. Stem cell transplantation has emerged as a potential therapeutic strategy for repopulating injured heart tissue. For myocardial regeneration therapies several stem cell sources are under investigation: human embryonic stem cells (hESCs), induced pluripotent stem cells (iPSCs) and human adult stem cells.

### **1.1.1 Human Embryonic Stem Cells**

In 1998, hESCs have been first derived from the inner cell mass of the blastocyst of the developing embryo. Due to their pluripotency, they have the potential to differentiate into cell types of all three germ layers (endoderm, ectoderm and mesoderm) [8]. In 2001, researchers for the first time succeeded in the differentiation of human embryonic stem cells into early stage cardiomyocytes. These cells showed spontaneous contractions and expressed both early cardiac transcription factors (e.g. GATA4, Nkx2.5 and MEF) and specific structural proteins of the heart muscle [9]. Therefore, with respect to their pluripotency and their high proliferation rate as well as the functionality of differentiated cells, hESCs show great potential for cardiac regeneration [10]. On the other hand, hESCs bear the risk of teratoma formation, the development of arrhythmias and the problem of immunological rejection of donor cells. In addition, previously it has been shown, that less than 5% of hESCs were able to differentiate into cardiomyocytes [11, 12]. Moreover, the use and research of hESCs are ethically problematic. Due to the ethical and legal restrictions in Germany (embryo protection law, ESchG, see BGBl. I 1990/2746), the realization of new regenerative therapies based on hESCs does not seem to be feasible in the near future.

### **1.1.2 Induced Pluripotent Stem Cells**

Based on the existing limitations of hESCs, researchers have been looking for a way to obtain pluripotent cells which can circumvent the ethical and political limitations. In 2012, the Nobel Prize in Physiology or Medicine was awarded to Dr. Yamanaka for his discovery of reprogramming mature differentiated cells into a pluripotent stem cell state. Initially, it was shown that mouse embryonic fibroblasts could be reprogrammed into iPSCs by introducing four transcription factors (Oct3/4, Sox2, c-Myc and Klf4) [13]. One year later, Yamanaka's group succeeded to convert adult human somatic cells into iPSCs using the same factor combination [14]. In the fast growing field of reprogramming, recently the world's first clinical trial involving iPSCs was approved by the Japanese Ministry of Health, Labor and Welfare. Thereby, an iPSC derived retinal pigment epithelium was transplanted into patients suffering from age related macular degeneration [15]. Moreover, it was shown, that iPSCs were able to differentiate into spontaneous beating cardiomyocytes which was proven by the expression of specific cardiac markers, morphology, cross-striation as well as calcium

transients [16, 17]. Recently, Kempf *et al* succeeded to develop a cardiac differentiation protocol with clinically applicable yields and purity (~ 85% iPSC derived cardiomyocytes) using chemical Wnt [18]. However, the currently produced iPSC derived cardiomyocytes retain in an immature state as indicated by an altered morphology and physiology when compared to mature cells (differences summarized in [19]). Thus, impaired electrical and mechanical integration within adult myocardium are still limiting the application of iPSC technology for cardiac regeneration at present [20]. Therefore, despite the great therapeutic potential of iPSCs for cardiac regeneration to generate autologous disease-specific pluripotent cells, further studies have to be performed before applying them in the clinic.

### 1.1.3 Human Mesenchymal Stem Cells

Other promising cell sources for cardiac regeneration are human adult stem cells. They are multipotent (differentiation into various cell types of one germ layer) and have the potential for self-renewing. Moreover, the use of these cells is ethically unproblematic. One of the most investigated adult stem cells are human mesenchymal stem cells (hMSCs). In 1968, Friedenstein *et al* first described mesenchymal stem cells (MSCs) as adherent spindle-shaped fibroblast-like cells. These cells were located in the bone marrow and were able to differentiate [21]. In order to standardize and characterize MSCs, the International Society for Cellular Therapy determined criteria to define MSCs in 2006. In this regard, cells must be adherent to plastic under common culture conditions. They have to express specific cell surface markers (e.g. cluster of differentiation (CD) 29, CD44, CD73, CD105) and lack the expression of CD11b, CD14, CD19, CD34, CD45, CD79 $\alpha$ , CD117 and human leukocyte antigen (HLA)-DR. Furthermore, MSCs must have the ability to differentiate into adipocytes, osteocytes and chondrocytes under certain culture conditions [22].

MSCs have been identified in various tissues, e.g. bone marrow, brain, liver, spleen, lung, kidney, skin, muscle, adipose tissue, aorta, vena cava, pancreas, thymus and umbilical cord blood [23, 24, 25, 26]. Yet, the most abundant organ is the bone marrow [27]. For efficient isolation of hMSCs from tissue, different methods can be used. One common technique is the isolation using plastic adherence. This is a cheap and easy but also unspecific and time consuming process. Furthermore, hMSCs can be obtained via magnetic activated cell sorting (MACS). Therefor magnetically labelled antibodies against specific stem cell surface markers are used. Previously, it was shown, that CD105 (endoglin) is a suitable surface marker for



efficient purification of hMSCs from bone marrow [28]. Endoglin, is a homodimeric integral membrane protein (180kDa) which acts as an accessory type III receptor (T $\beta$ R-III) and is able to bind different molecules of the transforming growth factor (TGF)- $\beta$  superfamily (e.g. TGF- $\beta$ 1, TGF- $\beta$ 3, activin-A, bone morphogenetic protein (BMP)-7 and BMP-2) in combination with T $\beta$ R-I or T $\beta$ R-II [29, 30, 31]. Though the specific function of endoglin yet needs to be analysed, previous publications claimed that CD105 is involved in angiogenesis and vascular remodelling [32, 33]. After efficient isolation, MSCs can be expanded *in vitro* to reach the desired cell number for autologous applications *in vivo* [34]. However, it has been proposed that cell expansion might influence their differentiation potential and homing ability [28, 35]. In March 2015, 265 clinical trials are using MSCs for a wide range of indications (cardiovascular diseases [36, 37], bone/ cartilage disorders [38], diabetes [39], liver diseases [40], autoimmune disorders [41] and neuromuscular diseases [42]) [43]. It was shown that MSCs exert their therapeutic effect by numerous mechanisms. They are able to migrate to the site of injury guided by a range of growth factors and chemokines like platelet-derived growth factor, insulin-like growth factor-1 (IGF-1) and C-C chemokine receptor (CCR) 2, CCR3, CCR4 [44]. Moreover, they can differentiate into various cell types, e.g. cartilage, bone, tendon, ligament, adipose tissue, marrow stroma and connective tissue as well as into endothelial cells and smooth muscle cells [37, 45, 46, 47, 48]. Previously, it was shown that a small number of MSCs had the ability to transdifferentiate into a cardiomyocyte-like phenotype *in vitro* and *in vivo* [48, 49]. However, these cells failed to generate functional cardiomyocytes indicating that their transdifferentiation potential might not be sufficient for cardiac regeneration [50]. Moreover, MSCs are able to secrete a large spectrum of trophic factors, e.g. soluble extracellular matrix glycoproteins (collagen type I and II, osteopontin), cytokines (TGF- $\beta$ , interleukin (IL)-10, IL-6) and growth factors (vascular endothelial growth factor (VEGF), keratinocyte growth factor, hepatocyte growth factor (HGF)), to activate cell regeneration and inhibit inflammation and apoptosis of damaged tissue [51]. Furthermore, they can perform immunomodulatory functions by suppressing T cells, dendritic cell maturation and B cell activation, stimulating regulatory T cells via IL-10 as well as inhibiting natural killer cells [52, 53, 54, 55, 56, 57, 58]. Moreover, MSCs can release soluble immunosuppressive factors like prostaglandins and various growth factors [59]. The clinical trials showed that MSCs seem to be well tolerated. Most studies reported no adverse effects [60]. Therefore, MSCs are promising cell sources for clinical applications in heart surgery.

## 1.2 Modifications of Mesenchymal Stem Cells for Cardiac Regeneration

Despite the great benefits of MSCs, clinical applications of MSC-based therapies are limited due to the poor viability of cells after transplantation into the myocardium [61]. In 2002, Toma *et al* showed that less than 0.5% of transplanted MSCs survived in the intact heart after 4 days [49]. To face the problem of low cell survival rates after cell injection, several strategies to specifically modify MSCs before transplantation have been investigated.

### 1.2.1 Pretreatment of Mesenchymal Stem Cells

MSCs can be pretreated with different growth and differentiation factors to facilitate their viability and engraftment in cardiac tissue [62, 63, 64]. Pasha *et al* showed that preconditioning of MSCs using stromal-derived factor 1 (SDF-1) enhanced cell survival, angiogenesis and cell homing in the infarcted heart compared to untreated cells by activating the Akt signaling pathway [64]. Moreover, it was shown that incubation of MSCs with TGF- $\alpha$  improved myocardial recovery by stimulating VEGF production after myocardial injury [65]. Furthermore, MSCs can be treated with pharmaceuticals before transplantation. Recently, it was demonstrated that pretreatment of MSCs with atorvastatin (competitive inhibitor of the HMG-CoA reductase) facilitated differentiation towards a cardiomyocyte-like phenotype and cell survival by activating endothelial nitric oxide synthase (eNOS) [66, 67]. Moreover, estradiol treatment of MSCs before transplantation into the heart improved cardiac function and cell viability by enhancing VEGF production [68]. Furthermore, Liu *et al* demonstrated that incubation of MSCs with lysophosphatidic acid prior transplantation enhanced MSC survival in ischemic myocardium [69].

### 1.2.2 Preconditioning of Mesenchymal Stem Cells

Additionally, different methods for preconditioning of MSCs prior to transplantation are under investigation. It was shown that preconditioning of MSCs using heat shock had a beneficial effect on the proliferation and differentiation potential of MSCs *in vitro* [70]. Moreover, hypoxic preconditioning of MSCs enhanced cell viability of transplanted cells and angiogenesis in the infarcted heart due to increased expression of pro-survival and pro-

angiogenic factors (e.g. hypoxia-inducible factor-1 $\alpha$  (HIF-1 $\alpha$ ), angiopoietin-1, VEGF, fetal liver kinase-1 (Flk-1), erythropoietin, IL-6, B-cell lymphoma-2 (Bcl-2)) as well as downregulation of apoptosis inducing genes (e.g. caspase-3, Bcl-2-associated X protein (Bax)) [71, 72, 73].

### 1.2.3 Genetic Modification of Mesenchymal Stem Cells

Both, preconditioning and pretreatment of MSCs have been shown to significantly influence gene expression patterns of the ischemic heart due to the upregulation of cytoprotective genes. However, both methods are unspecific which bears the risk of unwanted side effects. Moreover, they are potentially harmful for cells. Therefore, in recent years genetically modified MSCs mimicking preconditioning through expression of certain cardioprotective genes gained great attention for cell-based regeneration of the infarcted heart [74]. Specific delivery of defined genetic materials into host cells with the objective to treat cardiovascular diseases is termed as cell-based gene therapy [75]. Therefore cells are isolated, expanded in appropriate culture conditions and genetically manipulated. This *ex vivo* approach allows targeting of specific cell sources for gene delivery and controlled expression of certain proteins (e.g. growth factors). Moreover, it circumvents the safety concerns of directly applying viral vectors or transfection reagents *in vivo* [76].

Cell-based gene therapy can be sub-divided into two main approaches. The first approach uses the genetically modified cells as a passive carrier. Therefore cells are modified in a way that they secrete autocrine or paracrine factors to facilitate the tissue microenvironment for cardiac regeneration. It was shown that overexpression of heat shock protein-20 (Hsp-20) led to increased cell survival rates in genetically modified MSCs compared to conventional cells due to the activation of Akt and secretion of specific growth factors (VEGF, IGF-1, fibroblast growth factor-2 (FGF-2)) [77]. Moreover, our group demonstrated that overexpression of Bcl-2 in hMSCs led to improved cell viability and upregulated VEGF expression *in vitro*. *In vivo*, transplantation of Bcl-2 transfected MSCs into infarcted hearts led to increased cell survival and improved functional recovery [78].

In the alternative approach, cells are genetically modified to optimize cell properties, e.g. improvement of cell viability or differentiation into a specific phenotype. It was demonstrated that Akt-transfected MSCs significantly decreased apoptosis and enhanced MSC engraftment. Moreover, VEGF, HGF and IGF-1 were upregulated within the myocardium [79, 80].

Another promising strategy is focused on the overexpression of heme oxygenase-1 (HO-1). HO-1 enzymatically cleaves heme to bilirubin, carbon monoxide and free iron, thus having an anti-oxidative, anti-apoptotic and pro-angiogenic effect. It was shown that overexpression of HO-1 in MSCs increased cell viability and improved heart function *in vivo* [81]. Moreover, specific differentiation of MSCs into functional cardiomyocytes by genetic modifications using transcription factors is under investigation. Myocardin is a myogenic transcription factor regulating the expression of cardiac and smooth muscle cell genes. Grauss *et al* could show that overexpression of myocardin in hMSCs facilitated cell engraftment and induced differentiation towards a cardiomyocyte-like phenotype. However, electrophysiological analyses of hMSC derived cardiomyocytes were not investigated in this study [82].

### 1.3 Different Nucleic Acid Species for Gene Therapy

For gene therapy, various kinds of nucleic acids are utilized. They can be sub-divided into deoxyribonucleic acid (DNA)- and ribonucleic acid (RNA)- based approaches. Although, most of the nucleic acid-based therapeutics are in early stages of preclinical studies, these classes of compounds became promising candidates for treatment of a wide range of diseases, e.g. cardiovascular diseases, cancer, neurodegenerative diseases and genetic disorders [74, 75, 83, 84, 85, 86, 87, 88].

#### 1.3.1 DNA-based Gene Therapy

DNA-based gene therapy includes the application of short (e.g. DNA aptamers and DNazymes) and long DNA molecules (e.g. plasmids).

DNA aptamers are short, double-stranded DNA fragments (25-70 base pairs) that specifically bind proteins with high affinity. Aptamers are chemically synthesized. Therefore, they provide high specificity, non-immunogenicity and good stability *in vivo* [89]. In 2009, Spiel *et al* tested ARC1779, a DNA-aptamer against von Willebrand factor, in blood of patients with acute myocardial infarction *ex vivo*. It was shown that ARC1779 specifically decreased von Willebrand factor activity. Therefore, ARC1779 could become a novel tool to reduce the development of myocardial infarction [90].

DNAzymes are catalytically active DNA molecules. DNAzymes bind to the target mRNA sequence via their binding domains. Afterwards, the catalytic domain is activated and cleaves the target mRNA molecule. Thus, translation into a protein is blocked [91]. Recently, it was shown that a DNAzyme targeting the transcription factor early growth response protein-1 (Egr-1) decreased inflammation and apoptosis in the heart after myocardial infarction and enhanced cardiac function [92].

Among the DNA-based gene therapy, plasmids are predominantly used and most investigated for cardiac regeneration. Plasmids are circular, double-stranded DNA constructs (1 – 1,000 kilo base pairs) encoding genes for specific proteins. After cellular internalization into the cytoplasm, the DNA has to enter the nucleus for efficient transcription and translation of the therapeutic protein. To date, various plasmid-based gene therapy studies exist to treat ischemic heart diseases using diverse approaches, e.g. to influence cell differentiation, improve angiogenesis and cell survival (summarized in [74]). Advantages of using plasmid-based gene therapy are the transfer of several genes simultaneously, the possibility of externally controlled gene expression (e.g. drug-sensitive promoters, hypoxia-inducible promoters) and better stability compared to RNA nucleotides [93, 94, 95, 96]. However, for efficient gene expression foreign DNA has to cross the nuclear envelope into the nucleus which determines the limiting step [97]. Moreover, the application of DNA has the risk of mutational insertion into the host genome which could lead to cancer [98].

### 1.3.2 RNA-based Gene Therapy

Regarding the drawbacks of DNA-based gene therapy, the focus has turned to RNA-based approaches which can be distinguished between protein coding and non-protein coding RNAs. To date, recent progress has been achieved in the application of coding messenger RNAs (mRNAs). Potential mRNA approaches have been shown for reprogramming of fibroblasts into iPSCs, vaccination against HIV-1 and cancer therapy [99, 100]. However, further investigations have to be performed to prevent an immune response *in vivo* as well as to increase stability and efficiency of mRNAs for therapeutic applications.

A number of current studies have shown the great influence of non-coding RNAs (ncRNAs) on gene expression. Only 1% to 2% of the genome is coding for proteins. The remaining 98% represents the big class of ncRNAs [101]. NcRNAs are not translated into a protein but control various aspects of gene expression including control of transcription, post-

transcriptional processing and epigenetic targeting [102]. They are expressed dynamically during development and in response to environmental factors and stress [103]. Regulatory ncRNAs can be divided into long and short ncRNAs.

Long ncRNAs (lncRNAs) are transcripts larger than 200 nucleotides. They are involved in the regulation of many biological processes including chromosome X inactivation, imprinting, splicing and transcriptional regulation [104, 105, 106, 107]. However, the definite function of most lncRNAs has to be investigated. One recent example is the lncRNA *Braveheart* which is regulating cardiac differentiation in mouse ESCs. Additionally, it was shown that *Braveheart* is also enriched in the adult heart. Therefore, it is proposed that it might be an important lncRNA for cardiac lineage specification and differentiation [108]. Moreover, it was shown that overexpressing *lncRNA-RoR* modulated reprogramming of ESCs and increased the efficiency of iPSC-colony formation [109]. Therefore, lncRNAs might be used to promote direct reprogramming of cardiac fibroblasts into cardiomyocytes. However, further studies have to be performed to identify potential cardiac lncRNAs for treatment of myocardial infarction.

Recently, the most investigated short ncRNAs in research are small interfering RNAs (siRNAs) and microRNAs (miRs). SiRNAs can be used for treatment of disease causing genes through RNA interference (RNAi). For the discovery of RNAi, the Nobel Prize in Physiology or Medicine was awarded to Andrew Z. Fire and Craig C. Mello in 2006. RNAi provides a specific and efficient way to silence gene expression on the post-transcriptional level by inhibition of protein translation or direct mRNA degradation (Figure 1) [110]. Primarily, siRNAs originated from exogenously introduced double stranded RNAs (dsRNAs). More recently, it was shown that siRNAs could arise from endogenous genomic loci as well [111]. These dsRNAs are processed by Dicer into several mature siRNAs that direct gene silencing. SiRNAs are double-stranded nucleic acids composed of 21 – 23 nucleotides. After internalization into the cell, the siRNA is incorporated into a cytoplasmatic nuclease complex called RNA-induced silencing complex (RISC). In the RISC, Argonaute a catalytically active endonuclease binds to siRNA, degrades the passenger strand and leaves the guide strand intact to direct gene silencing. The guide siRNA strand specifically binds the target mRNA. Subsequently, the mRNA is cleaved and translation into a protein is stopped. Afterwards, the RISC is recycled and targets other mRNAs [112]. Regarding the function of siRNAs, they represent a promising approach for genetic research and drug targeting. Tu *et al* investigated the effect of p53 upregulated modulator of apoptosis (PUMA) in cardiomyocytes.

They could demonstrate that a specific inhibition of PUMA by siRNA protects cardiomyocytes from apoptosis *in vitro* [113]. Moreover, *in vivo* it was shown that the application of siRNA against Src homology region 2 domain-containing tyrosine phosphatase-1 significantly reduced apoptosis and infarction size after ischemic heart damage [114].

The best-characterized small ncRNAs in the heart are miRs [115]. miRs are key regulators of gene expression on the post-transcriptional level regulating more than 60% of all mammalian protein coding mRNAs [116]. They are endogenously expressed from either miR genes or intronic sequences of protein coding genes in the nucleus as pri-miR (Figure 1). Subsequently, pri-miR is cleaved by the enzyme Drosha into a stem-loop structured precursor miR (pre-miR). After exporting into the cytoplasm via Exportin-5, pre-miR is cleaved by the enzyme Dicer into one mature double-stranded miR (18 - 24 nucleotides). Mature miR enters the RISC where one strand is degraded while the other one interacts with the 3' untranslated regions of the target mRNA. Binding of RISC leads to blocking or degradation of mRNA translation [117]. Thus, miRs act as inhibitors of gene expression. In contrast to siRNA, a single miR can bind to several target genes connected with the potential to modulate multiple cell pathways. Eulalio *et al* could demonstrate that none of the investigated siRNAs could increase the proliferation of cardiomyocytes as highly as observed with miRs. They concluded that the remarkable effect of these miRs might be a cumulative effect on multiple, cellular mRNA targets [118]. Moreover, it is supposed that miR-based gene therapy might be less harmful for cells compared to siRNA treatment as it is closer to the innate regulation mechanism [119].

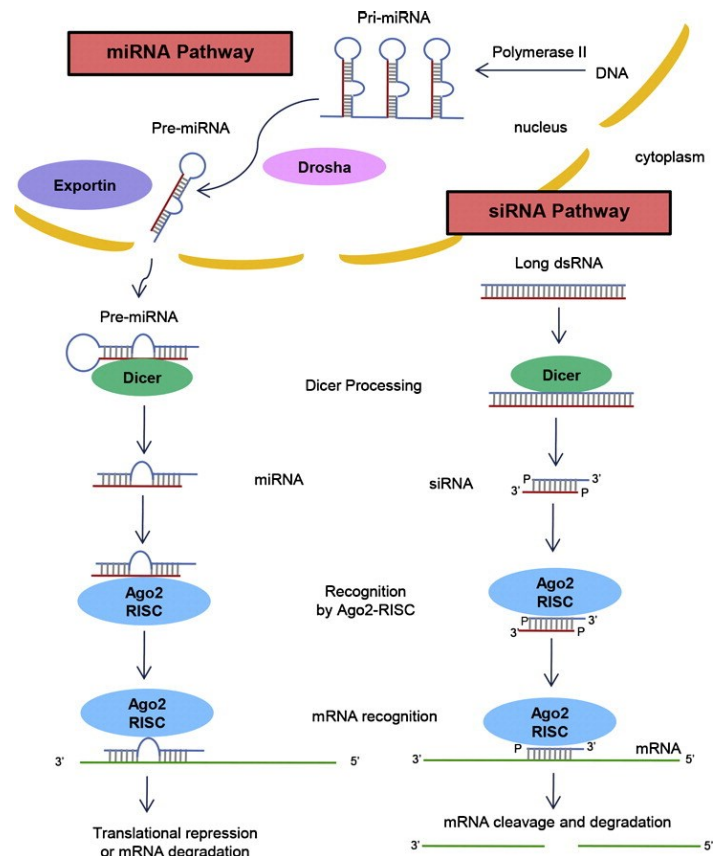


**Figure 1: Biogenesis and Function of miR and siRNA.** MiRs are expressed in the nucleus as pri-miR where they are subsequently cleaved by enzyme Drosha to stem-loop pre-miRs. Afterwards, the pre-miR is transferred via Exportin-5 into the cytoplasm where it is further processed by Dicer into a mature miR duplex. The functional miR strand is assembled in the RISC and thus able to repress translation of a set of mRNAs or to cleave the mRNA targets. SiRNA is mostly exogenously introduced into the cytosol as dsRNA. Then it is cleaved by Dicer into siRNA and is assembled in the RISC comparable to miR processing. However, siRNA perfectly matches to its specific target mRNA via Watson-Crick base pairing leading to inhibition of mRNA (taken from [120]).

To date, several miRs have been discovered that control cell differentiation, growth, proliferation and apoptosis [121, 122, 123]. In particular miRs play an essential role in heart development and cardiac diseases [124, 125]. The significance of miRs in cardiovascular development was demonstrated in Dicer-deficient mice where miR biogenesis was blocked. These mice showed seriously impaired heart and vessel development and died between days 12.5 and 14.5 of gestation [126]. Moreover, miRs show typical expression patterns after myocardial infarction, e.g. deregulated expression of miR-21, miR-1, miR-216 and miR-29 family [127, 128]. In addition, members of the miR-15 family (miR-15a, miR-15b, miR-16-1, miR-16-2, miR-195 and miR-497) were upregulated after ischemic damage in the heart resulting in death of cardiomyocytes and loss of pump function [129].



To date, different miR modulation strategies are available to treat myocardial infarction. The first possibility includes the inhibition of pathogenic miRs. Therefore miR inhibition can be achieved by the application of antagomiRs. AntagomiRs are small RNA oligonucleotides that perfectly match to the complementary miR. They are used to specifically silence endogenous miRs. It was shown that miR-15 inhibition reduced infarction size and improved cardiac function 2 weeks after myocardial infarction [130, 131]. Moreover, Bonauer *et al* showed that systemic administration of an antagomir-92a increased angiogenesis and functional recovery of the damaged tissue after myocardial infarction [132]. Recently, it was demonstrated that inhibition of miR-34a improved cell survival and heart functions following heart infarction by reducing telomere shortening, DNA damage responses and cardiomyocyte apoptosis [133]. Additionally, overexpression strategies of miRs are investigated. It was shown, that overexpression of miR-210 enhanced angiogenesis, inhibited apoptosis and improved cardiac function after myocardial infarction [134]. Recently, exogenously introduced miR-199a and miR-590 have been found to stimulate cardiac regeneration after heart infarction in mice [118]. Additionally, novel approaches to combine stem cell- and miR-based therapies are examined (Figure 2). It was shown, that overexpression of miR-499 in bone marrow MSCs increased the expression of cardiac specific genes (Nkx2.5, GATA4 and MEF2C) and induced cardiac differentiation [135]. In 2013, Huang *et al* overexpressed miR-1 in MSCs prior to transplantation in the infarcted heart. They could demonstrate enhanced survival of transplanted cells and cardiomyogenic differentiation thus improving heart function [136]. Recently, Dakhallallah *et al* showed that transfection of MSCs with miR-133a improved survival of MSCs *in vitro*. Moreover, transplantation of miR-133a modified MSCs in the heart led to a significant enhanced cell engraftment, cardiac function and decreased fibrotic remodeling after myocardial infarction by targeting pro-apoptotic genes (Apaf-1, caspase-9, caspase-3) [137]. Therefore, miR modified MSCs represent potential novel therapeutic approaches for treatment of ischemic heart diseases.

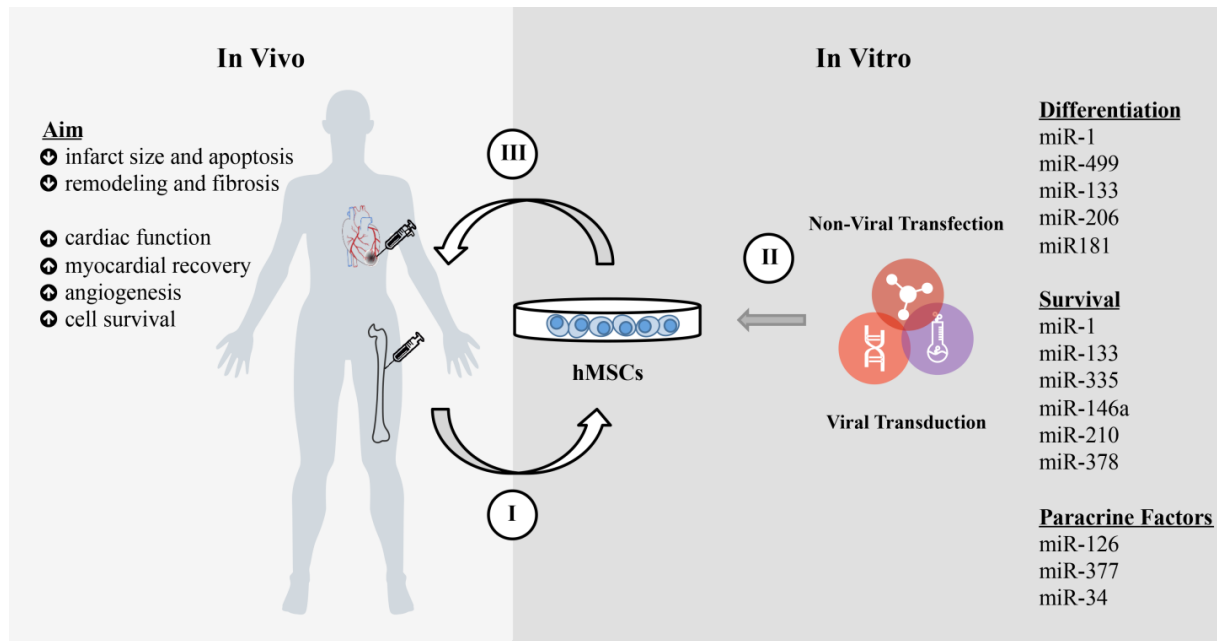


**Figure 2: Ex Vivo Genetic Modifications of hMSCs using miRs.** (I) hMSCs were obtained and purified from bone marrow aspirates. (II) Afterwards, freshly isolated or expanded hMSCs were genetically modified with miRs using viral transduction or non-viral transfection *in vitro*. (III) Subsequently, the modified cells were injected in the infarcted heart to improve tissue regeneration (data are summarized from [123, 135, 136, 137, 138, 139, 140, 141, 142, 143, 144]).

#### 1.4 Small RNA-Based Delivery Methods

Genetic modifications of MSCs using miRs have been shown to enhance the efficiency of stem cell therapy by influencing cell viability, differentiation and secretion of paracrine factors [145]. Various artificial precursor or mature miRs are commercially available. However, reduced *in vivo* stability, inappropriate biodistribution and unwanted side effects are limitations of successful miR-based therapy [146]. Therefore, safe and efficient miR transfer methods suitable for clinical applications have to be developed. To date, two delivery approaches are under investigation: viral and non-viral delivery methods.

Viruses are naturally evolved nano-scaled vehicles (viral vectors) that efficiently transfer their genes into host cells. They are the most efficient vectors to deliver DNA both *in vivo* and *in vitro* [147, 148, 149]. Advantages of using viral vectors are high transduction efficiencies and stable gene expression. However, the possibility of insertional mutagenesis, pathogenic vector mutation, cytotoxicity and immunogenicity limit the clinical use of this carrier [146, 150]. For investigating the regulatory role of miRs, primarily lentiviruses, adenoviruses and adeno-

associated viruses are used. However, none of these viral vectors deliver miR itself. All studies use miR expressing vectors like DNA sequences that require nuclear localization for efficient transcription into pri-miR and further processing by the RNA machinery [118, 133, 151, 152, 153, 154, 155]. Therefore, this belongs to the field of DNA delivery.

#### 1.4.1 Non-Viral Delivery Methods

Non-viral delivery methods were developed to overcome the drawbacks of viral vectors. They show less safety risks, high nucleic acid capacity, non-inflammatory and non-infectious behaviour [156]. Moreover, miRs and siRNAs can be delivered in their mature structure. In contrast to viral vectors, plasmid-based gene expression or RNAi is often transient which might be preferable due to a better control of the therapeutic effect [157]. In general, all non-viral transfection techniques can be divided into physical and chemical methods.

Over the past years, many physical methods have been investigated for gene delivery, e.g. electroporation, gene gun, sonoporation and microinjections. Recent developments propose that gene delivery using physical methods has reached the efficiency and expression duration that is clinically meaningful [158]. Here, physical forces (e.g. injection, particle impact, electric pulse, ultrasound or laser irradiation) are used to facilitate the transfer of nucleic acids inside the cell by creating transient membrane defects [150]. Primarily, electroporation which uses an electric field to generate transient pores in the cell membrane for nucleic acid entry is used [159, 160]. Tano *et al* could efficiently block miR-150 in bone marrow derived mononuclear cells by transferring the appropriate antagomiR using electroporation [161]. However, physical methods are potentially damaging cells due to deregulated ion influx or thermal heating. Moreover, application of naked small RNAs inside the cell is susceptible to the degradation by nucleases [162]. Additionally, all physical methods are preferentially used for *ex vivo* modulation of cells. *In vivo* applications are limited due to the accessibility to the internal organs.

Chemical methods use cationic synthetic or natural compounds to condense and protect negatively charged nucleic acids [150]. They show great potential as effective carriers for DNA, siRNA and miR [156, 163, 164]. Advantages of using chemical methods include the control of their molecular composition and their simplified manufacturing [165]. The most commonly used chemical transfection reagents are cationic lipids and cationic polymers.

In 1987, Felgner *et al* were the first who described cationic lipid-based gene delivery. They introduced the term lipofection which describes a lipid-based transfection procedure for nucleic acids [166]. Cationic lipids build vesicles composed of a phospholipid bilayer with an aqueous core. Moreover, they have the ability to build complexes with negatively charged nucleic acids through electrostatic interactions - so called lipoplexes [150]. The cellular pathway of lipoplexes was revealed by Xu *et al* in 1996. After association of cationic liposome/DNA complexes to the negatively charged cell membrane, lipoplexes were incorporated into the cell via endocytosis. In the early endosome, the endosomal membrane was destabilized by a flip-flop mechanism of anionic phospholipids. The anionic membrane lipids laterally diffused into the lipoplexes and formed neutrally charged ion pairs with the cationic lipids of the lipoplexes. As a result, DNA was released from the lipoplexes allowing cytoplasmatic entry [167]. Currently, there are several lipid-based delivery systems commercially available like Lipofectamine<sup>®</sup> (Invitrogen). Lipofectamine<sup>®</sup> is a mixture of the cationic lipid 2,3-dioleoyloxy-N-[2-(spermine-carboxamido)ethyl]-N,N-dimethyl-1-propanaminium trifluoroacetate (DOSPA) and neutral helper lipid dioleoyl phosphatidylethanolamine (DOPE). Alaiti *et al* used Lipofectamine<sup>®</sup> to transfect CD34<sup>+</sup> hematopoietic stem cells with miR-210 *in vitro*. They could demonstrate up to 60% transfection efficiency and good cell viability (87%) [168]. To date, lipofection belongs to the most extensively investigated and frequently used non-viral gene delivery methods *in vitro*. It provides several commercially available products with highly efficient gene delivery of both DNA and small RNAs connected with low costs [169]. However, safe and efficient delivery *in vivo* is restricted due to cytotoxicity, nonspecific uptake and unwanted immune response [170].

Cationic polymers represent an additional class of chemically based non-viral vectors with high transfection efficiency. One of the most widely used cationic polymer *in vitro* and *in vivo* is polyethylenimine (PEI) [171, 172, 173]. PEI consists of several units of two carbons and one nitrogen atom. Under physiological conditions, high amounts of amino groups in PEI are protonated providing its positive surface charge and good buffering capacity. Thus, PEI can be used to condense nucleic acids and form cationic complexes (termed as polyplexes) through electrostatic interactions [146]. Positively charged polyplexes can interact with negatively charged polysaccharides of the cell membrane. Once bound to the cell surface, it is proposed that polyplexes are taken up inside the cell via endocytosis [171]. In 1995, Boussif *et al* investigated the intracellular pathway of polyplexes and revealed the endosomal escape

mechanism of PEI polyplexes through ‘*proton sponge*’ effect as crucial step for efficient transfection [174]. During the endosomal maturation, the membrane-bound ATPase actively pumps protons from the cytosol into the endosomes leading to acidification of endosomal compartments and activation of hydrolytic enzymes. Additionally, incorporated polyplexes get protonated and resist acidification. Subsequently, more protons are transported into the endosomes to decrease the pH value. This leads to a passive entry of chloride ions and an increase of ionic concentration followed by a passive water influx. Subsequently, the osmotic pressure inside the vesicles increases and causes swelling and rupture of the endosomal membrane releasing polyplexes into the cytoplasm [174, 175]. Thus, nucleic acids are protected from lysosomal degradation. Urban-Klein *et al* successfully developed a PEI-based siRNA delivery approach. They could demonstrate that PEI efficiently protects siRNA against enzymatic degradation. Moreover, it was shown that siRNA/PEI complexes but not siRNA alone could deliver functional siRNA both *in vitro* and *in vivo* resulting in a significant reduction of human epidermal growth factor receptor-2 (HER-2) mRNA levels (~ 50%) compared to the untransfected group [172]. Additionally, Ibrahim *et al* demonstrated that PEI is also able to form stable complexes with miR and could efficiently transfect more than 80% of cells [176]. Although, cytotoxicity and non-biodegradability of PEI restrict its clinical applications [177], Grayson *et al* demonstrated that branched PEI with a molecular weight of 25 kDa was the most successfully tested polymer for siRNA delivery *in vitro* [178]. However, for directed miR delivery *in vivo*, PEI polyplexes are limited due to the lack of specificity. Therefore, specific targeting approaches could be applied to overcome these obstacles.

#### 1.4.2 Magnetic Gene Targeting Strategies

To date, numerous non-viral approaches for gene delivery are under investigations. However, there is still no perfect nano-scaled delivery system available, which achieves efficient, safe and selective delivery of the genetic material for translation into the clinic. Different targeting strategies have attracted attention as they provide specific and local gene delivery proposed for systemic administration. Targeted RNAi can be achieved either by functionalization of the non-viral vector with specific ligands (e.g. peptides, growth factors, antibodies) or by combination with magnetic nanoparticles (MNPs) which can be guided by an external magnetic field [179, 180, 181, 182, 183, 184]. MNPs have already been used for MACS,

hyperthermia for cancer treatment, protein purification and cell tracking [185, 186, 187, 188]. Additionally, iron oxide-based MNPs were approved by the US Food and Drug Administration as magnetic resonance imaging (MRI) contrast agents (Resovist<sup>®</sup>, Feridex IV<sup>®</sup>) [189]. Therefore, they have been well characterized in terms of biocompatibility and safety issues being essential for potential clinical applications. Moreover, the surface of MNPs can be functionalized with surfactants, ligands or biomolecules, e.g. streptavidin coating [190]. Additionally, size, charge and magnetic properties of MNPs can be modified during their production [189]. Previous studies have shown that MNP-mediated gene delivery enables both *in vivo* targeting of the magnetic complexes towards a specific organ and guiding of cells transfected with MNPs using an externally applied magnetic field [183, 191]. Therefore, it was proposed that a combination of MNPs with different non-viral gene delivery methods can be a promising strategy to increase their selectivity and efficiency.

In 2002, Scherer *et al* demonstrated a new technique called magnetofection, where common viral and non-viral gene delivery agents (e.g. adenovirus, Lipofectamine<sup>®</sup>, PEI) were combined with paramagnetic iron oxide nanoparticles via salt-induced aggregation. It was shown that an externally applied magnetic field increased sedimentation of the transfection complexes and efficiently improved transfection efficiency *in vitro* and *in vivo* [192]. However, magnetofection is not facilitating cellular uptake or intracellular pathways [193]. In recent years, MNP-mediated transfection (e.g. Magnetofectamine<sup>®</sup>) has become a powerful approach for highly effective and fast delivery of both DNA as well as siRNA [194, 195, 196, 197, 198]. Tan *et al* successfully delivered siRNA using Magnetofectamine<sup>®</sup>-based transfection which is a combination of the cationic lipid Lipofectamine<sup>®</sup> from Invitrogen with PEI-coated CombiMag MNPs from OZ Biosciences. They could demonstrate transfection efficiencies between 70% to 90% in a mouse N2A neuroblastoma cell line and 15% to 30% in primary neurons [199].

A different approach for magnetically targeted DNA transfection has been developed by our group in 2008. Li *et al* first condensed DNA by biotinylated PEI to form DNA/PEI polyplexes. Afterwards, DNA/PEI complexes were covalently bound to streptavidin-coated MNPs via biotin-streptavidin connections (Figure 3). *In vitro*, it was shown that reporter gene expression was up to 85-fold increased after transfection with magnetic polyplexes compared to DNA/PEI complexes alone in different cell lines (NIH3T3, HEK293, COS7) as well as in primary endothelial cells using magnetic forces. Moreover, DNA/PEI/MNP complexes were

further applied *in vivo*. After intravenous injection in the tail vein of mice, magnetic polyplexes could be targeted to the heart by an external magnetic field [200].

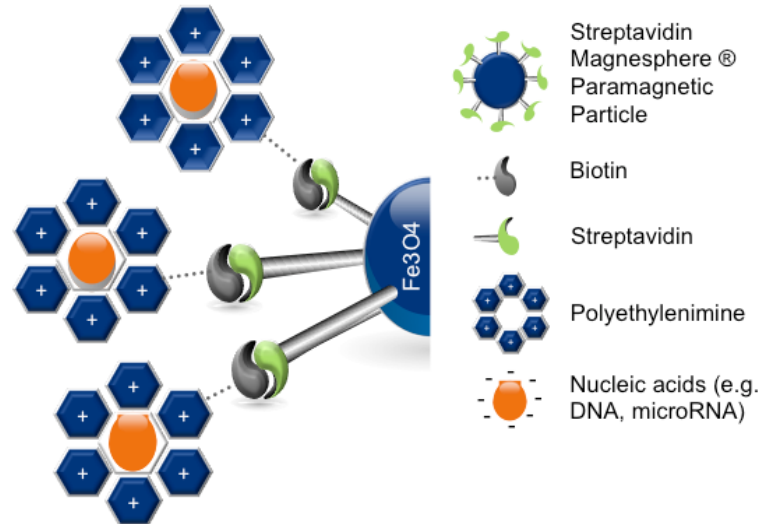


**Figure 3: Construction of Magnetic Transfection Complexes.** Negatively charged nucleic acids (e.g. DNA or miR) form complexes with biotinylated cationic PEI due to electrostatic interactions. Afterwards, PEI polyplexes are covalently bound to streptavidin coated paramagnetic iron oxide nanoparticles via streptavidin-biotin connections (adopted from [201]).

Recently, we have shown enhanced transfection efficiencies for DNA-based complexes after MNP-based transfection in hMSCs even without the application of a magnetic field [202]. Therefore, Delyagina *et al* proposed different transfection mechanisms for DNA/PEI/MNP and DNA/PEI complexes. It is assumed that MNP-bound polyplexes provide a faster release of DNA into the cytosol compared to PEI polyplexes. Furthermore, DNA/PEI/MNP complexes remain outside the nucleus due to the strong biotin-streptavidin binding between PEI and MNPs while condensed polyplexes were found inside the nucleus [202, 203]. Thus, MNP-containing complexes may be advantageous for miR delivery as opposed to DNA, miR-mediated RNAi takes place in the cytosol.

## 1.5 Aim of the Thesis

Based on the background described above, the aim of this thesis was to develop a non-viral miR delivery vector for efficient modification of freshly isolated hMSCs using magnetic miR/PEI/MNP complexes and show proof-of-principle for targeting of transfected hMSCs by an externally applied magnet *in vitro*. Initially, the optimal complex composition had to be found in expanded hMSCs by investigating different miR amounts, PEI concentrations and MNP quantities. In this study, delivery of miR-335 was chosen as exemplary model. MiR-335 had been shown to influence proliferation, differentiation and migration of hMSCs by targeting tenascin C (TNC) and runt-related transcription factor 2 (RUNX2), respectively [144]. Then, the intracellular processing of transfected pre-miR-335 into mature strand, RNAi of known target genes as well as functionality of delivered miR was investigated. Subsequently, the optimized magnetic vector should be applied to freshly isolated hMSC as they bear less safety risks and more relevance for clinical applications. Moreover, transfection performance of miR/PEI/MNP complexes should be compared to commonly used and commercially available magnetic vectors. Finally, the ability to specifically target magnetically transfected hMSCs using an externally applied magnetic field was investigated *in vitro*.



## 2 Materials and Methods

### 2.1 List of Chemicals

**Table 1: List of Chemicals Used in this Thesis**

Manufacturer	Chemicals
ATTO-TEC GmbH, Siegen, Germany	Atto 565 Biotin
Biozym Scientific GmbH, Hessisch Oldendorf, Germany	Agarose
Carl Roth, Karlsruhe, Germany	Boric Acid DMSO NaCl TRIS
Fermentas GmbH, Schwerte, Germany	6x DNA Loading Dye
Life Technologies Corporation, Austin, USA	Acid-Phenol Chloroform Cy3™ dye-Labeled Pre-miR Negative Control #1 DAPI UltraPure™ DNase/RNase-free Distilled Water hsa-miR-335-5p Pre-miR™ miRNA Precursor Lipofectamine® 2000 Opti-MEM® I Reduced Serum Medium Pre-miR™ miRNA Precursor Molecules - Negative Control #1 Recovery™ Cell Culture Freezing Medium TaqMan® 2x Universal PCR Master Mix with AmpErase®UNG α-MEM
Lonza, Walkersville, USA	MSCGM™
Merck, Darmstadt, Germany	FluorSave™
Merck Millipore, Billerica, USA	Human Plasma Fibronectin
Miltenyi Biotec GmbH, Bergisch-Gladbach, Germany	CD105 MicroBeads FcR Blocking Reagent
MP Biomedicals, Solon, USA	Glucose
OZ Biosciences, Marseille, France	CombiMag Reagent

---

PAA Laboratories GmbH, Pasching, Austria	EDTA Penicillin Streptomycin Trypsin/EDTA (10x)
Pan Biotech GmbH, Aidenbach, Germany	FBS Pancoll Separation Medium PBS RPMI 1640
Promega, Madison, WI, USA	Streptavidine    Magnesphere <sup>®</sup> Paramagnetic Particles
Roche Diagnostics GmbH, Mannheim, Germany	Collagenase B DNase I
Sigma-Aldrich Chemie GmbH, Munich, Germany	BSA Donkey Serum Ethidium Bromide Glycine Ninhydrin Reagent PEI 25 kDa PFA Triton X-100 Trypan Blue
Thermo Fisher Scientific, Rockford, USA	Sulfo-NHS-LC-Biotin Linker
Zentralapotheke der Universitätsmedizin Rostock, Rostock, Germany	Ethanol Absolute

---

## 2.2 List of Solutions

**Table 2: List of Solutions Used in this Thesis**

<b>Solution</b>	<b>Contents</b>
$\alpha$ -MEM Basal Medium	90% $\alpha$ -MEM 10% FBS 100 U/ml Penicillin 100 $\mu$ g/ml Streptomycin
Adipogenic Differentiation Medium	99% $\alpha$ -MEM Basal Medium 1% Adipogenic Supplement
Adipogenic Supplement	Hydrocortisone Indomethacin Isobutylmethylxanthine
Blocking Solution	0.3% Triton X-100 1% BSA 10% Donkey Serum PBS
MACS-Buffer	0.5% BSA 2mM PBS/EDTA
MSCGM™	500 ml MSCBM 50 ml MCGS 10 ml L-Glutamine 0.5 ml GA-1000 100 U/ml Penicillin 100 $\mu$ g/ml Streptomycin
Osteogenic Differentiation Medium	95% $\alpha$ -MEM Basal Medium 5% Osteogenic Supplement
Osteogenic Supplement	Ascorbatephosphate Dexamethasone $\beta$ -Glycerolphosphate
TBE Buffer	54 g TRIS 27.5 g Boric Acid 20 ml of 0.5 M EDTA Adjust to pH 8.0 Up to 1 l with dH <sub>2</sub> O
Washing Solution	1% BSA PBS

## 2.3 hMSC Isolation and Culture

hMSCs derived from bone marrow were obtained from sternal aspirates of patients undergoing artery bypass surgery at the Cardiac Surgery Department of the University of Rostock as described previously [204]. The donors gave their written consent to use their bone marrow for research purposes according to the Declaration of Helsinki.

### 2.3.1 Isolation of Mononuclear Cells

Mononuclear cells (MNCs) were isolated by density gradient centrifugation. Therefore, 10 ml of bone marrow aspirates were mixed with 6 ml phosphate buffered saline/ethylenediaminetetraacetic acid solution (PBS/EDTA), 20 ml RPMI 1640 medium, 175  $\mu$ l collagenase B (0.02%) and 175  $\mu$ l DNase I (100 U/ml) and incubated on the shaker (VWR International GmbH, Darmstadt, Germany) for 30 minutes at room temperature. Meanwhile, 15 ml Pancoll separation medium was pipetted into 50 ml Leucosep<sup>®</sup> tubes (Greiner Bio-One GmbH, Solingen, Germany) with subsequent centrifugation at 1,000 g for 10 seconds. After the incubation time, the cell suspension was transferred to the prepared Leucosep<sup>®</sup> tubes (Greiner Bio-One) and centrifuged at 445 g for 35 minutes at 22 °C. After aspiration of the MNC layer, the volume of the cell suspension was adjusted to 50 ml with PBS/EDTA solution and centrifuged at 300 g for 10 minutes at 22 °C. Then, cell numbers were determined and up to  $1.5 \times 10^8$  MNCs per 175 cm<sup>2</sup> culture flask (Greiner Bio-One) were cultivated in 20 ml Mesenchymal Stem Cell Growth Medium (MSCGM<sup>™</sup>) at 37 °C and 5% CO<sub>2</sub>.

### 2.3.2 Isolation of hMSCs by Plastic Adherence

For plastic adherence selection of hMSCs, the cell suspension was cultivated in MSCGM<sup>™</sup> at 37 °C and 5% CO<sub>2</sub> until the adherent hMSC population reached 80% confluency. Subsequently, the cells were passaged or frozen in 1 ml Recovery<sup>™</sup> Cell Culture Freezing medium at -170 °C in liquid nitrogen. For transfection optimization experiments using expanded cells, hMSCs in passage 3 and 4 were used. The morphology of the cells was analyzed using an Axiovert 40 CFL microscope (Carl Zeiss AG, Jena, Germany).

### 2.3.3 Isolation of hMSCs by Magnetic Cell Separation

For magnetic cell separation of CD105<sup>+</sup> hMSCs from the MNC fraction (cultivated overnight), MACS<sup>®</sup> technology was applied according to the manufacturer's protocol (Miltenyi Biotec GmbH, Bergisch-Gladbach, Germany). Briefly, MNC suspension was centrifuged at 300 g for 10 minutes at 4 °C and supernatant was discarded. Afterwards,  $1 \times 10^7$  MNCs were resuspended in 60 µl MACS-buffer. For magnetic cell labeling, the cell suspension was mixed with 20 µl FcR Blocking Reagent and 20 µl CD105 MicroBeads and incubated for 30 minutes at 4 °C. In the case of higher cell numbers, volume of reagents was scaled up accordingly. Afterwards, cells were washed with 2 ml MACS-buffer and centrifuged at 200 g for 10 minutes at 4 °C. Supernatant was removed and the cell pellet was resuspended in 500 µl MACS-buffer. Next, the magnetically labeled cell suspension was filtered through a 30 µm pre-separation filter (Miltenyi Biotec) to remove cell aggregates. Subsequently, the cell suspension was applied to equilibrated MS (up to  $2 \times 10^8$  MNCs) or LS ( $2 \times 10^8$  -  $2 \times 10^9$  MNCs) MACS<sup>®</sup> columns (Miltenyi Biotec) under the application of a magnetic field using a MiniMACS<sup>®</sup> or MidiMACS<sup>®</sup> separator (Miltenyi Biotec). Afterwards, columns were washed three times with 500 µl MACS-buffer for MS MACS<sup>®</sup> column or 3 ml MACS-buffer for LS MACS<sup>®</sup> column, respectively. After removing the magnetic field, the magnetically labeled CD105<sup>+</sup> cell fraction was eluted with 1 ml MSCGM<sup>™</sup> for MS MACS<sup>®</sup> columns or 3 ml MSCGM<sup>™</sup> for LS MACS<sup>®</sup> columns. To increase cell purity, the isolation process was repeated using a second rinsed MS or LS MACS<sup>®</sup> column, respectively. Subsequently, the number of living cells was determined by trypan blue staining (0.4%) and the cell morphology was analyzed using an Axiovert 40 CFL microscope (Carl Zeiss). For further *in vitro* experiments using freshly isolated cells, the positive CD105<sup>+</sup> cell fraction was suspended in MSCGM<sup>™</sup> and was transfected immediately after isolation.

## 2.4 Immunophenotyping of hMSCs

Cell surface markers of freshly isolated and cultured hMSCs were fluorescently labeled with anti-human antibodies CD29-APC, CD44-PerCP-Cy5.5, CD45-V500, CD73-PE, CD117-PE-Cy7 (BD Biosciences, Heidelberg, Germany) and CD105-AlexaFluor488 (AbD Serotec, Kidlington, UK). Appropriate mouse isotype antibodies served as negative controls. Therefore,  $5 \times 10^4$  hMSCs were labeled with respective fluorescent dye-conjugated antibodies

(Table 3). The total volume was adjusted to 100  $\mu$ l with MACS-buffer and the cells were incubated in the dark for 10 minutes at 4 °C. After the incubation time, cells were washed with 1 ml PBS and centrifuged at 300 g for 10 minutes. Supernatant was discarded and the cell pellet was resuspended in 100  $\mu$ l PBS and 33  $\mu$ l paraformaldehyde (4% PFA). Subsequently,  $2 \times 10^4$  cells were acquired using a BD FACS LSRII™ flow cytometer (BD Biosciences) and analyzed with BD FACSDiva Software 6 (BD Biosciences).

**Table 3: Immunofluorescent Labeling of hMSCs**

<b>Antigen</b>	<b>Dye</b>	<b>Company</b>	<b>Catalogue number</b>	<b>V (dye) per 100 <math>\mu</math>l</b>
CD29	APC	BD Biosciences	559883	10 $\mu$ l
CD44	PerCP-Cy5.5	BD Biosciences	560531	2.5 $\mu$ l
CD45	V500	BD Biosciences	560777	2.5 $\mu$ l
CD73	PE	BD Biosciences	550257	10 $\mu$ l
CD105	AF 488	AbD Serotech	MCA1557A488	5 $\mu$ l
CD117	PE-Cy7	BD Biosciences	339217	2.5 $\mu$ l
Isotype control CD29	APC	BD Biosciences	555751	10 $\mu$ l
Isotype control CD44	PerCP-Cy5.5	BD Biosciences	558304	10 $\mu$ l
Isotype control CD45	V500	BD Biosciences	560787	2.5 $\mu$ l
Isotype control CD73	PE	BD Biosciences	555749	10 $\mu$ l
Isotype control CD105	AF 488	AbD Serotech	MCA928A488	5 $\mu$ l
Isotype control CD117	PE-Cy7	BD Biosciences	557872	2.5 $\mu$ l

## 2.5 Functional Differentiation Assay

The differentiation capacity of hMSCs was analyzed using the Human Mesenchymal Stem Cell Function Identification Kit (R&D Systems, Minneapolis, USA).

### 2.5.1 Adipogenic Differentiation of hMSCs

For adipogenic differentiation,  $5 \times 10^4$  cells per well were expanded in a 24-well plate on sterilized coverslips (Carl Roth) in  $\alpha$ -Minimum-Essential-Medium ( $\alpha$ -MEM) Basal Medium at 37 °C and 5% CO<sub>2</sub>. When 100% confluency was reached, the cells were cultivated in Adipogenic Differentiation Medium (R&D Systems). Differentiation Medium was changed every 3 to 4 days. After 20 days under differentiation conditions, cells were washed twice with 1 ml PBS and fixed with 500  $\mu$ l PFA (4%) for 20 minutes at room temperature. Next, the cells were washed three times for 5 minutes with 500  $\mu$ l washing solution. Afterwards, hMSCs were permeabilized and blocked with 500  $\mu$ l blocking solution. Subsequently, staining for adipogenic differentiation was performed. Therefor, 300  $\mu$ l per well of goat anti-mouse fatty acid binding protein-4 (FABP-4) primary antibody (10  $\mu$ g/ml, R&D Systems) were incubated overnight at 4 °C. Then, the cells were washed three times for 5 minutes with 500  $\mu$ l washing solution. Afterwards, 300  $\mu$ l of Alexa Fluor 488 donkey anti-goat IgG secondary antibody (Life Technologies) diluted 1:200 in washing solution was incubated in the dark for 1 hour at room temperature. Cells were washed three times with 500  $\mu$ l washing solution and stained with 300  $\mu$ l 4',6-diamidino-2-phenylindole (DAPI) dihydrochloride (250 nM) in the dark for 15 minutes at room temperature. After three washing steps with 1 ml PBS on the microplate shaker (Grant Instruments, Cambridge, England), coverslips were mounted with FluorSave™ on a microscope slide (Paul Marienfeld GmbH & Co. KG, Lauda-Königshofen, Germany). Images were acquired using an ELYRA PS.1 LSM 780 microscope (Carl Zeiss) and analyzed by ZEN2011 software (Carl Zeiss, Göttingen, Germany).

### 2.5.2 Osteogenic Differentiation of hMSCs

For osteogenic differentiation,  $3 \times 10^4$  hMSCs per well were seeded in 500  $\mu$ l  $\alpha$ -MEM Basal Medium on human plasma fibronectin (10  $\mu$ g/ml) coated coverslips and incubated at 37 °C and 5% CO<sub>2</sub> until 50% to 70% confluency was reached. Subsequently, the cells were cultivated in Osteogenic Differentiation Medium (R&D Systems). Osteogenic Differentiation Medium was exchanged every 3 to 4 days. After 20 days in differentiation medium, the cells were fixed and stained as described above (see 2.5.1) using mouse anti-human osteocalcin primary antibody (R&D Systems) and Alexa Fluor 488 donkey anti-mouse IgG (Life Technologies).

## 2.6 Preparation of Transfection Complexes

### 2.6.1 Preparation of Polyplex-based Transfection Complexes

For preparation of miR/PEI, miR/PEI/MNP and miR/PEI/CombiMag complexes, Cy3<sup>TM</sup> dye-Labeled Pre-miR Negative Control #1, Pre-miR<sup>TM</sup> miRNA Precursor Molecules - Negative Control #1 or hsa-miR-335-5p Pre-miR<sup>TM</sup> miRNA Precursor were used. MiRs were diluted in 100 µl DNase/RNase free distilled water and stored in aliquots with a concentration of 50 mM at -20 °C.

Branched PEI (25 kDa) was biotinylated using a Sulfo-NHS-LC-Biotin linker and was kindly provided by Natalia Voronina (University of Rostock, Germany). To determine the biotinylation degree of PEI, EZ Biotin Quantitation Kit (Thermo Fisher Scientific) was used according to the manufacturer's protocol. PEI with 1.3 mMol Biotin/mMol PEI was obtained. To measure the α-amino group concentration in PEI, Ninhydrin reagent solution (2%) was used. Therefor 100 µl of PEI solution and 75 µl of Ninhydrin reagent were mixed and incubated for 30 minutes at 80 °C. Afterwards, 100 µl ethanol absolute were added and absorbance of PEI samples was measured at 550 nm against glycine standard curve of known concentrations. Biotinylated PEI was stored at amine concentrations of 27.6 mM at 4 °C.

#### 2.6.1.1 Preparation of miR/PEI Complexes

For preparation of miR/PEI complexes, different molar ratios of PEI nitrogen and miR phosphate (NP ratios) were prepared (Equation 1). Therefor miR and PEI were diluted in equal volumes of 5% glucose solution, well mixed and incubated for 30 minutes at room temperature (Table 4, 5).

$$NP \text{ ratio} = \frac{C(PEI) * V(PEI)}{0.12 * n(miR)}$$

**Equation 1: Calculation of the NP Ratio Referring to the Number of Nitrogen Atoms (N) in PEI per Phosphate Group (P) of miR** (C (PEI) = concentration of amine nitrogen in PEI in mM, V (PEI) = volume of PEI in µl, n (miR) = amount of substance of miR in pmol, 0.12 nmol/pmol = 0.12 nmol of phosphate in 1 pmol of miR).



**Table 4: Transfection Protocol for Cultured hMSCs.** Values are calculated according to 5pmol/cm<sup>2</sup> of miR. (n (miR) = amount of substance of miR, NP = number of N in PEI per P of miR, V (PEI) = volume of PEI, V (glucose) = volume of glucose for miR and PEI dilution).

Culture plate	Cell number/ well	n (miR)	V (PEI)			V (glucose)
			NP 2.5	NP 5	NP 10	
24-well	15,000	5 pmol	0.05 µl	0.11 µl	0.22 µl	50 µl
12-well	30,000	10 pmol	0.11 µl	0.22 µl	0.44 µl	100µl
6-well	100,000	50 pmol	0.54 µl	1.09 µl	2.17 µl	200 µl

**Table 5: Transfection Protocol for Freshly Isolated hMSCs.** (n (miR) = amount of substance of miR, NP = number of N in PEI per P of miR, V (PEI) = volume of PEI, V (glucose) = volume of glucose for miR and PEI dilution).

Culture plate	Cell number/ well	n (miR)	V (PEI)			V (glucose)
			NP 2.5	NP 5	NP 10	
48-well	200,000	5 pmol	0.05 µl	0.11 µl	0.22 µl	50 µl
	200,000	10 pmol	0.11 µl	0.22 µl	0.44 µl	50 µl
12-well	500,000	10 pmol	-	-	0.44 µl	100 µl

### 2.6.1.2 Preparation of miR/PEI/MNP Complexes

For the formation of miR/PEI/MNP complexes, Streptavidine Magnesphere<sup>®</sup> Paramagnetic Particles (in the following abbreviated as MNPs) were used. First, MNPs were sonicated and filtered using a 450 nm Millix-HV PVDF syringe driven filter (Millipore, Tullagreen, Ireland). Then, the iron concentration of the MNP solution was determined by measuring the absorbance at 351 nm with a spectrophotometer (Themo Electron, Waltham, USA) against iron standard solution of known concentrations. The MNP filtrate was stored in aliquots at 4 °C. After the preparation of miR/PEI complexes, 1 to 6 µg/ml iron in sonicated MNPs were

added and incubated for 30 minutes at room temperature. miR/PEI and miR/PEI/MNP complexes were freshly prepared before each transfection experiment.

### **2.6.1.3 Preparation of miR/PEI/CombiMag Complexes**

In order to form miR/PEI/CombiMag complexes, Cy3<sup>TM</sup> dye-Labeled Pre-miR Negative Control #1 was used. At first, CombiMag reagent was incubated for 20 minutes in an ultrasonic bath (Bandelin electronic GmbH & Co. KG, Berlin, Germany). Subsequently, 0.025  $\mu$ l CombiMag per 1 pmol miR were mixed with miR/PEI complexes. miR/PEI/CombiMag complexes were incubated for 20 minutes at room temperature. Transfection complexes were freshly prepared before transfection.

## **2.6.2 Preparation of Lipoplex-based Transfection Complexes**

### **2.6.2.1 Preparation of miR/Magnetofectamine<sup>®</sup> Complexes**

For the preparation of miR/Magnetofectamine<sup>®</sup> complexes, Cy3<sup>TM</sup> dye-Labeled Pre-miR Negative Control #1 was used. Initially, miR/Lipofectamine<sup>®</sup> complexes were formed. Therefor miR and Lipofectamine<sup>®</sup> 2000 transfection reagent (0.05  $\mu$ l Lipofectamine<sup>®</sup>2000/pmol miR) were diluted each in 25  $\mu$ l of Opti-MEM<sup>®</sup> I Reduced Serum Medium and incubated for 5 minutes at room temperature. Afterwards, miR solution and Lipofectamine<sup>®</sup> solution were mixed and incubated for 20 minutes at room temperature. In order to form miR/Magnetofectamine<sup>®</sup> complexes, CombiMag reagent was sonicated for 20 minutes. Then, 0.025  $\mu$ l CombiMag/pmol miR were mixed with miR/Lipofectamine<sup>®</sup> complexes and incubated for 20 minutes at room temperature. MiR/Magnetofectamine<sup>®</sup> complexes were freshly prepared before use.

## **2.7 Characterization of miR/PEI and miR/PEI/MNP Complexes**

### **2.7.1 Condensation Assay**

Condensation of miR by PEI was evaluated by gel electrophoresis. Therefore miR and miR/PEI complexes composed of 20 pmol Pre-miR<sup>TM</sup> miRNA Precursor Molecules - Negative Control #1 with NP ratios ranging from 0.1 to 33 were prepared as described above (see 2.6.1.1). Afterwards, the samples were mixed with 2.5 µl 6x loading dye and loaded onto a 2% agarose gel containing 6 µl ethidium bromide solution in TRIS-borate-EDTA (TBE) buffer. Gel electrophoresis was performed for 15 minutes at 100 V. Afterwards, the gel was analyzed using the Gel Doc 2000 system (BioRad Laboratories GmbH, Munich, Germany).

### **2.7.2 Particle Size and Zeta Potential Measurement**

To determine particle size and surface charge, transfection complexes composed of an NP ratio of 10 combined with 20 pmol Cy3<sup>TM</sup> Labeled Pre-miR<sup>TM</sup> Negative Control #1 and 1 to 6 µg/ml iron in MNPs were prepared as described above (see 2.6.1.1, 2.6.1.2). MNPs and miR/PEI/MNP complexes were diluted in 1 ml glucose solution (5%). The mean hydrodynamic diameter was determined by dynamic light scattering (DLS) technique with a Brookhaven 90 Plus Nanoparticle Size Analyzer (Brookhaven Instruments Corporation, New York, NY, USA). Surface charge was evaluated by a ZetaPALS Analyzer (Brookhaven Instruments) using the phase analysis light scattering (PALS) method.

## **2.8 Transfection Experiments**

For experiments in a well plate, appropriate numbers of hMSCs were seeded (Table 4, 5) 24 hours before transfection of cultured hMSCs or immediately before transfection of freshly isolated cells. At the day of transfection, complexes were prepared as described above (see 2.6) and added dropwise to the cells. Subsequently, the cells were treated with or without the application of a magnetic field using a Super Magnetic Plate (OZ Biosciences) for 20 minutes. Afterwards, the cells were incubated for 5, 24 or 72 hours at 37 °C and 5% CO<sub>2</sub>.

## 2.9 Uptake Efficiency and Cytotoxicity

For quantification of uptake efficiency and cytotoxicity, hMSCs were transfected with complexes containing Cy3<sup>TM</sup> dye-Labeled Pre-miR Negative Control #1 as described above (see 2.6, 2.8). After transfection, cultured or freshly isolated cells were washed with 1 M sodium chloride (NaCl) solution for 5 minutes and centrifuged at 300 g for 10 minutes at 4 °C. Supernatant was discarded and the cell pellet was resuspended in 100 µl MACS-buffer. To evaluate cytotoxicity, the cells were stained with Near-IR LIVE/DEAD<sup>®</sup> Fixable Dead Cell Stain Kit (Life Technologies). Therefor 0.5 µl dye was mixed with the cell suspension and incubated for 10 minutes at 4 °C in the dark. Additionally, freshly isolated cells were labeled with 10 µl Alexa Fluor 488 mouse anti-human CD105 (clone SN6, AbD Serotec). After incubation time, the cells were washed with 1 ml PBS and centrifuged at 300 g for 10 minutes at 4 °C. The cell pellet was resuspended in 100 µl PBS and fixed with 33 µl PFA (4%). 3x10<sup>4</sup> events were acquired using BD FACS LSRII<sup>TM</sup> flow cytometer (BD Biosciences) and analyzed with BD FACSDiva Software 6 (BD Biosciences). To determine the uptake efficiency and cytotoxicity of cultured hMSCs, the number of living Cy3<sup>+</sup> cells in relation to total living cells and the percentage of dead cells in relation to the total cell number were calculated, respectively. For freshly isolated cells, the uptake efficiency was evaluated by the number of living CD105<sup>+</sup> Cy3<sup>+</sup> cells in relation to living CD105<sup>+</sup> cells. To determine the cytotoxicity of transfection complexes, the percentage of dead CD105<sup>+</sup> cells in relation to total CD105<sup>+</sup> cells was calculated.

## 2.10 Intracellular Visualization of miR/PEI/MNP Transfection Complexes

### 2.10.1 Fluorescent Labeling of miR/PEI/MNP Transfection Complexes

Labeling of hsa-miR-335-5p Pre-miR<sup>TM</sup> miRNA Precursor was performed using LabelIT<sup>®</sup> miRNA Labeling Kit, Version 2 with Cy5<sup>TM</sup> (Mirus Bio LLC, Madison, USA). According to the manufacturer's protocol, 1 µg miR was mixed with 8 µl Label IT reagent and incubated for 2 hours at 37 °C in the dark. Unbound dye was removed using a purification column. Labeled miR-Cy5 solution was stored at -20 °C.

Staining of PEI was carried out using the FluoReporter<sup>®</sup> Oregon Green<sup>®</sup> 488 Protein Labeling Kit (Life Technologies). Therefor 650 µl PEI were mixed with 65 µl sodium bicarbonate

solution (1 M). Subsequently, 25  $\mu$ l Oregon Green<sup>®</sup> solution (10 mg/mL in DMSO) was added to PEI solution and incubated for 1 hour in the dark. For efficient purification of unreacted dye, the PEI-488 solution was loaded onto a spin column and centrifuged at 1,100 g for 5 minutes. Labeled PEI-488 solution was stored at 4 °C.

Labeling of MNPs was performed with Atto 565 dye conjugated to biotin during miR/PEI/MNP complex formation. Therefore MNPs and Atto 565 at a ratio of 1:1,000 (w/w) were mixed with miR/PEI complexes simultaneously. miR/PEI/MNP-565 complexes were incubated for 30 minutes in the dark. Labeling of MNPs was freshly performed before each transfection.

Images of labeled complexes were acquired using structured illumination microscopy (SIM) mode of an ELYRA PS.1 LSM 780 microscope (Carl Zeiss) with Plan-Apochromat 63x objective (1.4 numerical aperture) and analyzed with ZEN 2011 Software (Carl Zeiss).

### 2.10.2 Confocal Laser Scanning Microscopy

For intracellular visualization of miR/PEI/MNP complexes,  $1.5 \times 10^4$  cultured hMSCs were seeded on sterilized glass coverslips placed in a 24-well plate with 1 ml MSCGM<sup>™</sup> on day before transfection. For transfection, labeled miR-Cy5/PEI-488 and miR-Cy5/PEI-488/MNP-565 complexes composed of an NP ratio of 10 combined with 5 pmol/cm<sup>2</sup> miR and 1  $\mu$ g/ml iron in MNPs were used. After 72 hours incubation time, the cells were washed with 1 ml NaCl solution (1 M) for 1 minute. Then, the cells were fixed with 500  $\mu$ l PFA solution (4%) for 20 minutes at room temperature. After washing with 1 ml PBS, nuclei were stained with 300  $\mu$ l DAPI (250 nM) in the dark for 15 minutes at room temperature. Coverslips were washed three times with 1 ml PBS on the shaker and were mounted with FluorSave<sup>™</sup> on a microscope slide. Images were acquired using confocal laser scanning microscopy (LSM) mode of an ELYRA PS.1 LSM 780 microscope (Carl Zeiss) with Plan-Apochromat 63x objective (1.4 numerical aperture) and analyzed with ZEN 2011 Software (Carl Zeiss).

## 2.11 Real-Time PCR

For real-time polymerase chain reaction (PCR),  $1 \times 10^5$  cultured hMSCs per well and  $5 \times 10^5$  freshly isolated hMSCs per well were seeded in a 6-well plate with 4 ml MSCGM™ and a 12-well plate with 2 ml MSCGM™, respectively. Cells were transfected with miR, miR/PEI or miR/PEI/MNP complexes containing hsa-miR-335-5p Pre-miR™ miRNA Precursor (Life Technologies) as described above (see 2.6.1.1, 2.6.1.2, 2.8).

### 2.11.1 RNA Isolation of Cultured hMSCs

Total RNA of cultured hMSCs was isolated using the mirVana™ miRNA Isolation Kit (Life Technologies) 5, 24 and 72 hours after transfection according to the manufacturer's protocol. Therefore, medium was removed and attached cells were washed with 1 ml PBS. Then, the cells were lysed with 500 µl Lysis/Binding Buffer and detached using a cell scraper (Sarstedt AG & Co., Nümbrecht, Germany). 50 µl miRNA Homogenate Additive was added to the lysed cells and incubation was performed for 10 minutes on ice. Next, 500 µl acid-phenol chloroform was added and the cell lysate was centrifuged at 10,000 g for 5 minutes. The upper aqueous phase was transferred into a new tube and mixed with 625 µl ethanol absolute. The solution was loaded onto a filter cartridge and centrifuged at 12,000 g for 30 seconds. Afterwards, the filter was washed once with 700 µl miRNA wash solution 1 and twice with 500 µl wash solution 2/3. Then, the filter was centrifuged for drying and transferred into a new collection tube. RNA was eluted using 100 µl of 95 °C pre-heated DNase/RNase free distilled water. Subsequently, RNA concentration was measured using NanoDrop 1000 spectrophotometer (Thermo Fisher Scientific).

### 2.11.2 RNA Isolation of Freshly Isolated hMSCs

Total RNA of fresh hMSCs was isolated using the mirVana™ miRNA Isolation Kit (Life Technologies) 72 hours after transfection according to the manufacturer's protocol. Therefore, suspension cells were centrifuged at 300 g for 10 minutes and washed with 1.5 ml PBS. After an additional centrifugation step, the cell pellet was resuspended in 500 µl Lysis/Binding Buffer. Further RNA isolation was performed as described above (see 2.11.1).

### 2.11.3 Real-Time PCR of miRs

Reverse transcription (RT) of miRs was performed using the TaqMan<sup>®</sup> MicroRNA Reverse Transcription Kit (Life Technologies). First, the RT master mix was prepared according to the manufacturer's instructions (Table 6). Next, 7  $\mu$ l RT master mix were mixed with 5  $\mu$ l RNA (10 ng) and 3  $\mu$ l 5x RT primer for hsa-miR-335-5p (Assay ID 000546), hsa-miR-16-5p (Assay ID 000391), hsa-miR-191-5p (Assay ID 002299) and RNU6B (Assay ID 001093). The mixture was incubated for 5 minutes on ice. RT was performed according to the manufacturer's protocol (Table 7) using a MJ Mini<sup>™</sup> Personal Thermal Cycler (BioRad Laboratories).

**Table 6: Preparation of RT Master Mix for RT of miRs**

Components	V [ $\mu$ l]
100 mM dNTP mix	0.15
MultiScribe <sup>™</sup> Reverse Transcriptase (50 U/ $\mu$ l)	1.00
10x Reverse Transcription Buffer	1.50
RNase Inhibitor (20 U/ $\mu$ l)	0.19
DNase/RNase free distilled water	4.16
<b>Total volume</b>	<b>7</b>

**Table 7: Program for RT of miRs**

Step	Time [minutes]	Temperature [ $^{\circ}$ C]
Hold	30	16
Hold	30	42
Hold	5	85
Hold	$\infty$	4

Real-time PCR was performed using TaqMan<sup>®</sup> MicroRNA Assays (Life Technologies) for human mature miR-335, miR-16, miR-191 and RNU6B. The PCR reaction mix was prepared according to the manufacturer's protocol (Table 8) using TaqMan<sup>®</sup> 2x Universal PCR Master Mix with AmpErase<sup>®</sup>UNG. Afterwards, real-time PCR was performed in a 96-well plate

according to the manufacturer's instructions (Table 9) using the StepOnePlus™ Real-Time PCR System (Life Technologies). For each TaqMan® MicroRNA Assay a no template control was used. All experiments were performed in triplicates.

**Table 8: Real-Time PCR Pipetting Scheme for miR Quantification**

Components	V [μl]
TaqMan® 2x Universal PCR Master Mix with UNG	10.00
nuclease free water	7.67
20x TaqMan® MicroRNA Assay	1.00
cDNA product from RT reaction	1.33
<b>Total volume</b>	<b>20</b>

**Table 9: Program for Real-Time PCR**

Step	Time [seconds]	Temperature [°C]
Hold	120	50
Hold	600	95
40 cycles	15	95
	60	60
Hold	∞	4

To calculate the relative expression ratio (R) the  $\Delta\Delta C_T$  (threshold cycle) method was used as described previously by Livak *et al* (Equation 2) [205]. Therefor miR-16, miR-191 and RNU6B were used as endogenous normalization controls and untransfected cells served as reference.

$$\Delta C_T = C_T \text{ target} - C_T \text{ endogenous control}$$

$$R = 2^{-(\Delta C_T \text{ sample} - \Delta C_T \text{ reference})}$$

**Equation 2: Calculation of the Relative Expression Ratio (R) using the  $\Delta\Delta C_T$  Method.**



### 2.11.4 Real-Time PCR of Target Genes

RT of target genes was performed using the High Capacity cDNA Reverse Transcription Kit with RNase Inhibitor (Life Technologies). At first, 2x RT master mix was prepared according to the manufacturer's protocol (Table 10). Then, 10  $\mu$ l 2x RT master mix were combined with 10  $\mu$ l RNA (400 ng). RT was performed according to the manufacturer's protocol (Table 11) using a MJ Mini™ Personal Thermal Cycler (BioRad Laboratories).

**Table 10: Preparation of 2x RT Master Mix for RT of Target Genes**

Components	V [ $\mu$ l]
100 mM 25x dNTP mix	0.8
MultiScribe™ Reverse Transcriptase (50 U/ $\mu$ l)	1.0
10x RT Buffer	2.0
RNase Inhibitor (20 U/ $\mu$ l)	1.0
DNase/RNase free distilled water	3.2
10x RT Random Primers	2.0
<b>Total volume</b>	<b>10.0</b>

**Table 11: Program for RT of Target Genes**

Step	Time [minutes]	Temperature [°C]
Hold	10	25
Hold	120	37
Hold	5	85
Hold	$\infty$	4

Real-time PCR was performed using TaqMan® Gene Expression Assays (Life Technologies) for TNC (Assay ID Hs01115665\_m1), RUNX2 (Assay ID Hs00231692\_m1) and Human GAPDH as Endogenous Control (Assay ID Hs99999905\_m1). The PCR reaction mix was prepared according to the manufacturer's protocol (Table 12). Real-time PCR was performed in 96-well plates using the StepOnePlus™ Real-Time PCR System (Life Technologies, Table 9). For each TaqMan® Gene Expression Assay a no template control was used. All

experiments were performed in triplicates. To quantify gene expression values of target genes the  $\Delta\Delta C_t$  method was used (Equation 2). Therefor Human GAPD Endogenous Control was used as endogenous normalization control for protein coding genes. Untransfected cells were used as reference.

**Table 12: Real-Time PCR Pipetting Scheme for Target Gene Quantification**

Components	V [ $\mu$ l]
TaqMan <sup>®</sup> 2x Universal PCR Master Mix with UNG	10.0
nuclease free water	5.0
20x TaqMan <sup>®</sup> Gene Expression Assay	1.0
cDNA product from RT reaction (20 ng)	4.0
<b>Total volume</b>	<b>20</b>

## 2.12 Migration Assay

For functional analysis,  $4 \times 10^5$  cultured hMSCs per well were seeded in a 24-well plate with 1 ml MSCGM<sup>™</sup> and transfected with miR/PEI/MNP complexes composed of an NP ratio of 10 combined with 5 pmol/cm<sup>2</sup> miR (hsa-miR-335-5p Pre-miR<sup>™</sup> miRNA Precursor, Pre-miR<sup>™</sup> miRNA Precursor Molecules - Negative Control #1) and 1  $\mu$ g/ml iron in MNPs as described above (see 2.6.1.2, 2.8). 24 hours after transfection, the cells were washed with 500  $\mu$ l NaCl solution (1 M) for 1 minute and twice with 500  $\mu$ l PBS for 30 seconds. Afterwards, fresh medium was added and a scratch was created using a sterile plastic tip. Live cell imaging was performed by sequential acquisition of images every 3 minutes using an ELYRA PS.1 LSM 780 microscope (Carl Zeiss) for 12 hours at 37 °C and 5% CO<sub>2</sub>. At the beginning and at the end of the experiment, the overgrown surface area was determined with ZEN 2011 Software (Carl Zeiss).

### 2.13 Magnetic Targeting of MNPs

For magnetic targeting, MNP solution was vortexed properly and sonicated for 15 minutes. Afterwards, one drop of the MNP solution was pipetted onto a coverslip and a neodymium-iron-boron magnet (1,080–1,120 mT; IBS Magnet, Berlin, Germany) was applied for 10 minutes. The influence on the MNP behavior in the presence or absence of a magnetic field was investigated using an Axiovert 40 CFL microscope (Carl Zeiss).

### 2.14 *In Vitro* Magnetic Targeting of hMSCs

For *in vitro* targeting of cells,  $3 \times 10^4$  cultured hMSCs per well and  $5 \times 10^5$  freshly isolated hMSCs per well were seeded in a 12-well plate with 2 ml MSCGM™. After 24 hours incubation time, the cells were transfected with miR/PEI and miR/PEI/MNP complexes composed of an NP ratio of 10 combined with 5 pmol/cm<sup>2</sup> miR (Pre-miR™ miRNA Precursor Molecules - Negative Control #1) and 1 µg/ml iron in MNPs as described above (see 2.6.1.2, 2.8). 24 hours after transfection, the cells were detached with 1 ml trypsin/EDTA and centrifuged at 300 g for 10 minutes at 4 °C. The cell pellet was resuspended in 2 ml MSCGM™ and seeded in a 12-well plate with or without the application of a neodymium-iron-boron magnet (1,080–1,120 mT; IBS Magnet). After 4 hours incubation time, images were acquired using an Axiovert 40 CFL microscope (Carl Zeiss).

### 2.15 Statistical Analysis

For all experiments the Student's t-test was performed using SigmaPlot® 11.0 software (Systat Software GmbH, Erkrath, Germany). Relative expression data of CD markers and particle size data are shown as mean ± standard deviation (SD). All other values are presented as mean ± standard error of the mean (SEM). A *p*-value < 0.05 was considered to be statistically significant.

### 3 Results

#### 3.1 Characterization of Freshly Isolated and Expanded CD105<sup>+</sup> hMSCs

##### 3.1.1 Evaluation of Cell Morphology

Bone marrow derived CD105<sup>+</sup> hMSCs were characterized regarding their cell morphology (Figure 4), multilineage differentiation (Figure 5) and surface marker expression (Figure 6) before use in further experiments. Immediately after MACS isolation of CD105<sup>+</sup> cells, freshly isolated hMSCs showed a small and rounded morphology comparable to typical suspension cells (Figure 4 A). After 20 days under common culture conditions, cells attached to the surface of the culture flask thereby increasing in size. Expanded hMSCs formed fibroblast-like structures with irregularly formed cell extensions (Figure 4 B).

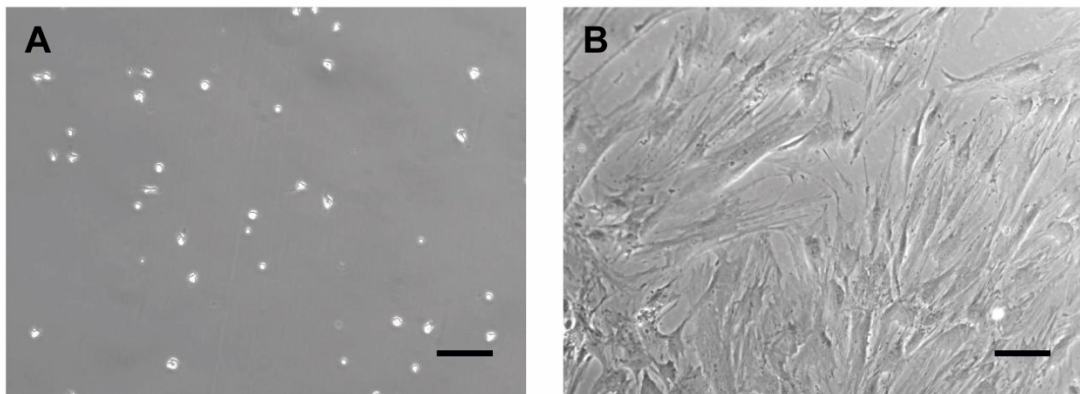


**Figure 4: Cell Morphology of Freshly Isolated (A) and Expanded hMSCs (B).** Scale bar = 10  $\mu\text{m}$ .

### 3.1.2 Determination of Differentiation Capacity

Subsequently, the differentiation capacity of freshly isolated and cultivated hMSCs was investigated (Figure 5). Therefore cells were cultured in adipogenic or osteogenic differentiation medium and examined by fluorescent microscopy. Figure 5 demonstrates that both freshly isolated and expanded hMSCs were able to differentiate into adipocytes (Figure 5 A,C) and osteocytes (Figure 5 B,D), respectively.

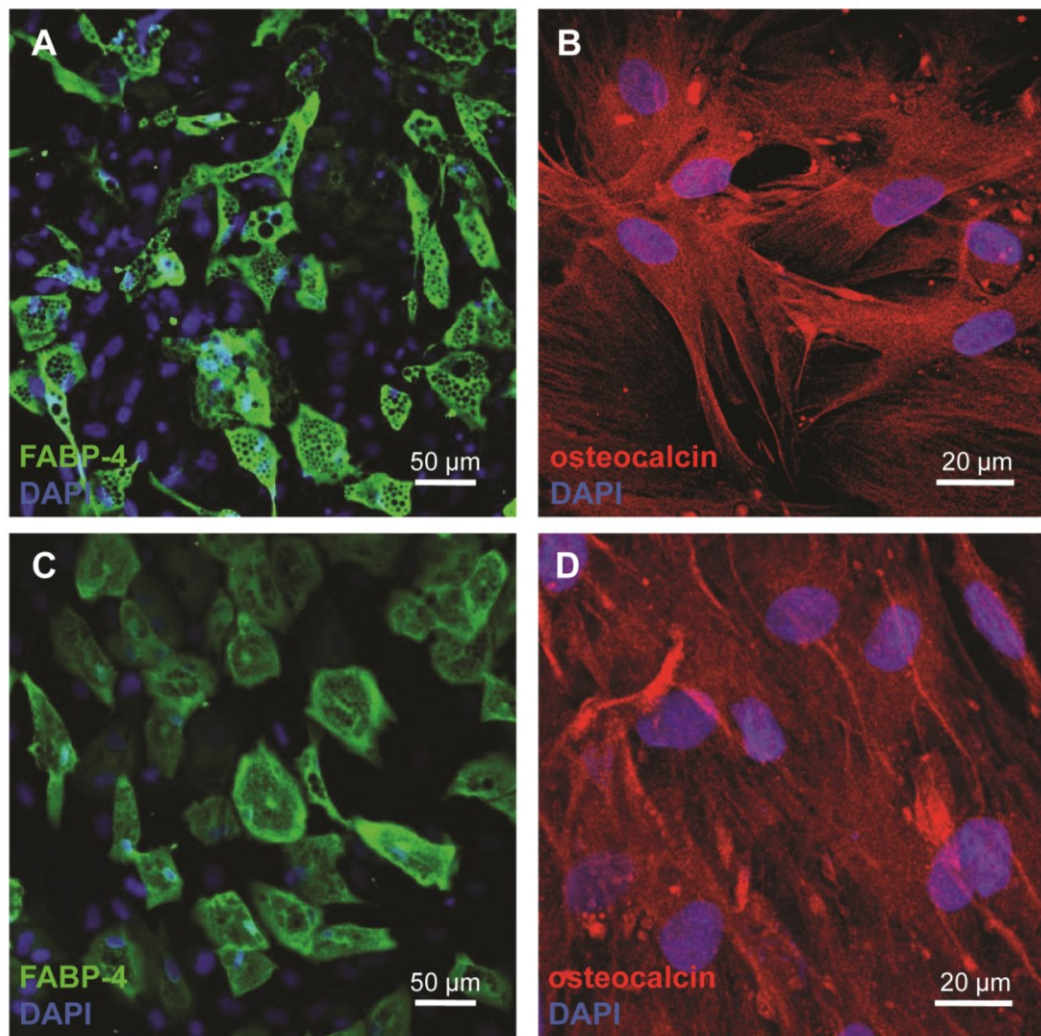
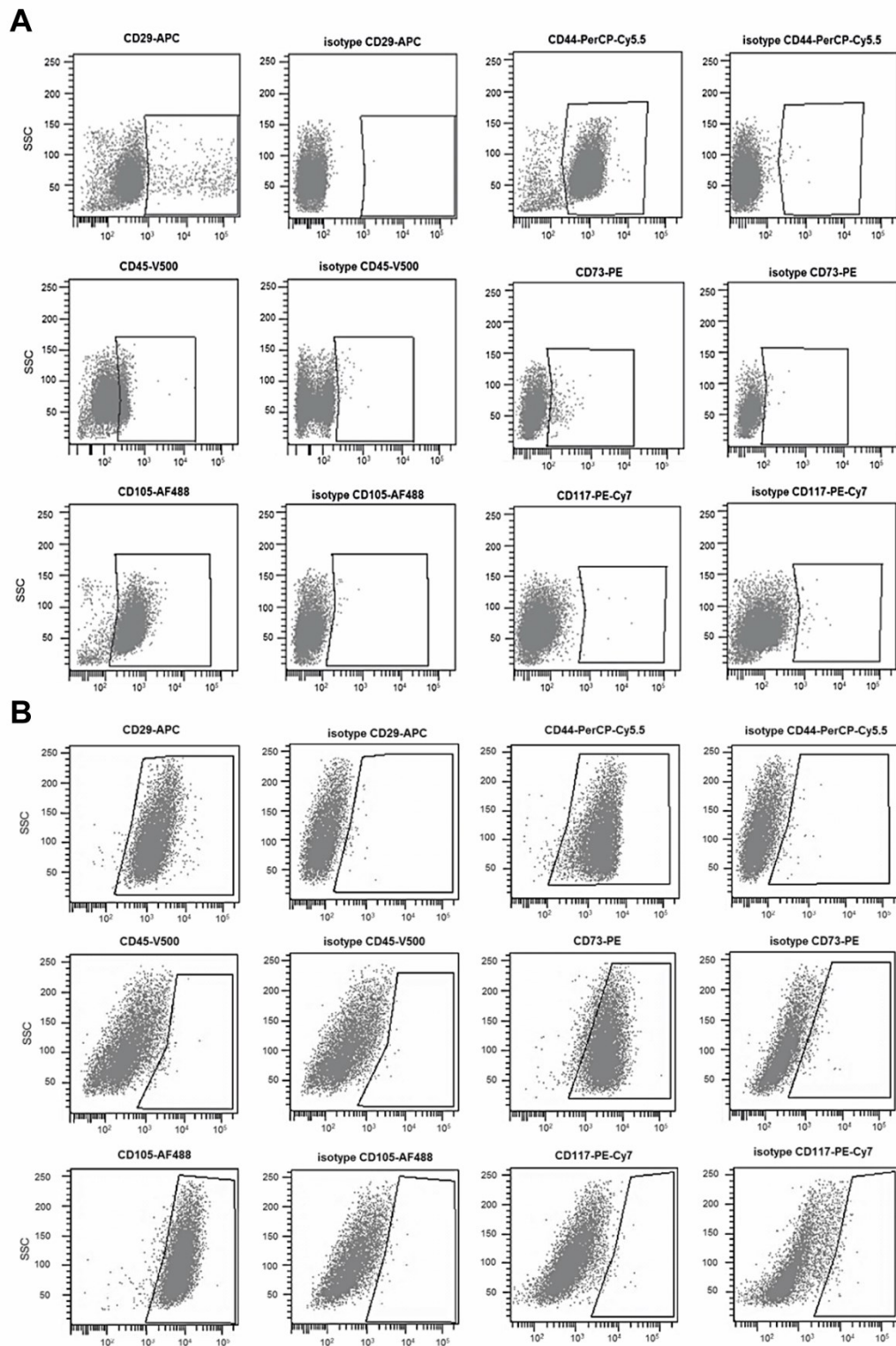


**Figure 5: Differentiation Capacity of hMSCs.** Functional differentiation of freshly isolated (A,B) and cultured hMSCs (C,D) was shown by immunostaining of FABP-4 (green) for adipocytes (A,C) and osteocalcin (red) for osteocytes (B,D) after 20 days under differentiation conditions. Nuclei were counterstained with DAPI (blue). Scale bar for adipocytes = 50 μm; Scale bar for osteocytes = 20 μm (A is taken from [206, 207], C and D are taken from [201, 208]).

### 3.1.3 Evaluation of the hMSC-Immunophenotype

To determine the surface marker expression of hMSCs, freshly isolated and cultured cells were analyzed by flow cytometry (Figure 6). Freshly isolated CD105<sup>+</sup> cells were highly positive for the surface markers CD44 and CD105. They had low expression values of CD29 and CD45 and no detectable expression of CD73 and CD117 (Figure 6 A,C). In contrast, the immunophenotype of cultivated CD105<sup>+</sup> hMSCs showed high expression of stem cell markers CD29, CD44, CD73 and CD105, but the cells were negative for the expression of hematopoietic markers CD45 and CD117 (Figure 6 B,C).



**C**

	CD29	CD44	CD45	CD73	CD105	CD117
<b>Fresh hMSCs</b>	4.8% ± 2.4	93.8% ± 1.3	23.8% ± 0.6	1.4% ± 0.9	93.0% ± 4.6	0.1% ± 0.1
<b>Cultured hMSCs</b>	99.6% ± 0.4	99.7% ± 0.3	0.5% ± 0.5	97.5% ± 3.3	98.5% ± 0.4	0.2% ± 0.2

**Figure 6: Immunophenotyping of hMSCs.** Immunophenotyping of freshly isolated (A,C) and cultured hMSCs (B,C) was investigated by flow cytometry after staining of specific CD surface markers. Appropriate isotype controls were used. CD marker expression values are represented as mean  $\pm$  SD; n = 2 (C). (A and C are taken from [206, 207], B is taken from [207]).

## 3.2 Optimization of Transfection Complexes in Cultured hMSCs

### 3.2.1 Optimization of miR Amounts

In order to optimize transfection efficiencies in cultivated hMSCs, miR/PEI and miR/PEI/MNP complexes with different miR amounts (2.5 to 15 pmol/cm<sup>2</sup> miR) consisting of an NP ratio of 10 were tested using flow cytometry (Figure 7). Transfection complexes composed of 2.5 pmol/cm<sup>2</sup> miR showed no significant differences in uptake rates (ranging from 27% to 11%) when compared to miR transfection (46%, Figure 7 A). After transfection with 5 pmol/cm<sup>2</sup> miR, miR/PEI and miR/PEI/MNP complexes showed the highest uptake rates (ranging from 78% to 71%) and were moderately increased compared to transfection with miR alone (62%). Interestingly, a further increase in miR amounts (15 pmol/cm<sup>2</sup> miR) did not lead to further enhancement of uptake rates using miR/PEI and miR/PEI/MNP complexes, respectively.

Additionally, the cytotoxicity of different complex compositions was investigated (Figure 7 B). miR/PEI and miR/PEI/MNP complexes composed of 2.5 pmol/cm<sup>2</sup> miR combined with 1  $\mu$ g/ml iron in MNPs (~ 11%) showed no cytotoxic effect compared to transfection with miR only (9%). Magnetic polyplexes consisting of higher MNP concentrations (2  $\mu$ g/ml iron in MNPs) significantly increased cell mortality about 5% compared to miR transfection. Cytotoxicity of transfection complexes with 5 pmol/cm<sup>2</sup> miR (~ 15%) was moderately increased compared to transfection with miR alone (8%). Moreover, cell mortality was further enhanced after transfection with miR/PEI and miR/PEI/MNP complexes composed of 15 pmol/cm<sup>2</sup> miR reaching highest values under these conditions (~ 25%). Considering the highest uptake rates and moderate cell mortality, transfection complexes composed of 5 pmol/cm<sup>2</sup> miR were used in further optimization experiments.



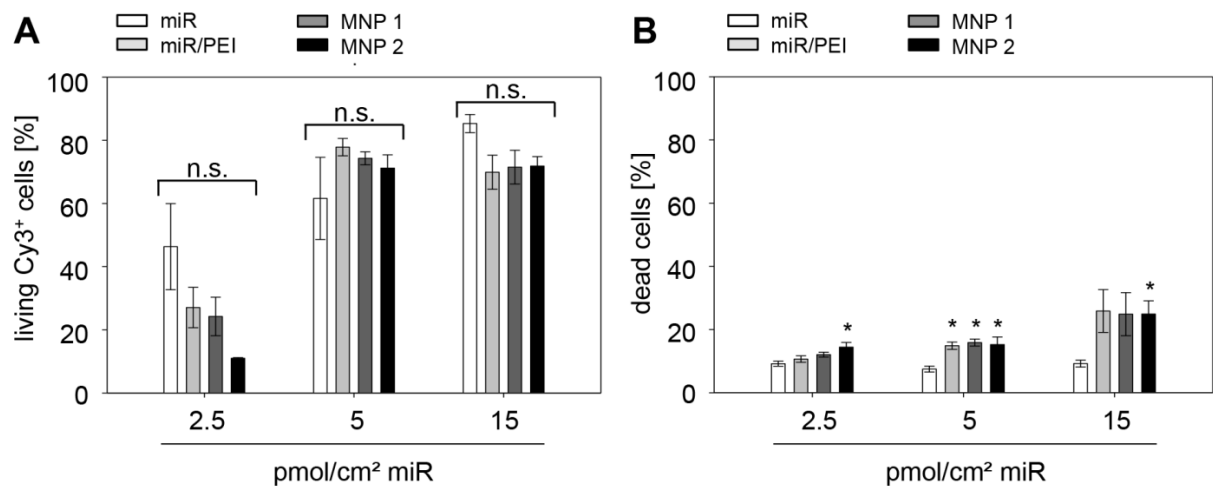


**Figure 7: Transfection Optimization of miR Amounts in Cultured hMSCs.** Uptake efficiency (A) and cytotoxicity (B) of Cy3<sup>TM</sup> labeled miR, miR/PEI or miR/PEI/MNP complexes were determined by flow cytometry 5 hours post transfection. Transfection complexes were composed of various miR amounts (2.5, 5, 15 pmol/cm<sup>2</sup> miR) combined with an NP ratio of 10 coupled to 1 or 2 µg/ml iron in MNPs (MNP 1, MNP 2). Data are represented as mean ± SEM, n = 3, \*  $p \leq 0.05$  vs miR, n.s. = no significant difference. (A and B are adopted from [201, 208]).

### 3.2.2 Optimization of PEI Amounts

In order to increase transfection performance in expanded hMSCs, miR/PEI complexes with different NP ratios were tested using flow cytometry (Figure 8). Therefor the miR amount (5 pmol/cm<sup>2</sup> miR) was kept constant. miR/PEI complexes with low NP ratios (NP ratio 1 to 5) resulted in decreased transfection efficiencies (< 20%) compared to miR transfection (~ 48%, Figure 8 A). Polyplexes with an NP ratio of 10 (77%) and 33 (70%) showed the highest uptake rates. To further enhance the uptake efficiency, a higher NP ratio was investigated. However, after transfection with an NP ratio of 50, uptake efficiencies were significantly decreased to 2%.

Moreover, cytotoxicity of the transfection complexes was examined (Figure 8 B). Polyplexes with NP ratios from 1 to 10 (ranging from 9% to 18%) showed no significant differences compared to transfection with miR only (7%). miR/PEI complexes with an NP ratio of 33 moderately increased cell mortality (28%) compared to miR transfection. However, an increase in the NP ratio (NP ratio 50) led to the highest cytotoxicity value (96%). Thus, with respect to highest uptake rates combined with lowest cytotoxicity, polyplexes composed of an

NP ratio of 10 and 33 were considered to represent optimal polyplex compositions and were utilized in further experiments. Moreover, regarding previous findings with plasmid DNA [202], miR/PEI complexes with an NP ratio of 2.5 were further investigated.

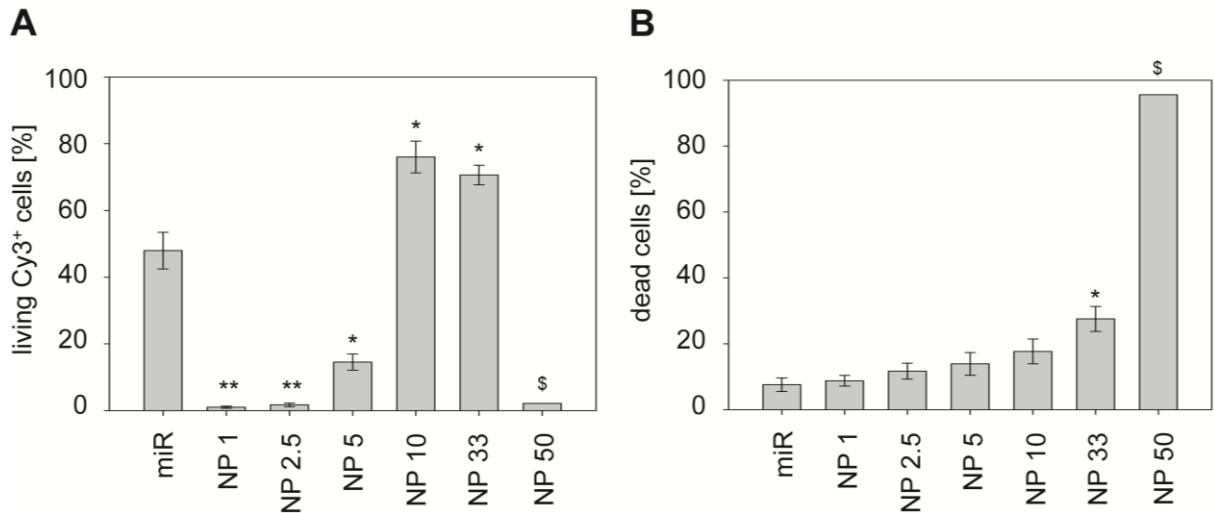


**Figure 8: Transfection Optimization of PEI Amounts in Cultured hMSCs.** Uptake efficiency (A) and cytotoxicity (B) of Cy3<sup>TM</sup> labeled miR/PEI complexes were evaluated by flow cytometry 5 hours after transfection. Polyplexes were composed of various NP ratios (ranging from NP 1 to NP 50) combined with 5 pmol/cm<sup>2</sup> miR. Cells transfected with miR alone were used as control. Data are presented as mean  $\pm$  SEM, \*  $p \leq 0.05$  vs miR, \*\*  $p \leq 0.001$  vs miR. For transfection with miR alone and polyplexes composed of NP ratios from 1 to 33, experiments were repeated 3 times ( $n = 3$ ). For polyplexes consisting of an NP ratio of 33, the experiment was performed once ( $n = 1$ ) as cytotoxicity reached approximately 100% which is in correspondence with previous publications [209, 210].

### 3.2.3 Optimization of MNP Amounts

To enhance selectivity of the transfections complexes as well as safety for clinical applications, miR/PEI complexes composed of the optimized miR amount (5 pmol/cm<sup>2</sup> miR) and the preselected NP ratios (NP ratio 2.5, NP ratio 10, NP ratio 33) were combined with different MNP amounts (from 1 to 6  $\mu$ g/ml iron in MNPs). Transfection complexes consisting of an NP ratio of 2.5 resulted in the lowest uptake efficiencies ( $\sim 1\%$ , Figure 9 A). In contrast, miR/PEI and miR/PEI/MNP complexes with an NP ratio of 10 showed the highest uptake rates compared to miR transfection (48%). The uptake rates of miR/PEI (76%) and miR/PEI/MNP complexes composed of 1 to 2  $\mu$ g/ml iron in MNPs (ranging from 75% to

79%) were significantly enhanced compared to transfection with miR alone. However, magnetic polyplexes consisting of higher MNP concentrations (4 and 6  $\mu\text{g/ml}$  iron in MNPs) led to a decrease in uptake efficiencies (66% and 62%, respectively) and no significant differences compared to miR transfection were observed. The uptake rates at an NP ratio of 33 were significantly increased after transfection with miR/PEI (71%) and miR/PEI/MNP complexes composed of 1 to 4  $\mu\text{g/ml}$  iron in MNPs (ranging from 67% to 70%). However, no significant difference was observed after transfection with miR/PEI/MNP complexes consisting of 6  $\mu\text{g/ml}$  iron in MNPs (64%) compared to miR transfection.

Furthermore, cell mortality of different transfection complexes was investigated (Figure 9 B). miR/PEI and miR/PEI/MNP complexes composed of an NP ratio of 2.5 (~ 14%) and 10 (ranging from 16% to 19%) showed no cytotoxic effect when compared to miR transfection (7%). However, complexes with an NP ratio of 33 appeared to be toxic for the cells (ranging from 24% to 27%). Therefore, with respect to the highest uptake efficiencies accompanied by good cell viability, transfection complexes composed of an NP ratio of 10 with 5  $\text{pmol/cm}^2$  miR combined with 1 or 2  $\mu\text{g/ml}$  iron in MNPs were selected as optimal conditions for efficient and safe miR delivery in cultured hMSCs.

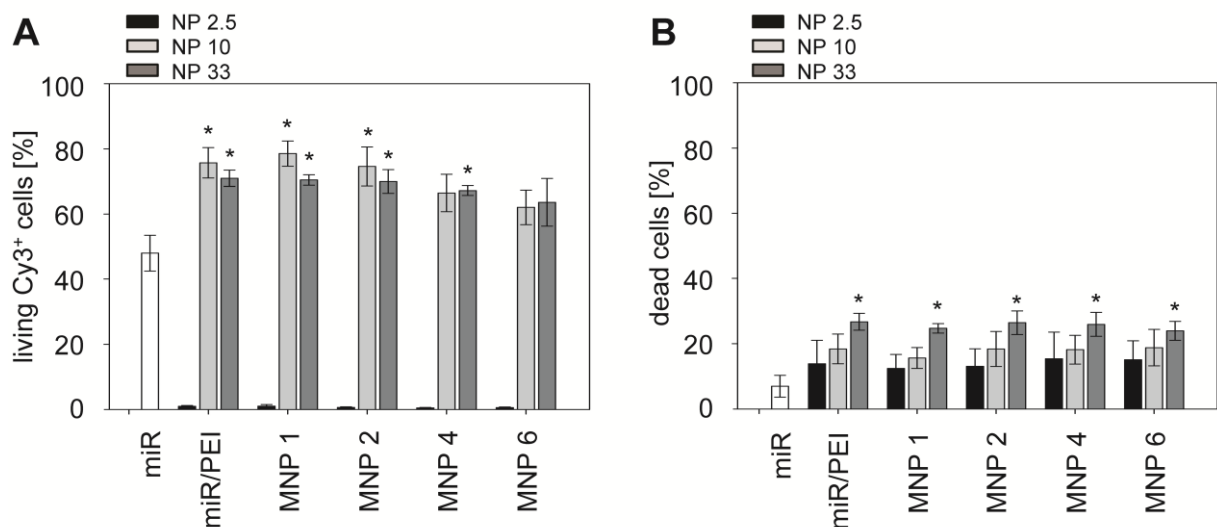


**Figure 9: Transfection Optimization of MNP Amounts in Cultured hMSCs.** Uptake efficiency (A) and cytotoxicity (B) of Cy3<sup>TM</sup> labeled miR/PEI and miR/PEI/MNP complexes were investigated by flow cytometry after 5 hours incubation time. Transfection complexes were composed of various NP ratios (NP 2.5, NP 10, NP 33) combined with 5  $\text{pmol/cm}^2$  miR coupled to different MNP concentrations ranging from 1 to 6  $\mu\text{g/ml}$  iron in MNPs (MNP 1 to MNP 6). miR transfection was used as reference. Values are represented as mean  $\pm$  SEM,  $n = 3$ , \*  $p \leq 0.05$  vs miR. (A and B are taken from [201, 208]).

### 3.3 Characterization of Transfection Complexes

#### 3.3.1 Condensation Assay

Condensation of miR by PEI was investigated using gel electrophoresis (Figure 10 A). miR without PEI showed a strong and distinct main band which was used as reference. At an NP ratio of 0.25 this band disappeared and the complexes migrated slower in the gel. Starting at an NP ratio of 0.5, the miR signal in the gel disappeared entirely and miR/PEI complexes remained in the slots.

#### 3.3.2 Determination of Particle Size and Zeta Potential

MNPs, miR/PEI and miR/PEI/MNP complexes were characterized regarding their surface charge using PALS (Figure 10 B). MNPs alone were negatively charged (-17.0 mV). In contrast, miR/PEI complexes had a strong positive surface charge (+41.6 mV). The surface charge of miR/PEI/MNP complexes composed of 1  $\mu\text{g/ml}$  iron in MNPs was slightly decreased to +32.8mV compared to polyplexes alone. However, magnetic polyplexes with higher MNP amounts (from 2 to 6  $\mu\text{g/ml}$  iron in MNPs) had significantly decreased surface charges (ranging from +15.6 to +7.7 mV) compared to miR/PEI complexes.

Particle size of MNPs, miR/PEI and miR/PEI/MNP complexes was determined by DLS (Figure 10 C). Both, MNPs and miR/PEI complexes had effective diameters around 100 nm. Moreover, particle size of miR/PEI/MNP complexes with 1 to 6  $\mu\text{g/ml}$  iron in MNPs was increased and ranged between 150 to 200 nm.

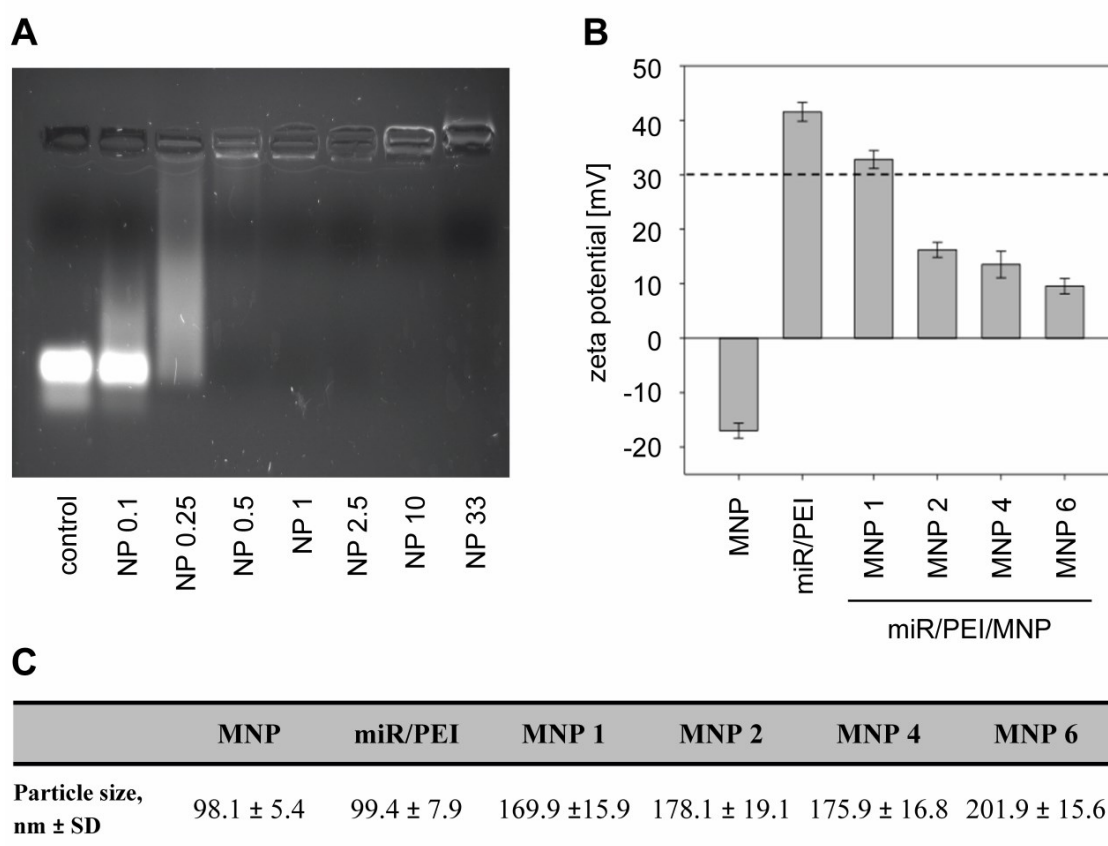


**Figure 10: Classification of Transfection Complexes.** (A) Condensation behavior of miR by PEI was investigated using gel electrophoresis. Polyplexes were composed of several NP ratios (ranging from NP 0.1 to NP 33) and 20 pmol miR. The miR band served as positive control. (B,C) Zeta potential (B) and particle size (C) of MNPs, miR/PEI and miR/PEI/MNP complexes were evaluated by PALS and DLS. Transfection complexes were composed of an NP ratio of 10 combined with 20 pmol miR coupled to various MNP concentrations ranging from 1 to 6  $\mu\text{g/ml}$  iron in MNPs (MNP 1 to MNP 6). Zeta potential values are represented as mean  $\pm$  SEM,  $n = 10$ . Particle size data are shown as mean  $\pm$  SD,  $n = 10$ . (A, B and C are taken from [201], A is taken from [208]).

### **3.4 Evaluation of miR Processing in Cultured hMSCs over Time**

#### **3.4.1 Investigation of Mature miR Expression Levels**

Cultivated hMSCs were transfected with miR, miR/PEI and miR/PEI/MNP complexes and the expression level of mature miR-335 was quantified by real-time PCR (Figure 11). Initially, different potential endogenous normalization controls were tested 5 hours after transfection (Figure 11 A). Results indicated no significant differences in miR-335 levels when miR-16, miR191 or RNU-6B were used as internal normalization controls.

Moreover, the processing of pre-miR into mature miR-335 was monitored 5, 24 and 72 hours post transfection, respectively (Figure 11 B). 5 hours after transfection, the level of miR-335 was increased about 10-fold after transfection with miR only. A significant increase of miR-335 levels (about 10-fold) was observed after transfection with miR/PEI or miR/PEI/MNP complexes compared to miR only transfection. Furthermore, in the latter case the miR-335 expression level was decreased, equaling that of untransfected cells after 24 hours. Moreover, cells transfected with miR/PEI and miR/PEI/MNP complexes reached highest values and showed a more than 1,000-fold enhancement compared to cells treated with miR alone. After 72 hours incubation time, miR-335 expression remained at a constant level after transfection with miR/PEI/MNP complexes. However, after transfection with miR/PEI complexes, miR-335 values were decreased about 3-fold compared to MNP-mediated transfection.

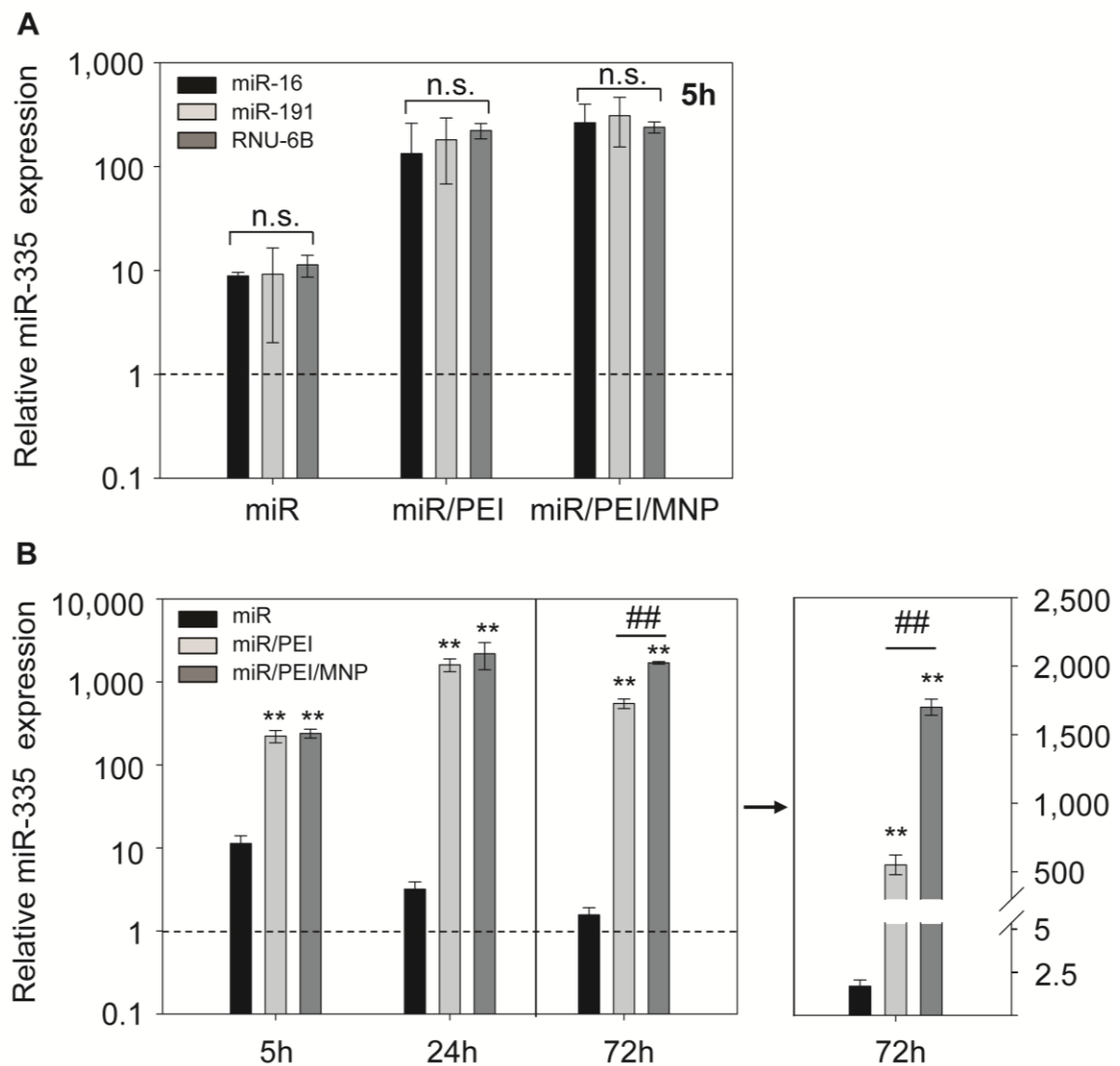


**Figure 11: Monitoring of pre-miR-335 Processing in Cultured hMSCs.** (A) hMSCs were transfected with optimized transfection complexes and the level of the mature miR-335 strand was detected by real-time PCR 5 hours after transfection with respect to different endogenous normalization controls (miR-16, miR-191, RNU-6B). (B) Processing of pre-miR-335 into mature miR-335 after transfection with miR/PEI or miR/PEI/MNP complexes was examined by real-time PCR after 5, 24 and 72 hours incubation time. hMSCs transfected with miR alone served as control. The miR-335 expression level in untransfected cells is indicated by a dashed line. Right plot demonstrates a linear representation of the relative miR-335 expression 72 hours after transfection. RNU-6B was used as normalization control. Data are represented as mean  $\pm$  SEM,  $n = 5$ , \*\*  $p \leq 0.001$  vs miR, ##  $p \leq 0.001$  vs PEI-mediated transfection, n.s. = no significant difference. (B is taken from [201]).

### 3.4.2 Microscopic Observations of Transfection Complexes

Initially, the quality of 3-color labeling of miR/PEI/MNP complexes was investigated using SIM (Figure 12). After investigating the single channels, visual co-localization of miR together with PEI and MNPs was observed.

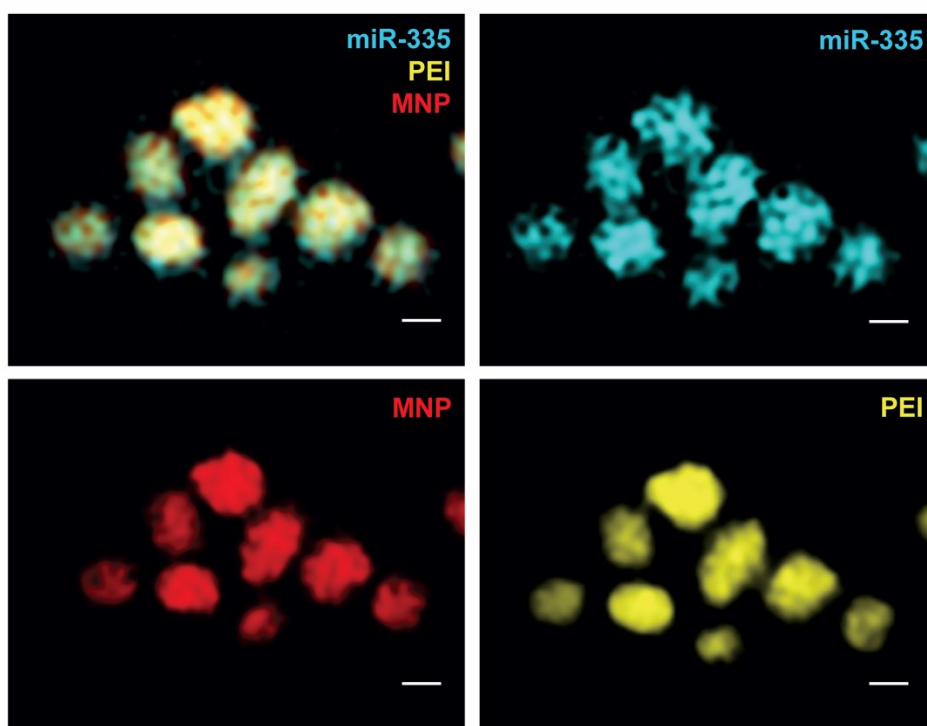


**Figure 12: Visualization of Transfection Complexes.** miR/PEI/MNP complexes were fluorescently labeled and visualized using SIM. Staining of miR-335 was performed using Cy5™ dye (cyan). PEI was labeled with Oregon Green® 488 (yellow) and MNP staining was done with Atto 565 (red). Scale bar = 0.25  $\mu\text{m}$ .

Furthermore, labeled miR/PEI/MNP complexes were visualized inside the cell 72 hours post transfection using confocal LSM and were compared to PEI-mediated transfection. Figure 13 A demonstrates that condensed miR/PEI complexes were distributed inside the cytoplasm but also inside the nucleus. In contrast, magnetic polyplexes were randomly distributed exclusively in the cytoplasm but did not enter the nucleus (Figure 13 B).



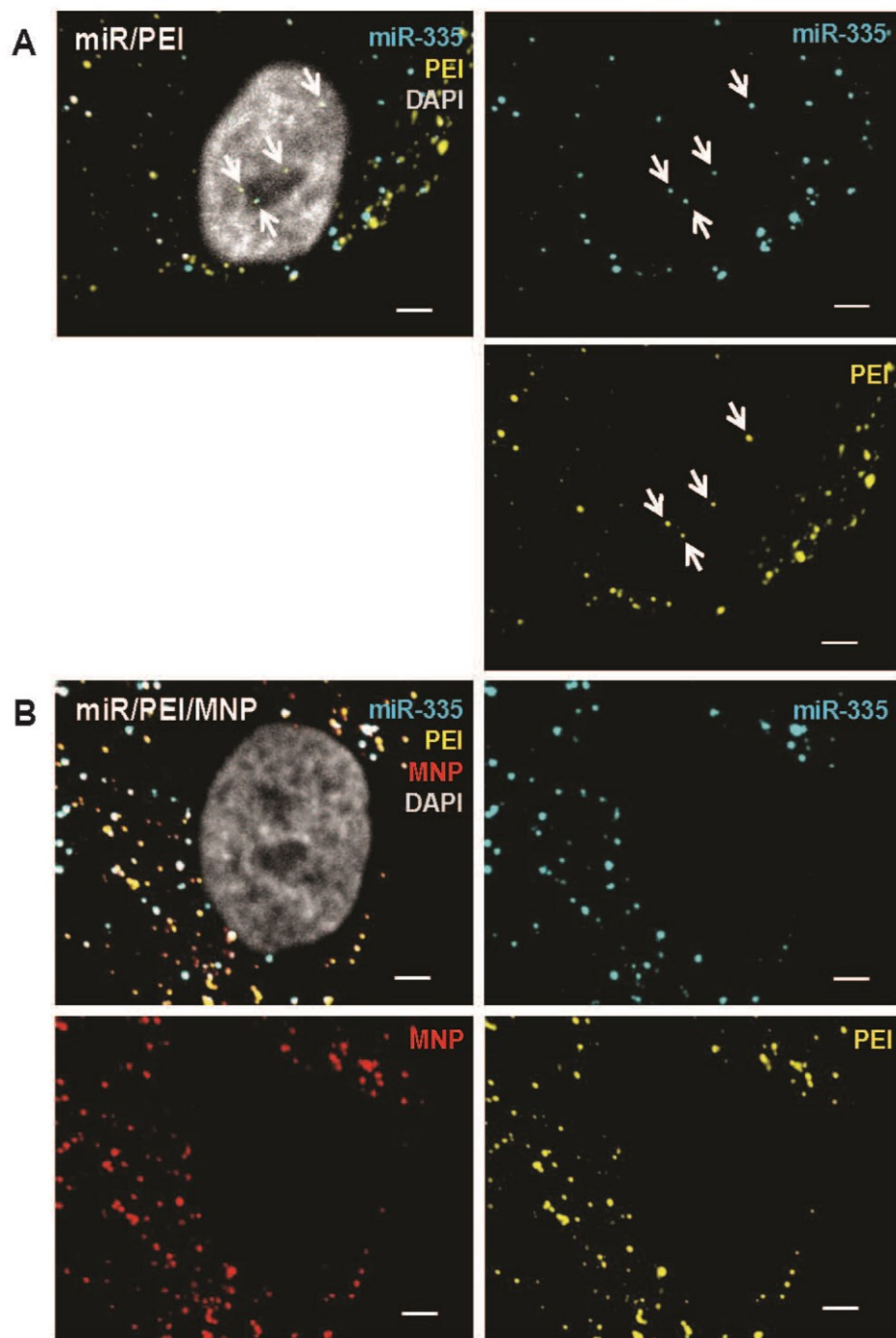


**Figure 13: Intracellular Visualization of Transfection Complexes in Cultured hMSCs.** hMSCs were transfected with fluorescently labeled miR/PEI (A) or miR/PEI/MNP complexes (B) and observed by confocal LSM 72 hours after transfection. miR-335 staining was performed with Cy5™ dye (cyan). PEI was labeled with Oregon Green® 488 (yellow). MNPs were stained with Atto 565 (red). Nuclei were counterstained with DAPI (gray). The arrows show condensed polyplexes inside the nucleus. Scale bar = 5  $\mu$ m. (A and B are taken from [201]).

### 3.4.3 Evaluation of Target Genes Expression

Expanded hMSCs were transfected with miR, miR/PEI or miR/PEI/MNP complexes and the expression levels of miR-335 target genes TNC and RUNX2 were detected 5, 24 and 72 hours post transfection by real-time PCR (Figure 14). Transfection with miR-335 alone did not lead to an efficient knockdown of the investigated target genes compared to untransfected cells over time. However, 24 hours after transfection with both miR/PEI and miR/PEI/MNP complexes, a significant knockdown of TNC (65% vs 61%) and RUNX2 (56% vs 60%) was observed when compared to control. 72 hours after polyplex transfection, the expression of TNC remained at the same level, while the RUNX2 expression level rose to 62%. In contrast, after MNP-mediated transfection the mRNA levels of TNC and RUNX2 were further down-regulated to 41% and 52%, respectively, compared to untransfected cells and were significantly reduced compared to PEI-mediated transfection.

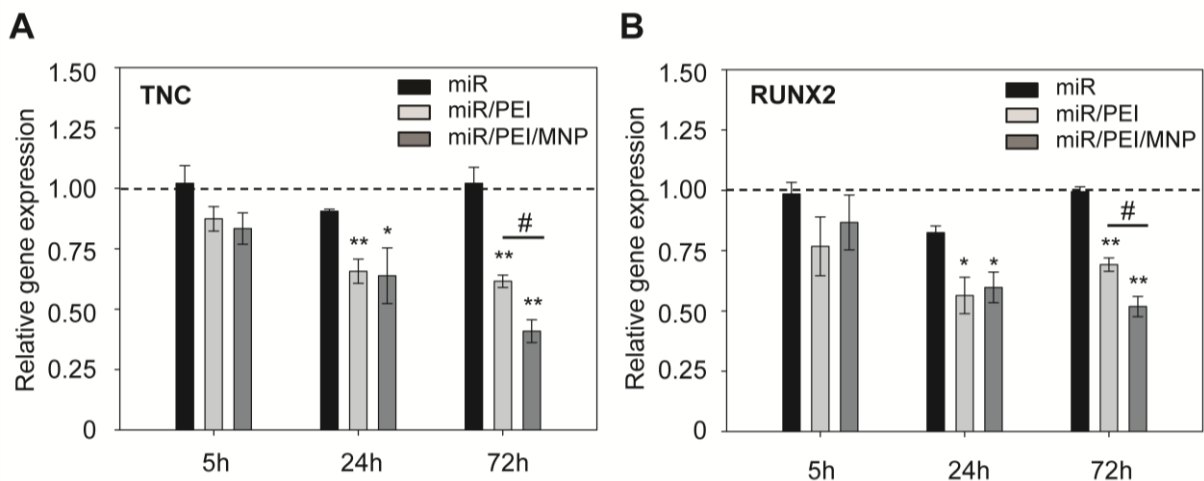


**Figure 14: Gene Knockdown of TNC and RUNX2 after miR-335 Transfection in Cultured hMSCs.** After transfection with optimized transfection complexes, relative gene expression of TNC (A) and RUNX2 (B) was determined by real-time PCR 5, 24 and 72 hours after transfection. miR transfection was used as control. The miR-335 expression level in untransfected cells is indicated by a dashed line. GAPDH served as endogenous normalization control. Values are represented as mean  $\pm$  SEM,  $n = 5$ , \*  $p \leq 0.05$  vs miR, \*\*  $p \leq 0.001$  vs miR, ##  $p \leq 0.001$  vs PEI-mediated transfection. (A and B are taken from [201]).

### 3.4.4 Analysis of Migratory Potential

Cultured hMSCs were transfected with miR/PEI/MNP complexes and their migratory behavior was investigated 24 hours after miR-335 transfection using live cell imaging (Figure 15). MNP-containing complexes composed of scrambled miR (53.5%) had no influence on cell migration compared to control (57.2%). However, after transfection with miR/PEI/MNP complexes consisting of functional miR-335, the migratory ability of hMSCs (25.7%) was significantly reduced compared to untransfected cells.

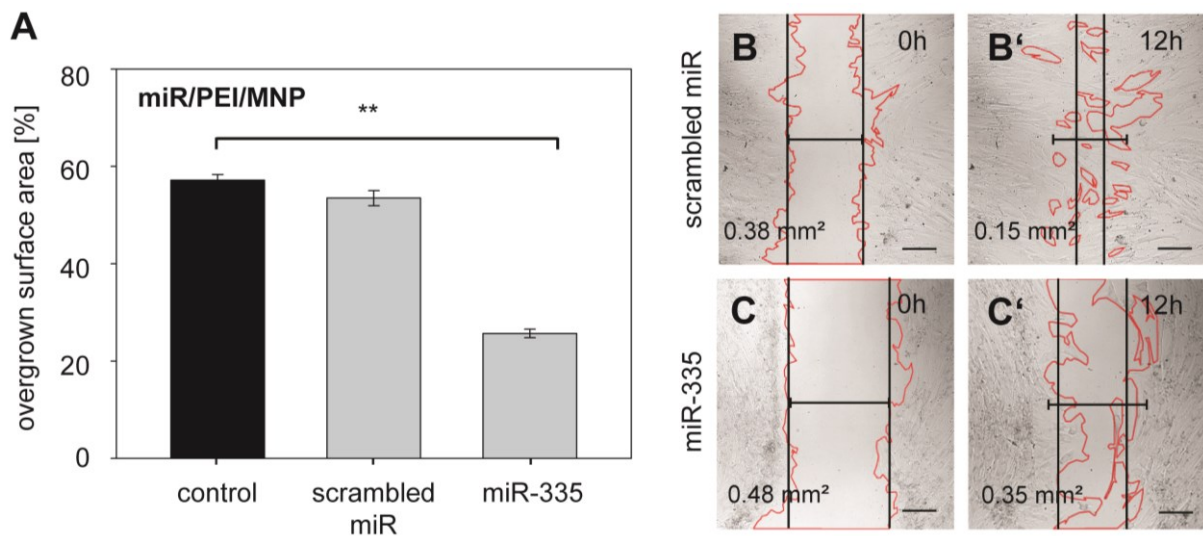


**Figure 15: Inhibition of the Migratory Ability of Cultured hMSCs after miR-335 Transfection.**

(A) 24 hours after transfection with optimized miR/PEI/MNP complexes, migratory behavior of cultured hMSCs was tested over a period of 12 hours using live cell imaging. Untransfected cells served as control. Data are shown as mean  $\pm$  SEM,  $n = 5$ , \*\*  $p \leq 0.001$ . (B,C) Expanded hMSCs were transfected with magnetic polyplexes consisting of scrambled miR (B,B') or miR-335 (C,C'). Directly after (B,C) and 12 hours after scratching (B',C'), images were taken. Values reflect the free surface area. Scale bar = 200  $\mu$ m. (A,B and C are taken from [201]).

### 3.5 Optimization of Transfection Complexes in Freshly Isolated hMSCs

#### 3.5.1 Optimization of miR Amount

In order to optimize transfection efficiencies in freshly isolated hMSCs, miR/PEI complexes with different miR amounts (2.5 to 15 pmol/cm<sup>2</sup> miR) at an NP ratio of 10 were tested using flow cytometry (Figure 16). Transfection with polyplexes consisting of 2.5 pmol/cm<sup>2</sup> miR resulted in the lowest uptake rates (1%, Figure 16 C). miR/PEI complexes composed of 5 pmol/cm<sup>2</sup> miR led to the highest uptake efficiencies (58%) which were significantly enhanced compared to miR transfection alone (37%). Moreover, an increase in miR amounts (10 and 15 pmol/cm<sup>2</sup> miR) showed a stepwise enhancement of uptake rates (38% vs 62%). However, after PEI-mediated transfection, uptake efficiencies were reduced to 20% and 8%, respectively.

Additionally, potential cytotoxicity of polyplexes was examined (Figure 16 D). Thereby, untransfected cells served as control (23%) reflecting toxicity of the isolation process. Transfection complexes composed of 2.5 pmol/cm<sup>2</sup> miR (28% after miR transfection, 22% after PEI-mediated transfection) showed no cytotoxic effect when compared to control. Moreover, cytotoxicity of miR/PEI complexes consisting of 5 and 10 pmol/cm<sup>2</sup> miR (~ 47%), respectively, was increased compared to transfection with miR alone (22% vs 26%). However, polyplexes and miR transfection with 15 pmol/cm<sup>2</sup> miR showed the highest values (78% vs 56%) and were significantly increased compared to control. With respect to the highest uptake rates and lowest cytotoxicity, 5 and 10 pmol/cm<sup>2</sup> miR were selected and utilized in further experiments.

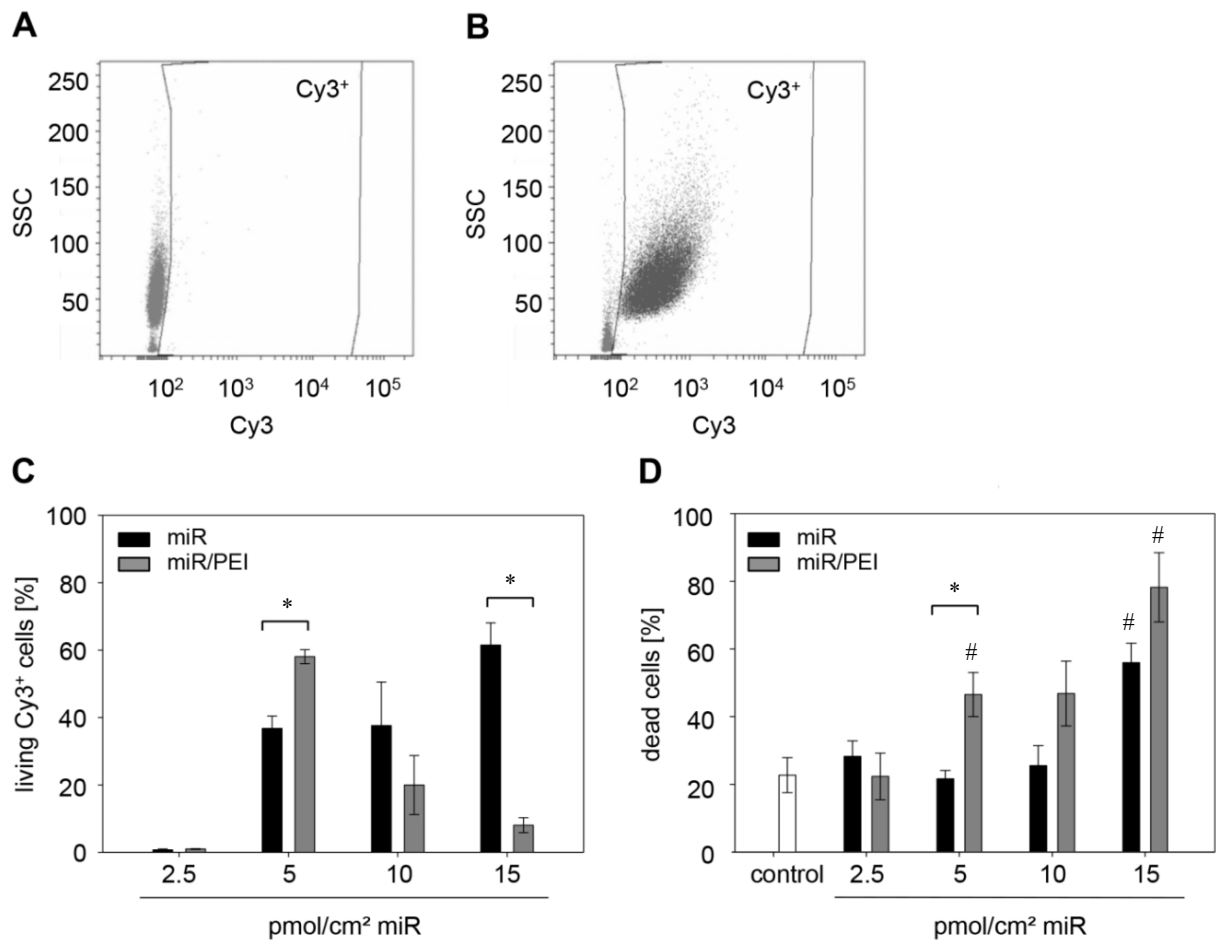


**Figure 16: Transfection Optimization of miR Amounts in Freshly Isolated hMSCs.** (A,B) Gating strategy to determine the uptake efficiency. (A) Untreated living CD105<sup>+</sup> cells served as negative control. (B) hMSCs were transfected with Cy3<sup>TM</sup> labeled transfection complexes and the number of living CD105<sup>+</sup> Cy3<sup>+</sup> cells in relation to living CD105<sup>+</sup> cells was determined. (C,D) Uptake efficiency (C) and cytotoxicity (D) of Cy3<sup>TM</sup> labeled miR and miR/PEI complexes were determined by flow cytometry 24 hours after transfection. Transfection complexes were composed of an NP ratio of 10 combined with various miR amounts (2.5, 5, 10 and 15 pmol/cm<sup>2</sup> miR). Untransfected cells were used as control. Data are represented as mean  $\pm$  SEM,  $n = 3$ , \*  $p \leq 0.05$  vs miR, #  $p \leq 0.05$  vs control. (A and B are taken from [206, 207]).

### 3.5.2 Optimization of PEI Amount

To further improve transfection performance in freshly isolated hMSCs, miR/PEI complexes with different NP ratios (NP ratio 2.5, NP ratio 10, NP ratio 33) and two selected miR amounts (5 pmol/cm<sup>2</sup> miR, 10 pmol/cm<sup>2</sup> miR) were investigated by flow cytometry (Figure 17). Polyplexes composed of 5 pmol/cm<sup>2</sup> miR with an NP ratio of 2.5 resulted in moderate uptake rates (32%, Figure 17 A). To further enhance uptake efficiency, higher NP ratios (NP ratio 10, NP ratio 33) were tested. PEI-mediated transfection using an NP ratio of 10 showed the highest uptake efficiencies (56%). However, PEI-based transfection with an NP ratio of 33 significantly decreased the uptake rates (1%). Moreover, miR/PEI complexes composed of 10pmol/cm<sup>2</sup> miR were investigated. The best uptake rates were achieved using transfection complexes composed of an NP ratio of 2.5 (69%). Nevertheless, an increase in NP ratios (NP ratio 10, NP ratio 33) led to a significant decrease in uptake efficiencies (12% vs 2%).

Furthermore, cytotoxicity of polyplex transfection was investigated (Figure 17 B). Therefore untransfected cells were used as control (29%). miR/PEI complexes composed of an NP ratio of 2.5 (35% vs 32%) showed no significant differences compared to control. Moreover, transfection complexes composed of an NP ratio of 10 and 5 pmol/cm<sup>2</sup> miR (46%) moderately increased cell mortality. However, transfection complexes composed of an NP ratio of 10 and 10 pmol/cm<sup>2</sup> miR (67%) showed the highest cytotoxicity levels. Likewise, an increase in the NP ratio (NP ratio 33) led to high cytotoxicity values after PEI-mediated transfection with 5pmol/cm<sup>2</sup> miR (57%) and with 10 pmol/cm<sup>2</sup> miR (55%), respectively. Therefore, regarding the highest uptake rates and lowest cytotoxicity, miR/PEI complexes composed of an NP ratio of 10 combined with 5 pmol/cm<sup>2</sup> miR and transfection complexes with an NP ratio of 2.5 combined with 10 pmol/cm<sup>2</sup> miR were selected and used in further experiments.

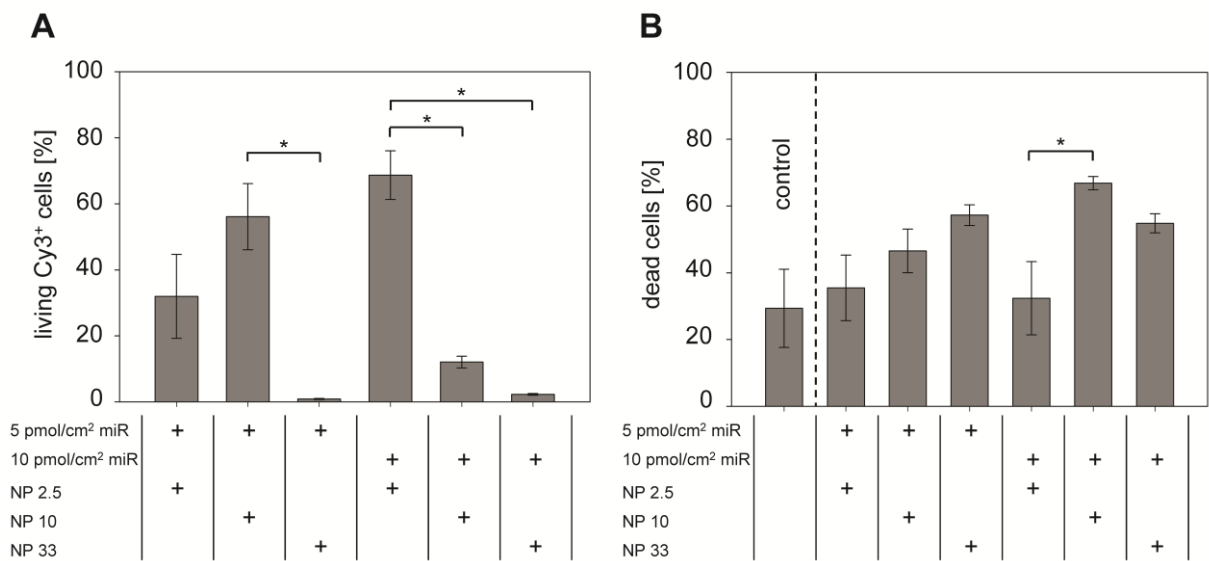


**Figure 17: Transfection Optimization of PEI Amounts in Freshly Isolated hMSCs.** Uptake efficiency (A) and cytotoxicity (B) of Cy3<sup>TM</sup> labeled miR/PEI complexes were investigated by flow cytometry 24 hours after transfection. Polyplexes were composed of various NP ratios (NP 2.5, NP 10, NP 33) combined with 5 or 10 pmol/cm<sup>2</sup> miR. Untransfected cells served as control. Data are represented as mean  $\pm$  SEM,  $n = 3$ , \*  $p \leq 0.05$ . (A and B are adopted from [206, 207]).

### 3.5.3 Optimization of MNP Amount

In order to increase the specificity of our transfection system, different MNP amounts (1 or 2  $\mu\text{g/ml}$  iron in MNPs) were combined with the two optimized miR/PEI complex variants. A potential influence of different complex compositions on uptake efficiency (Figure 18 A,C) and cytotoxicity (Figure 18 B,D) with or without the application of a magnetic field was investigated by flow cytometry. Uptake rates of miR/PEI/MNP complexes composed of an NP ratio of 10 combined with 5 pmol/cm<sup>2</sup> miR showed no significant differences (ranging from 62% to 76%) compared to miR/PEI complexes (81%) in the absence of a magnetic field (Figure 18 A). Moreover, cytotoxicity of these complexes showed no cytotoxic effect (24% vs 27%) when compared to miR/PEI complexes (30%) and control (20%, Figure 18 B), respectively.

Similarly, miR/PEI complexes consisting of an NP ratio of 2.5 combined with 10 pmol/cm<sup>2</sup> miR coupled to 1 or 2  $\mu\text{g/ml}$  iron in MNPs were tested. Uptake rates of MNP-mediated transfection (ranging from 57% to 65%) did not lead to significant differences compared to

corresponding miR/PEI complexes (77%) without the application of a magnetic field (Figure 18 C). Additionally, similar values of cytotoxicity were observed for transfected cells (ranging from 15% to 18%) and untransfected controls (17%, Figure 18 D). Moreover, a magnetic field was applied and the influence on uptake efficiency and cytotoxicity was examined. However, no significant differences were observed in the presence of an external magnetic field. In the following experiments, miR/PEI/MNP complexes composed of an NP ratio of 10 combined with 5 pmol/cm<sup>2</sup> miR coupled to 1 µg/ml iron in MNPs and magnetic complexes consisting of an NP ratio of 2.5 combined with 10 pmol/cm<sup>2</sup> miR bound to 1 µg/ml iron in MNPs were used.

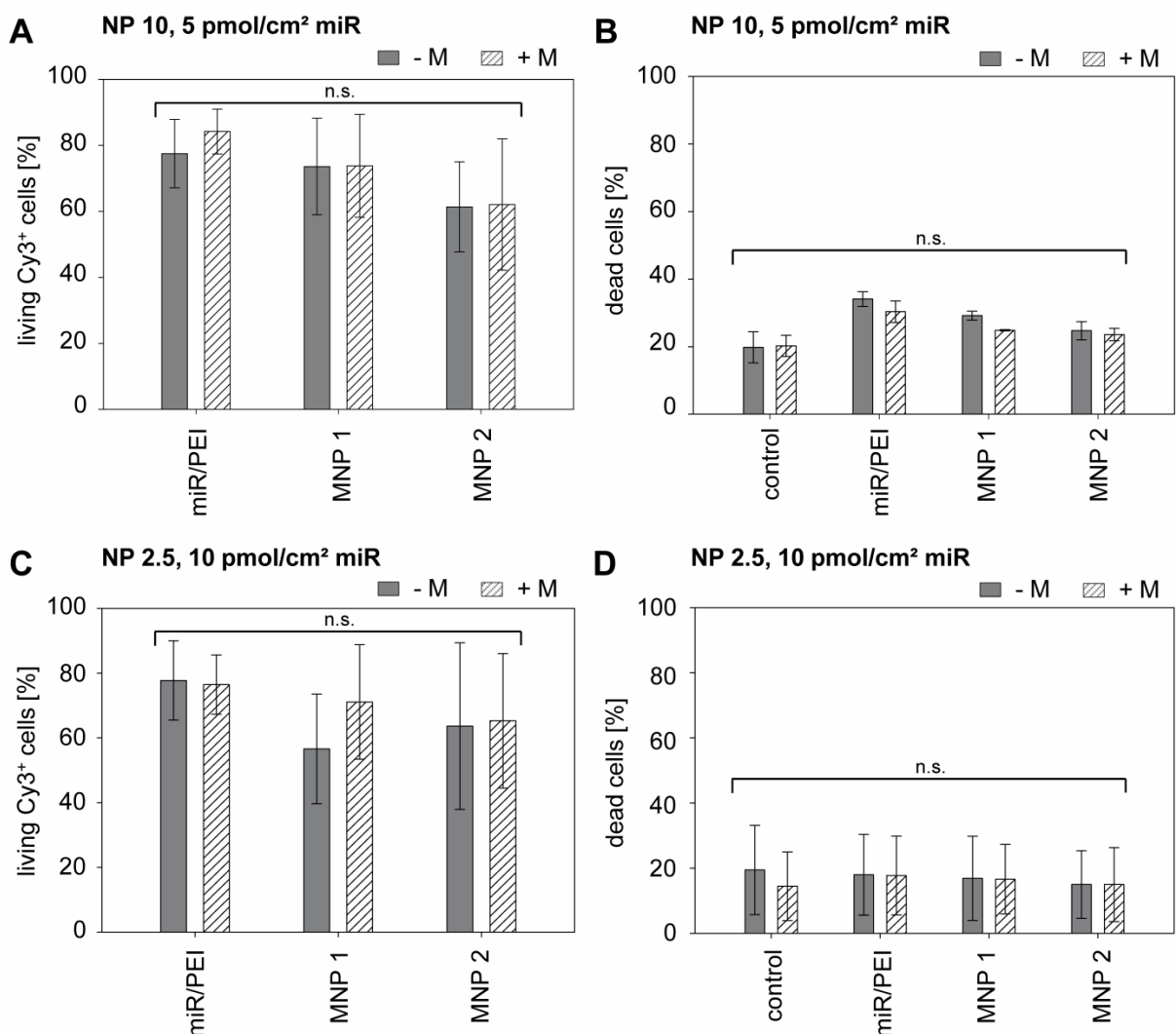


**Figure 18: Transfection Optimization of MNP Amounts in Freshly Isolated hMSCs with (+ M) and without (- M) the Application of a Magnetic Field.** Uptake efficiency (A,C) and cytotoxicity (B,D) of Cy3<sup>TM</sup> labeled miR/PEI and miR/PEI/MNP complexes were investigated by flow cytometry after 24 hours incubation time. Polyplexes were composed either of an NP ratio of 10 combined with



5 pmol/cm<sup>2</sup> miR (A,B) or of an NP ratio of 2.5 combined with 10 pmol/cm<sup>2</sup> miR (C,D). Furthermore, miR/PEI complexes could be bound to 1 or 2 µg/ml iron in MNPs (MNP 1, MNP 2). Values are represented as mean ± SEM, n = 3, n.s. = no significant difference. (A, B, C and D are taken from [206, 207]).

### 3.6 Evaluation of miR Processing in Freshly Isolated hMSCs

In order to differentiate between the transfection performances of the two optimized magnetic complexes, the expression levels of mature miR-335 in freshly isolated hMSC were quantified by real-time PCR 72 hours post transfection (Figure 19). After transfection with miR/PEI/MNP complexes consisting of an NP ratio of 10 combined with 5 pmol/cm<sup>2</sup> miR coupled to 1 µg/ml iron in MNPs, miR-335 expression levels were increased about 70-fold compared to untransfected cells. Moreover, transfection complexes composed of an NP ratio of 2.5 combined with 10 pmol/cm<sup>2</sup> miR bound to 1 µg/ml iron in MNPs further enhanced the miR-335 levels about 220-fold as compared to untreated controls. However, no significant differences between the investigated magnetic polyplexes were observed.

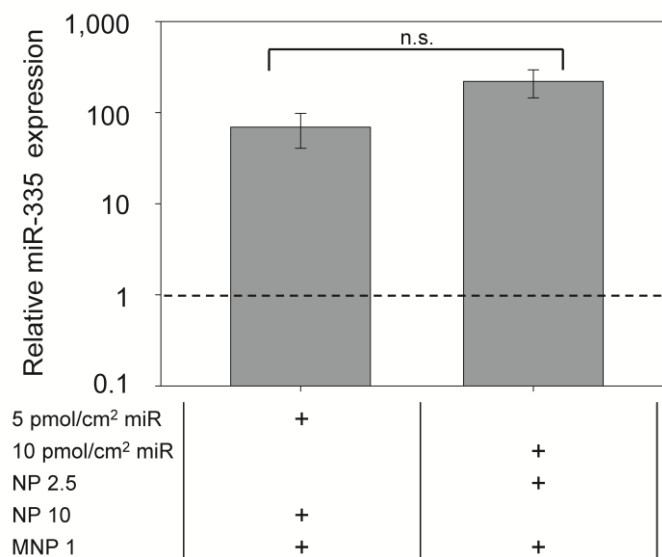


**Figure 19: Processing of pre-miR-335 in Freshly Isolated hMSCs.** hMSCs were transfected with the two optimized miR/PEI/MNP complexes (composed of 5 pmol/cm<sup>2</sup> miR with an NP ratio of 10 bound to 1 µg/ml iron in MNPs (MNP 1) or 10 pmol/cm<sup>2</sup> miR with an NP ratio of 2.5 bound to 1 µg/ml iron in MNPs (MNP 1)) and the level of the mature miR-335 strand was detected by real-time PCR 72 hours after transfection. The dashed line shows the miR-335 expression level in untreated cells. RNU-6B was used as endogenous normalization control. Data are represented as mean ± SEM, n = 3, n.s. = no significant difference.

### 3.7 Evaluation of MNP-mediated Transfection in Comparison to Established Magnetic Transfection Reagents in Freshly Isolated hMSCs

Uptake efficiency (Figure 20 A,C) and cytotoxicity (Figure 20 B,D) of optimized magnetic polyplexes were compared to commercially available magnetic carrier systems (CombiMag particles and Magnetofectamine<sup>®</sup>) using flow cytometry. Transfection with miR/PEI/MNP complexes composed of an NP ratio of 10 combined with 5 pmol/cm<sup>2</sup> miR bound to 1 µg/ml iron in MNPs resulted in high uptake rates of about 68% (Figure 20 A). Furthermore, uptake efficiencies of miR/PEI/CombiMag (64%) and miR/Magnetofectamine<sup>®</sup> (59%) complexes were comparable to those of MNP-mediated transfection. Moreover, no significant differences in cell mortality between transfected and control cells were observed (ranged from 11% to 17%, Figure 20 B).

Likewise, uptake efficiency (Figure 20 C) and cytotoxicity (Figure 20 D) of miR/PEI/MNP complexes composed of an NP ratio of 2.5 combined with 10 pmol/cm<sup>2</sup> miR bound to 1 µg/ml iron in MNPs were tested. Highest uptake rates (79%) were obtained after transfection with miR/PEI/MNP complexes. Moreover, miR/PEI/CombiMag (56%) and miR/Magnetofectamine<sup>®</sup> (75%) reached similar uptake levels. Besides, cell mortality values of transfected (ranging from 9% to 14%) and control cells were not significantly different.

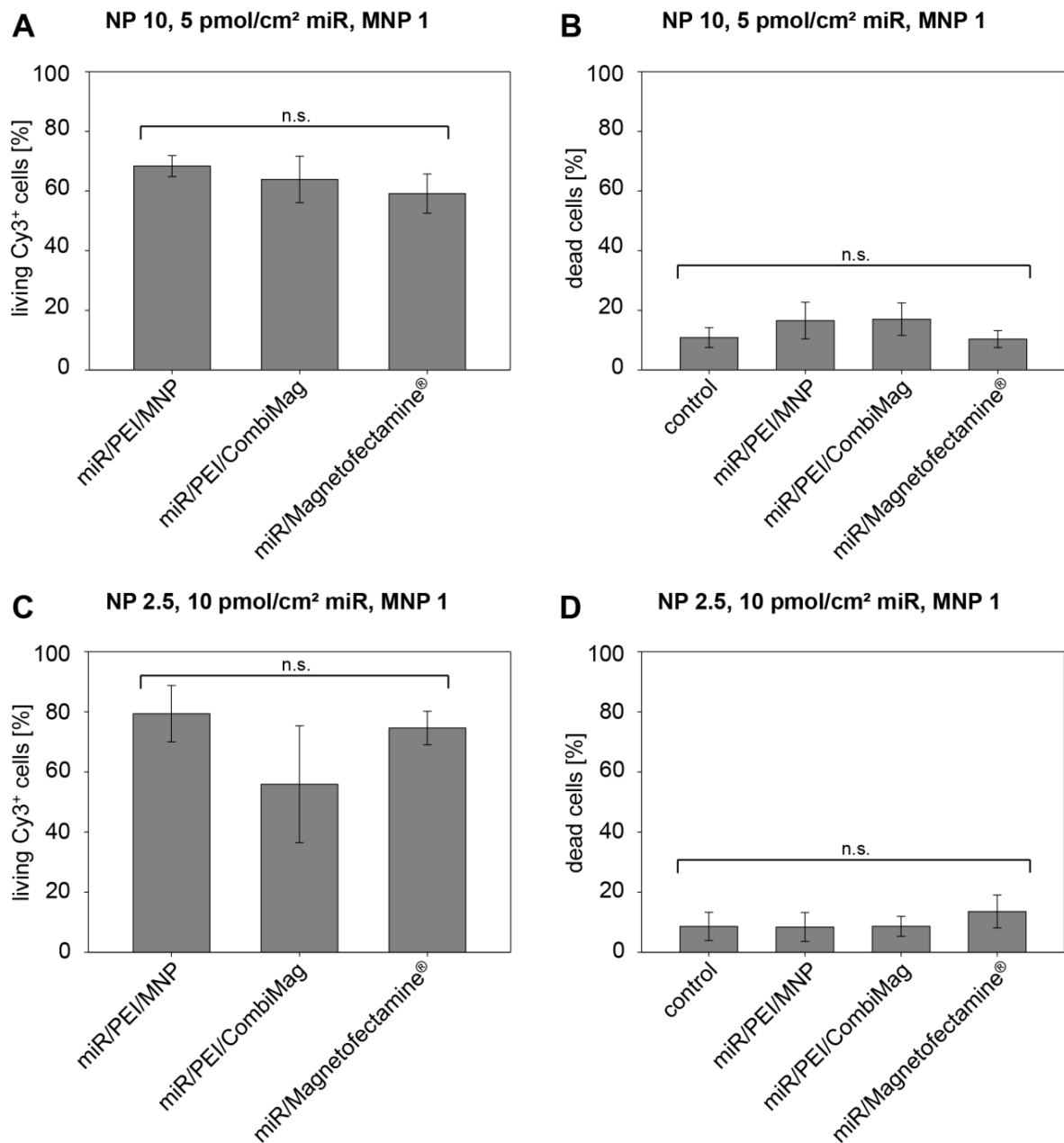


**Figure 20: Transfection Performances of Optimized miR/PEI/MNP Complexes in Comparison with Commercially Available Magnetic Transfection Carriers in Freshly Isolated hMSCs.** Uptake efficiency (A,C) and cytotoxicity (B,D) of Cy3<sup>TM</sup> labeled miR/PEI/MNP, miR/PEI/CombiMag and miR/Magnetofectamine<sup>®</sup> complexes were investigated by flow cytometry 24 hours after transfection in the presence of a magnetic field. miR/PEI/MNP complexes were composed either of an NP ratio of 10 combined with 5 pmol/cm<sup>2</sup> miR coupled to 1 µg/ml iron in MNPs (MNP 1; A,B) or of an NP ratio of 2.5 combined with 10 pmol/cm<sup>2</sup> miR bound to 1 µg/ml iron in MNPs (MNP 1; C,D). For the preparation of commercially available magnetic transfection complexes, corresponding amounts of Lipofectamine<sup>®</sup> 2000 and CombiMag particles were used. Untreated cells were used as control. Values are presented as mean ± SEM, n = 3, n.s. = no significant difference. (A, B, C and D are taken from [206, 207]).

### 3.8 *In Vitro* Magnetic Targeting of hMSCs

Initially, paramagnetic properties of the filtered MNP suspension were investigated using transmitted light microscopy. In the absence of a magnetic field, MNPs were properly dispersed in solution and did not perform any targeted movements (Figure 21 A). However, with the application of a magnetic field, MNPs started to move directly towards the magnet (Figure 21 B). After removing the magnet, MNPs stopped their directed movement and were evenly dispersed (Figure 21 C).

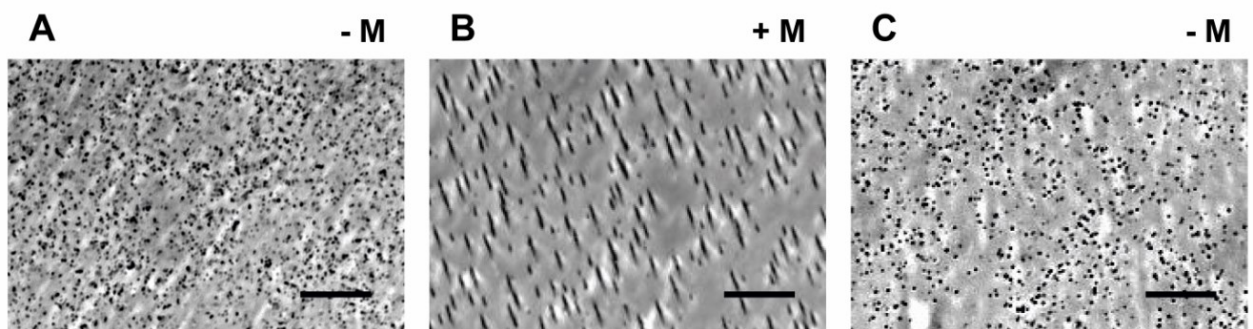


**Figure 21: Paramagnetic Properties of MNPs.** (A-C) The paramagnetic properties of MNPs were analyzed by transmitted light microscopy with (+ M) or without the application of a magnetic field (- M). Scale bar = 10  $\mu\text{m}$ .

Furthermore, hMSCs were transfected with optimized miR/PEI and miR/PEI/MNP complexes composed of an NP ratio of 10 combined with 5 pmol/cm<sup>2</sup> miR bound to 1  $\mu\text{g}/\text{ml}$  iron in MNPs and the effect of magnetic targeting was determined using transmitted light microscopy (Figure 22 A,B). Untransfected cells were used as control (Figure 22 C). After transfection with magnetic polyplexes, cultured hMSCs could be targeted by an external magnetic field (Figure 22 A). The majority of the cells accumulated in the area of the magnet. However, few hMSCs were randomly distributed at the border zone, where no magnetic field was applied. On the contrary, hMSCs transfected with miR/PEI/MNP complexes without the application of a magnet (Figure 22 A') were equally distributed in the whole well. After polyplex transfection, no specific targeting of hMSCs was observed in the presence (Figure 22 B) or absence (Figure 22 B') of a magnetic field and the distribution of cells were comparable to untransfected cells (Figure 22 C,C'). Moreover, targeting experiments using freshly isolated cells showed comparable results (data not shown).

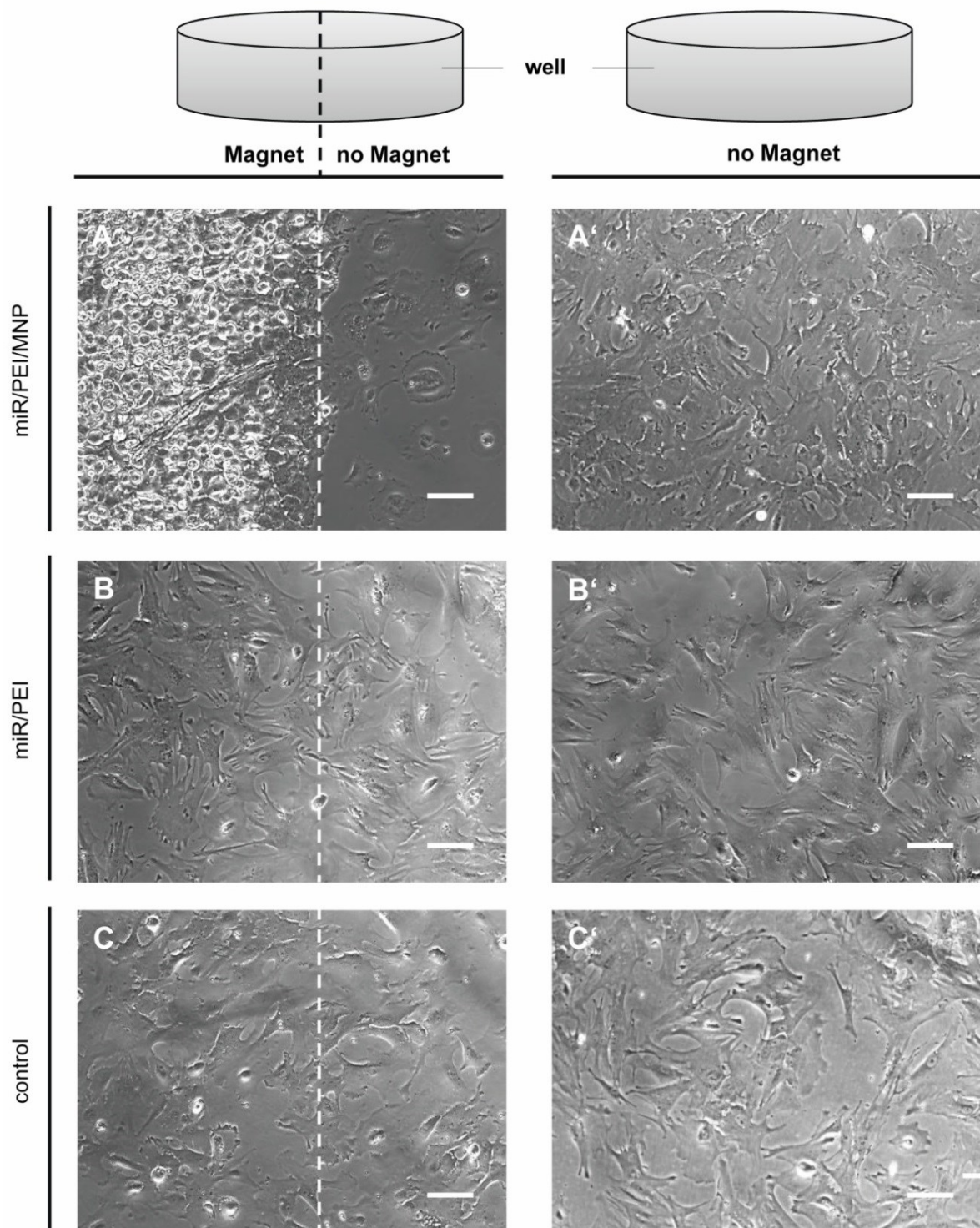


**Figure 22: *In Vitro* Magnetic Targeting of Cultured hMSCs.** 24 hours after transfection with optimized miR/PEI/MNP (A, A') and miR/PEI complexes (B, B'), magnetic targeting of cultured hMSCs in the presence (A, B, C) or absence of a magnetic field (A', B', C') was tested using transmitted light microscopy. Untransfected cells were used as control (C, C'). Scale bar = 10  $\mu$ m.

## 4 Discussion

### 4.1 Comparison of Freshly Isolated and Expanded CD105<sup>+</sup> hMSCs

CVDs are the leading cause of death worldwide [59]. Beside conventional therapies, cell-based approaches gained huge attention for regeneration of the injured heart during the last years. Cell-based therapies have the potential to replace damaged cardiac tissue and improve heart function after myocardial infarction with the aim to avoid heart transplantation. In recent years, bone marrow derived hMSCs have shown great therapeutic potential in treatment of CVDs [211]. Their protective function has been explained by different mechanisms, e.g. by secretion of anti-apoptotic, angiogenic, anti-inflammatory or matrix-mediating factors as well as by differentiation into various cell types [51, 212]. In general, MSCs are characterized by their expression of specific surface markers (e.g. CD29, CD44, CD73, CD105) as well as by their multilineage differentiation capacity [22]. In this work, hMSCs were isolated using anti-CD105 antibodies as it was shown, that CD105 is a suitable antigen for effective hMSCs purification [28]. Moreover, our group has demonstrated that CD105 purified and expanded hMSCs showed better cell survival in the infarcted heart and an improved effect on cardiac regeneration [204]. However, *in vitro* expanded MSCs were shown to develop altered gene expression patterns, loss of the C-X-C chemokine receptor type 4 (CXCR4) which is important for stem cell homing *in vivo* and a loss of their differentiation potential [213, 214, 215]. Furthermore, cell expansion is a time consuming and potentially harmful process [35]. Therefore, freshly isolated cells might be preferable for clinical applications. While the low cell number seems to limit the use of uncultured primary cells, Wise *et al* could demonstrate similar differentiation performances for freshly isolated MSCs as well as for expanded cells, even though the number of uncultured MSCs was by far smaller [216]. In our studies, immunophenotyping of freshly isolated CD105<sup>+</sup> cells was compared to expanded hMSCs (Figure 6). Our results showed a slightly different surface marker expression pattern of uncultured cells when compared to expanded hMSCs. While CD44, CD105 and CD117 are equally expressed in both freshly isolated and cultured hMSCs, the expression of CD45 was altered. Previously, it was shown that freshly isolated CD105<sup>+</sup> cells moderately expressed CD45 which was down-regulated during culture expansion [28]. Moreover, CD29 was weakly expressed on the surface of freshly isolated CD105<sup>+</sup> cells, while after culture all cells

were positive for CD29. CD29 is a membrane receptor involved in cell adhesion [217]. Therefore, it might be upregulated during cell expansion as hMSCs become adherent over time. Furthermore, in freshly isolated hMSCs CD73 surface expression was significantly decreased when compared to expanded cells which is in line with previous findings by Boiret *et al* [213]. Equally to our study, Aslan *et al* investigated bone marrow derived freshly isolated CD105<sup>+</sup> cells. Interestingly, though freshly isolated CD105<sup>+</sup> cells showed a different immunophenotype compared to expanded cells, they could demonstrate that uncultured cells were able to develop all typical properties of hMSCs after expansion [28]. Moreover, in our experiments freshly isolated hMSCs were able to be plastic adherent and showed a typical spindle-shaped morphology after 20 days in cell culture (Figure 4) as it is required by the International Society for Cellular Therapy [22]. To confirm the stem cell character of freshly isolated hMSCs, cells were characterized by their multilineage differentiation. It was shown, that freshly isolated hMSCs were able to differentiate into adipocytes and osteocytes similar to expanded hMSCs (Figure 5), which is in agreement with previous publications [45, 218, 219].

## **4.2 Establishment of a Standardized miR Transfection Protocol in Expanded hMSCs**

Beside the beneficial properties of hMSCs, their clinical applications are restricted, e.g. due to poor cell viability after transplantation into the heart [61]. Therefore, the therapeutic potential of hMSCs in cardiac regeneration can be improved by genetic modifications using specific miRs [135, 136, 137]. Recently, our group developed a magnetic non-viral vector system consisting of biotinylated PEI bound to streptavidin coated MNPs for DNA delivery (up to 10%) in cultivated hMSCs [220]. Therefore, we aimed to transfer this non-viral approach for miR delivery to hMSCs. Initially, we performed transfection optimization experiments in cultured hMSCs due to the high cell number that is required. Uptake efficiency and cytotoxicity of different complex formulations were investigated 5 hours after transfection. At this time point, it was shown that magnetic iron oxide containing PEI nanospheres were attached to the cell membrane and internalized inside the cell via endocytosis [221]. Moreover, we intended to avoid paracrine secretion of transfection complexes within microvesicles towards adjacent cells. Silva *et al* showed that under stress, MSCs released iron oxide nanoparticles throughout the organism where they can be taken up by host cells [222].



Thus, it would lead to misinterpretation of our uptake efficiency data. At first, hMSCs were transfected with miR alone, miR/PEI or magnetic miR/PEI/MNP complexes using different miR amounts (2.5 to 15 pmol/cm<sup>2</sup> miR) at an NP ratio of 10 (Figure 7). In all optimization experiments, negative control miR was used which has no function inside the cell. Thus, the observed effects on uptake efficiency and cell viability can be correlated to the different complex compositions. Interestingly, the uptake rates after transfection of expanded hMSCs with miR alone were relatively high (between 45% and 85%). However, Urban-Klein *et al* demonstrated that more than 90% of unprotected siRNA was degraded already after 15 minutes. In contrast, PEI complexes efficiently protected siRNA against enzymatic degradation and released bioactive siRNA inside the cell [172]. Additionally, systemic administration of naked siRNA *in vivo* was shown to have no therapeutically relevant effect [223]. As miR and siRNA have comparable structure, size and intracellular functionality, siRNA results can be transferred as a basis for miR delivery. Moreover, miR/PEI and miR/PEI/MNP complexes composed of 5 pmol/cm<sup>2</sup> miR transfected highly efficient around 75% cultured hMSCs with low cytotoxic effect (~ 15%). Although in previous studies higher amounts of small RNAs were used [178, 224, 225], in our experiments it did not further enhance uptake efficiency. However, a higher miR amount (15 pmol/cm<sup>2</sup> miR) increased cytotoxicity (~ 25%). Scholz *et al* stated that for successful siRNA delivery, a high cargo loading is required [157]. Therefore, regarding the highest uptake rates and the lowest cytotoxicity, transfection complexes composed of 5 pmol/cm<sup>2</sup> miR were used in the following experiments.

To further optimize transfection in expanded hMSCs, PEI polyplexes with different NP ratios (NP ratio 1 to NP ratio 50) and 5 pmol/cm<sup>2</sup> miR were tested (Figure 8). Previously it was demonstrated, that distinct NP ratios were remarkably influencing uptake efficiency of transfection complexes - thus we selected a broad range from NP ratio 1 to NP ratio 50 [226]. Moreover, in recent publications it was shown that PEI can deliver siRNA both *in vitro* and *in vivo* [172, 227, 228]. Although in former studies for DNA delivery NP ratios of 2.5 and 5 showed the highest transfection efficiencies [220], in our experiments miR/PEI complexes composed of low NP ratios (NP ratio 1, NP ratio 2.5, NP ratio 5) did not improve uptake rates. Moreover, Grayson *et al* could demonstrate that NP ratios higher than 6 have to be used for successful siRNA delivery [178]. hMSC transfection using polyplexes with an NP ratio of 10 or 33 showed the highest uptake rates (70% to 80%) which is in agreement with previous studies for PEI-mediated siRNA delivery [172, 176, 224, 229]. However, a further increase



of the PEI concentration (NP ratio 50) dramatically decreased the uptake efficiency due to the highest cytotoxicity of approximately 100%. It is known, that higher NP ratios resulted in increased cytotoxicity due to the higher PEI amount that is used to form complexes [230]. In previous studies it was demonstrated, that PEI can cause toxicity by randomly binding various negatively charged nuclear components and destructing membrane integrity, thus interfering with critical cell functions and inducing apoptosis [231, 232]. Moreover, it was shown that an NP ratio of 50 was correlated with high cytotoxicity in a human embryonal kidney cell line and a rat liver cell line [209, 210]. Thus, PEI polyplexes composed of an NP ratio of 50 were tested just once (n=1). Regarding the highest uptake efficiencies, polyplexes with an NP ratio of 10 and 33 as well as polyplexes with an NP ratio of 2.5 which performed best in combination with MNP for DNA transfection in expanded hMSCs were selected for additional transfection experiments [220].

To improve the selectivity of the transfection vector, preselected polyplexes were coupled to MNPs (ranging from 1 to 6  $\mu\text{g/ml}$  iron in MNPs) to enable specific magnetic targeting. Previously, it was shown by our group, that MNP-based complexes significantly enhanced DNA transfection in hMSCs even without the application of a magnetic field which was explained by different transfection mechanisms of DNA/PEI and DNA/PEI/MNP complexes [202]. Therefore, in the following experiments no magnetic field was preliminary applied. We could demonstrate that transfection complexes composed of an NP ratio of 2.5 resulted in the lowest uptake rates ( $\sim 1\%$ , Figure 9). Although, an NP ratio of 2.5 performed well in DNA transfection of COS7 cells [220], for miR delivery it was not suitable which could be explained by different structure, function and stability of miR when compared to DNA [157, 228]. Additionally, it was shown that for condensation of siRNAs higher PEI concentrations were needed due to the lower charge density and higher stiffness when compared to DNA [233]. Moreover, miR/PEI and miR/PEI/MNP complexes composed of an NP ratio of 33 significantly increased cytotoxicity by about 20% when compared to transfection using miR alone. In line with our findings, Kwok *et al* demonstrated that NP ratios higher than 20 significantly increased cytotoxicity. They explained this effect by the excess of free PEI within the transfection solution [228]. Interestingly, magnetic polyplexes composed of an NP ratio of 10 showed highest uptake rates at low MNP dosage (1 to 2  $\mu\text{g/ml}$  iron in MNPs) when compared to control (75% vs 50%) without cytotoxic effects. It is known, that higher MNP concentrations are correlated with higher transfection rates [234]. However, in our experiments an increase in MNP amounts (4 to 6  $\mu\text{g/ml}$  iron in MNPs) did

not lead to a further enhancement of uptake rates. Thus, magnetic polyplexes composed of 4 to 6  $\mu\text{g/ml}$  iron in MNPs were not used in further experiments as they did not show any beneficial effects for successful hMSC transfection. In the following investigations, magnetic complexes containing 1 to 2  $\mu\text{g/ml}$  iron in MNPs were used. Moreover, miR/PEI and miR/PEI/MNP complexes (1 to 2  $\mu\text{g/ml}$  iron in MNPs) showed similar performances regarding their uptake efficiencies which might indicate maximal transfection values possible in hMSCs. Therefore, uptake rates cannot be further enhanced by MNPs. However, magnetic complexes can be targeted by an external magnetic field and monitored via MRI which may become important for future *in vivo* applications [200, 235]. Additionally, magnetic targeting can enhance transfection efficiency and safety which is necessary for clinical applications as well as reduce cytotoxicity, dosage and costs [236]. Moreover, it was shown that MNP transfected cells could be guided by an externally applied magnet [183, 191]. Cheng *et al* demonstrated that cardiosphere derived cells transfected with iron oxide MNPs improved cell engraftment and cardiac function after myocardial infarction [237]. Thus, MNP-mediated stem cell targeting offers new perspectives for heart regeneration.

### 4.3 Physicochemical Characterization of Transfection Complexes

The physicochemical properties of the transfection vector are important factors influencing miR delivery and release inside the cell. An essential requirement for successful miR-mediated transfection is the ability to form stable complexes. Thus, binding properties of PEI with miR were tested using electrophoresis (Figure 10 A). It was shown, that miR polyplexes composed of an NP ratio greater than 0.5 completely retarded miR migration in the gel. Therefore, we concluded that at our optimized NP ratio 10, PEI polyplexes efficiently bound miR and formed tight complexes which is in line with previous findings [172, 228]. Thereby, miR is protected against enzymatic degradation by nucleases [238]. Moreover, PEI polyplexes provide a tool to avoid activation of the innate immune system by small RNAs [239].

Successful miR delivery has to face many challenges, e.g. cell targeting, uptake and endosomal release [178]. It was shown, that the size of nanoparticles can influence cellular uptake thus playing an essential role for *in vitro* and *in vivo* applications [240]. In our experiments, miR/PEI complexes composed of an NP ratio of 10 had a hydrodynamic diameter around 100 nm (Figure 10 C). Although siRNAs are small sized molecules around

7 nm length, also in previous studies it was shown that PEI formed complexes between 70 to 100 nm size which was explained by the complexation of several siRNAs into one complex [157, 228]. Binding of miR/PEI complexes to MNPs further increased particle sizes between 150 to 200 nm. However, previous studies have shown that a particle size between 50 to 200 nm was optimal for efficient uptake via endocytosis [178, 241]. Thus, both miR/PEI and miR/PEI/MNP complexes should be taken up and processed inside the cell in a similar way and speed [242]. Hence, this might be an explanation for comparable uptake efficiencies of MNP-containing complexes and PEI polyplexes (Figure 9).

Moreover, surface charge of transfection complexes was investigated (Figure 10 B). While MNPs alone were negatively charged ( $\sim -17$  mV), miR/PEI complexes with an NP ratio of 10 had a positive surface charge ( $\sim +40$  mV). Compared to our results, Kwok *et al* showed similar surface charges for siRNA/PEI complexes at an NP ratio of 10 [228]. It can therefore be concluded that due to its presence on the surface, PEI formed a protective cover around miR to avoid degradation by endonucleases [238]. Moreover, cell uptake was enhanced by positively charged complexes which efficiently bind to negatively charged cell membranes [226]. Furthermore, PEI provides efficient endosomal escape due to the “*proton sponge effect*” [174, 243]. Magnetic complexes containing 1  $\mu\text{g/ml}$  iron in MNPs showed a strong positive surface charge ( $\sim +33$  mV) providing optimal stability of transfection complexes in suspension by repulsive forces. In contrast, miR/PEI/MNP complexes with higher MNP concentrations (2 to 6  $\mu\text{g/ml}$  iron in MNPs) had a surface charge between +8 to +15 mV. Previously, it was shown that nanoparticles with a surface charge below +30 mV were less stable and tended to build aggregates over time [244, 245]. Summarizing highest uptake rates, lowest cytotoxicity and optimal physicochemical properties, magnetic transfection complexes composed of an NP ratio of 10 combined with 5 pmol/cm<sup>2</sup> miR and 1  $\mu\text{g/ml}$  iron in MNPs were selected as optimal parameters for all following experiments in expanded hMSCs.

#### **4.4 Intracellular Transfection Performance of miR/PEI/MNP Complexes in Expanded hMSCs**

After the optimization of stable complexes for successful miR delivery into expanded hMSCs, we investigated release and processing of pre-miR-335 from our optimized magnetic vector. Thereby, miR-335 served as proof-of-concept model which is known to target defined genes

(e.g. TNC, RUNX2) that are influencing proliferation, differentiation and migration of hMSCs [144, 246]. In these experiments, pre-miR was chosen due to its higher stability compared to mature miR. Moreover, pre-miR contains more nucleotides (~ 70 nucleotides) providing higher number of negatively charged phosphate groups in their backbone which are required for sufficient PEI complexation compared to less stable mature miR (~ 22 nucleotides) [125]. Beside the benefits regarding complex formation, transfected pre-miR has to undergo an additional processing step in the cytosol comparable to endogenously expressed miRs following the RNAi cascade [117]. Initially, processing of pre-miR into the mature strand was investigated by real-time PCR with respect to different endogenous normalization controls (miR-16, miR-191, RNU-6B; Figure 11 A). The accuracy of this method is critically dependent on appropriate reference RNA targets for normalization. For an optimal normalization, controls should be stably expressed along with the target being independent of environmental influences or experimental treatment [247]. Moreover, they are necessary for correct evaluation of quantitative data. In previous studies, miR-16 and RNU-6B were frequently used for miR expression normalization [248, 249, 250]. Moreover, Peltier and Latham suggested miR-191 as an optimal normalization target [251]. Our results demonstrated no significant differences of miR-335 levels when RNU-6B, miR-16 or miR-191 were used for normalization after transfection of expanded hMSCs with miR, miR/PEI or miR/PEI/MNP complexes. Thus, we concluded that RNU-6B, miR-16 or miR-191 were all suitable normalization controls for miR expression experiments. For the following real-time PCR experiments, RNU-6B was selected as standard normalization control.

Subsequently, we investigated the processing of pre-miR-335 and the kinetics of mature miR-335 levels 5, 24 and 72 hours after transfection in expanded hMSCs (Figure 11 B). Although transfection with mere pre-miR resulted in high uptake rates (Figure 7, 8, 9), 5 hours after transfection mature miR-335 level was just slightly increased by 10-fold compared to untreated hMSCs. Moreover, miR-335 values were decreased to normal expression levels within 72 hours of observation indicating a fast degradation of unprotected miR. Thus, transfection using miR alone seemed to be not suitable for *in vitro* applications. Furthermore, transfection performances of miR/PEI and miR/PEI/MNP complexes were investigated. Already 5 hours after transfection, miR-335 levels were significantly increased using miR/PEI or miR/PEI/MNP complexes when compared to mere miR transfection. After 24 hours, miR-335 levels were further increased by more than 1,000-fold after transfection with PEI- or MNP-containing complexes, respectively, and reached a maximum. In contrast to previous

results for DNA delivery, after 24 hours no differences between miR/PEI- and miR/PEI/MNP-mediated transfection in expanded hMSCs were observed indicating different release kinetics for miR delivery [220]. Interestingly, after 3 days miR-335 values remained at the same level after MNP-based transfection indicating a steady release of miRs. In contrast, miR-335 level was decreased by more than 3-fold after transfection using miR/PEI complexes when compared to magnetic miR/PEI/MNP complexes. Hence, we concluded a better consistent long term effect of MNP-mediated transfection which might be beneficial for clinical applications.

In order to explain the different transfection performances of MNP-containing complexes and PEI polyplexes 72 hours after transfection, we intended to visualize transfection complexes inside the cell. Therefore, all components of miR/PEI and miR/PEI/MNP complexes were selectively labeled with different fluorochromes. Recently, our group developed a labeling technique for DNA-based transfection complexes. Although the selected fluorochromes had close emission and excitation spectra, it was shown that no interactions between the dyes occurred. Moreover, it was demonstrated, that 3-color labeling of DNA/PEI/MNP complexes slightly enhanced particle size (~ 200 nm). However, it did not affect transfection efficiency and cell viability. Therefore, it was concluded that microscopic observations could be correlated to transfection data [220]. Hence, we adopted this labeling protocol for miR/PEI/MNP complexes. Initially, magnetic polyplexes were visualized in the absence of cells (Figure 12). Thus, we could investigate quality of labeling as well as shape of complexes. Labeled magnetic polyplexes showed rounded complexes with a good signal-to-noise ratio of all components. Moreover, miR was visually co-localized with PEI together with MNPs. Thus, modification of magnetic complexes by fluorescent labeling was not influencing complex formation. Subsequently, we applied labeled complexes in expanded hMSCs and investigated the performance of miR/PEI and miR/PEI/MNP complexes 72 hours after transfection (Figure 13). After transfection with PEI polyplexes, miR was found inside the nucleus still condensed by PEI. In line with our results, previous studies have shown comparable results after transfection with PEI using DNA or siRNA, respectively [220, 228, 252]. However, miR-mediated RNAi requires cytoplasmatic release. Therefore, mature miR levels might be decreased 72 hours after transfection as processing of delivered pre-miR is hindered due to the wrong cellular localization of transfection complexes (Figure 11). In contrast, in our experiments MNP-based complexes were randomly distributed entirely in the cytoplasm but not in the nucleus. For DNA transfection using magnetic polyplexes, similar

effects were observed. It was stated that due to the strong biotin-streptavidin binding between MNPs and PEI resulting in bigger particle size when compared to PEI polyplexes, magnetic complexes cannot enter the nucleus. Consequently, DNA has to be released in the cytosol following nuclear entry [202, 203]. Therefore, MNP-based transfection may provide benefits particularly for miR delivery as miR exert their function in the cytosol. Consequently, the different transfection mechanisms of miR/PEI and miR/PEI/MNP complexes might be an explanation for the better long term effect of MNP-containing complexes.

After testing release and processing of mature miR-335 from transfection complexes, we investigated functionality by knockdown of target genes 5, 24 and 72 hours after transfection (Figure 14). Previous studies revealed TNC and RUNX2 as target genes of miR-335 [144, 246]. It was shown, that the extracellular matrix protein TNC is involved in the regulation of proliferation and migration in cancer cells [253, 254]. Moreover, RUNX2 is a transcription factor and regulating osteogenic differentiation [144, 255]. In our experiments, transfection with mere miR did not significantly down-regulate TNC and RUNX2 compared to control within 72 hours after transfection. In agreement with our result, previously it was shown that unprotected siRNA was not able to perform efficient gene knockdown due to the lower stability and faster degradation when compared to PEI polyplexes [157, 172, 229]. However, after 24 hours, transfection with miR/PEI or miR/PEI/MNP complexes resulted in a significant knockdown of TNC and RUNX2 mRNA levels, respectively, when compared to untreated cells. Corresponding to our miR-335 processing data (Figure 11), 72 hour after miR/PEI transfection, the expression level of RUNX2 started to increase again which might be a reason of PEI-mediated nuclear delivery of transfection complexes into the wrong compartment as shown in Figure 13. Moreover, it might indicate the beginning of a depletion of delivered miR and a temporal limited effect of these complexes. Interestingly, after MNP-mediated transfection target genes expression was further decreased by 50% to 60% and was significantly down-regulated as compared to miR/PEI transfection. This effect might be a consequence of a constant release of miR from MNP-containing complexes into the cytosol for efficient RNAi within 72 hours as shown in our previous results (Figure 11, 13). Moreover, it underlines our hypothesis of a sustained effect by MNPs.

In addition, we investigated the influence of TNC knockdown by miR-335 on cell migration after transfection using magnetic complexes (Figure 15). In this experiment a wound healing assay was started 24 hours after transfection to observe the time frame in which TNC expression was maximally reduced by 40% to 60% (Figure 14). Our results showed no

difference after miR/PEI/MNP transfection containing not functional scrambled miR compared to untransfected control. Therefore, we could exclude an influence on cell motility by MNP-based complexes. Interestingly, after transfection with magnetic polyplexes using miR-335, cell migration was significantly decreased as shown by a minor overgrown surface area compared to untransfected cells. In line with our results, Tavazoie *et al* showed a significant reduction by 30% of cell migration in two cancer cell lines after retroviral-mediated transduction of miR-335 [246]. Moreover, Tomé *et al* could demonstrate similar results in expanded hMSCs [144]. Conclusively, we developed stable magnetic, non-viral transfection complexes for effective miR delivery and release following significant gene silencing of target genes in expanded hMSCs.

#### 4.5 Optimization of MNP-Mediated Transfection in Freshly Isolated hMSCs

To avoid the risks related to cell expansion (e.g. contaminations, altered gene expression, loss of stem cell markers and differentiation capacity), we adopted our optimized non-viral approach for transfection of freshly isolated hMSCs, thus making it more relevant for clinical applications. As uncultured hMSCs showed a different cell morphology and a slightly altered immunophenotype (Figure 4, 6) we started to optimize miR amounts (ranging between 2.5 to 15 pmol/cm<sup>2</sup> miR) of transfection complexes (Figure 16) taking advantage of previous experiments using expanded cells (Figure 7). In contrast to transfection in cultivated hMSCs, transfection complexes composed of 2.5 pmol/cm<sup>2</sup> miR were not taken up by freshly isolated cells. However, after transfection with polyplexes using 5 pmol/cm<sup>2</sup> miR uptake rates were significantly enhanced compared to mere miR transfection. In line with our previous results (Figure 7), an increase in miR amounts (10 to 15 pmol/cm<sup>2</sup> miR) did not lead to a further enhancement of uptake rates after polyplex-mediated transfection. Moreover, cytotoxicity of the different complex formulations was investigated. Therefore, untreated cells were used as control representing about 20% cytotoxicity which was caused by the isolation process. Increasing miR amounts showed a dose-dependent enhancement of cytotoxicity when compared to control. Similar to our results in expanded hMSCs, after transfection with polyplexes composed of 15 pmol/cm<sup>2</sup> miR highest cytotoxicity values (about 80%) were reached in freshly isolated cells. Although transfection experiments in freshly isolated hMSCs showed mostly comparable trends to cultured cells, absolute values of uptake rates ( $\Delta$  20%) and cytotoxicity ( $\Delta$  55%) were different. It was shown by others, that suspension cells

comparable to our freshly isolated hMSCs are more difficult to transfect than adherent cells similar to our cultivated cells [256, 257]. Therefore, altered cell size and morphology which was previously shown (Figure 4) might influence the transfection performance. Moreover, the different surface marker expression (Figure 6) might lead to changes on the cell membrane which could affect uptake of transfection complexes. To further improve the uptake efficiency of polyplexes, we selected two miR amounts (5 and 10 pmol/cm<sup>2</sup> miR) with moderate uptake rates but still no cytotoxic effect when compared to untreated cells for the following experiments. According to PEI-based transfection in expanded hMSCs, the selected miR amounts were combined with previously tested NP ratios (NP ratio 2.5, NP ratio 5, NP ratio 10) and transferred to efficient miR delivery into freshly isolated CD105<sup>+</sup> cells (Figure 17). In accordance with our previous results in cultured cells (Figure 9), we could show that PEI-based complexes composed of an NP ratio of 10 combined with 5 pmol/cm<sup>2</sup> miR yielded highest uptake rates (56%) in uncultivated hMSCs. In contrast to miR transfection in expanded hMSCs, polyplexes with a higher NP ratio (NP ratio 33) were not taken up by fresh hMSCs and resulted in enhanced cytotoxicity. Thus, freshly isolated hMSCs might react more sensitive to potentially detrimental agents. Interestingly, the uptake efficiency could be further enhanced in non-cultured cells (69%) by using polyplexes composed of a lower NP ratio (NP ratio 2.5) and combined with a higher miR amount (10 pmol/cm<sup>2</sup> miR). Additionally, the strategy of reducing the NP ratio decreased cytotoxicity to values comparable to the control group due to the lower amount of PEI used. Thus, PEI polyplexes consisting of an NP ratio of 2.5 combined with 10 pmol/cm<sup>2</sup> miR were investigated in further experiments and compared to miR/PEI complexes previously optimized for expanded cells (NP ratio 10, 5 pmol/cm<sup>2</sup> miR).

Targeted gene delivery is an essential requirement for clinical applications. Previously, it was shown that MNP-based gene delivery enables both *in vivo* targeting of transfection complexes towards the desired area and guiding of magnetically modified cells using an externally applied magnetic field [183, 191]. Therefore, the combination of MNPs with the optimal miR/PEI complex formulations (NP ratio 2.5, 10 pmol/cm<sup>2</sup> miR vs NP ratio 10, 5 pmol/cm<sup>2</sup> miR) might be a promising strategy to increase selectivity and efficiency in freshly isolated hMSCs (Figure 18). Regarding previous results in expanded cells (Figure 9), miR/PEI complexes were coupled to 1 or 2 µg/ml iron in MNPs, respectively. Similar to MNP-mediated transfection in expanded hMSCs, uptake efficiencies of different magnetic complex formulations did not significantly differ when compared to polyplex transfection in freshly



isolated cells. Moreover, absolute values were comparable to those obtained in cultured hMSCs (~ 75%). Additionally, magnetic complexes had no cytotoxic effect in fresh hMSCs when compared to controls indicating that the investigated MNP concentrations were well tolerated by the cells. Therefore, with respect to previous characterization of MNP-containing complexes (Figure 10), magnetic polyplexes composed of 1 µg/ml iron in MNPs were considered for the following experiments. Furthermore, in this experiment we applied a magnetic field for magnetofection and examined the impact on miR delivery into freshly isolated hMSCs (Figure 18). Interestingly, after 5 hours, magnetic forces did not lead to an enhanced miR transfection. Moreover, no significant differences in uptake efficiency and cytotoxicity in the presence or absence of a magnetic field were observed. In line with our results, Huth *et al* showed that the application of a magnetic field did not alter uptake mechanisms or processing of transfection complexes inside the cell [193]. Moreover, it was demonstrated *in vitro* that the enhanced transfection efficiency of MNP-based complexes was only caused by an accelerated sedimentation of complexes on the cell membrane facilitated by an external magnet [192, 193]. However, Plank *et al* showed that the enhanced efficiencies of magnetically assisted transfection were observed just for a short time. 4 hours after transfection, efficiencies of magnetic complexes under the exposure of a magnetic field were comparable to those without the application of a magnet [258].

After optimization of the magnetic vectors for efficient miR delivery into freshly isolated hMSCs, we investigated release and processing of transfected miR-335 (Figure 19) as it was previously done in expanded cells. It was shown that both tested miR/PEI/MNP complexes were capable of efficiently deliver and release miR-335 inside fresh hMSCs shown by 70-fold to 220-fold enhancement of miR-335 expression levels. Although similar uptake efficiencies of MNP-based transfection in freshly isolated and expanded hMSCs were reached, miR-335 levels were about 10-times lower in freshly isolated cells when compared to cultured hMSCs. This could be a reason of different cell morphologies as shown in Figure 4. In contrast to freshly isolated hMSCs, expanded cells were big cells with a large cell surface capable of taking up relatively more transfection complexes within one cell (Figure 13). Therefore, the amount of released miR might be enhanced in cultivated cells compared to fresh hMSCs. Interestingly, magnetic polyplexes consisting of an NP ratio of 2.5 combined with 10 pmol/cm<sup>2</sup> miR, which were shown to be less stable [228], showed 3-fold higher miR-335 levels when compared to MNP-containing complexes optimized for transfection in cultured hMSCs (NP ratio 10, 5 pmol/cm<sup>2</sup> miR). It seemed that the lower stability of magnetic

polyplexes composed of an NP ratio of 2.5 may allow a faster release of miR inside the cytosol promoting higher miR-335 levels. Moreover, due to the smaller size of freshly isolated hMSCs, the transport distance of transfection complexes to reach the perinuclear region for RNAi is shorter when compared to expanded cells. Hence, transfection complexes composed of a lower NP ratio (NP ratio 2.5) might be beneficial in fresh hMSCs.

#### 4.6 Comparison of Different Magnetic miR Carrier Systems in Freshly Isolated hMSCs

Additionally, miR delivery of our selected miR/PEI/MNP vectors were compared to commercially available magnetic transfection reagents in freshly isolated hMSCs (Figure 20). As standard transfection reagents commonly used for magnetofection, we combined miR with Magnetofectamine<sup>®</sup>. Being a combination of Lipofectamine<sup>®</sup> 2000 and CombiMag particles, Magnetofectamine<sup>®</sup> was successfully applied in various cell types for the delivery of different nucleic acids (e.g. DNA, siRNA) using an external magnetic field [194, 195, 196, 199]. Besides the combination with cationic lipids, it is proposed that CombiMag particles can be further combined with cationic polymers (e.g. PEI). Although these magnetic transfection reagents were widely applied in a broad range of indications, none of them were used for miR delivery before. In our experiments, both miR/PEI/MNP vectors showed highest uptake rates which were comparable to those reached with miR/PEI/CombiMag complexes. Underlining our results, Huth *et al* showed that magnetic vector assembly is essentially influencing transfection efficiency. Both, miR/PEI/MNP and miR/PEI/CombiMag complexes were prepared in a similar manner. At first, miR was complexed by PEI providing its positive surface charge (Figure 10) followed by coupling to MNPs or CombiMag particles, respectively. Thus, it is likely that both magnetic polyplexes were equally taken up and processed inside the cell, resulting in comparable miR uptake rates. Moreover, we compared our optimized polyplex-based miR/PEI/MNP complexes to lipoplex-mediated Magnetofectamine<sup>®</sup>. Cationic lipids were suggested as the most efficient chemical transfection reagents in suspension cells [259]. However, our magnetic polyplexes reached similar values. Although polyplexes and lipoplexes show different chemical structures, interactions with nucleic acids and intracellular transfection mechanisms, previously it was proposed that they might have similar uptake mechanisms via endocytosis [260, 261]. Furthermore, polyplex- and lipoplex-mediated transfection seems to underlie comparable

kinetics thus leading to equal miR uptake efficiencies. Furthermore, no cytotoxic effects of the different magnetic transfection complexes were observed when compared to control indicating that the investigated magnetic transfection reagents were well tolerated in freshly isolated hMSCs. Therefore, the investigated magnetic vectors may provide direct genetic modifications of damaged tissue by introducing therapeutic miRs *in vivo* [183]. Furthermore, *in vitro* magnetic modifications of stem cells before transplantation may allow specific guiding or retention of transplanted cells by an externally applied magnetic field [191].

#### 4.7 *In Vitro* Targeting of Magnetically Modified hMSCs

In 2013, Lang *et al* investigated engraftment of intramyocardially transplanted stem cell derivatives for treatment of heart infarction. It was shown, that only 5% of the transplanted cells retained at the site of injection due to massive washout of the beating heart [262]. Thus, magnetic targeting of transplanted cells may provide a strategy to increase the cell engraftment and therapeutic outcome of stem cells after myocardial infarction. Recently, Vandergriff *et al* labeled human cardiosphere derived stem cells with paramagnetic iron oxide nanoparticles and investigated magnetic targeting of magnetically modified cells in the infarcted heart. After intracoronary injection, labeled cells were visibly targeted towards the magnet and accumulated around the ischemic zone. In contrast, without magnetic targeting the majority of stem cells were washed out directly after injection. Conclusively, they could demonstrate that magnetic targeting of labeled cardiac stem cells facilitated cell retention and engraftment thus improving cardiac regeneration [263]. Besides the ability of targeted delivery of magnetically modified stem cells towards the side of interest, the combination of magnetic targeting with simultaneous gene delivery by using the same vector might further enhance therapeutic benefits. Previously, we have shown efficient miR delivery in both freshly isolated and expanded hMSCs after transfection with our optimized miR/PEI/MNP vector (Figure 9, 18). Furthermore, we investigated magnetic targeting of transfected cells *in vitro*. Initially, paramagnetic properties of MNPs were tested (Figure 21). According to the definition of paramagnetic nanoparticles [240], our MNPs exhibited magnetization only in the presence of a magnetic field. Without the application of a magnet, MNPs stopped their targeted movements and remained a stable colloidal suspension. Furthermore, magnetic targeting of freshly isolated and expanded hMSCs was investigated after transfection with our optimized magnetic complexes (Figure 22). We could demonstrate specific targeting of

hMSCs after MNP-mediated transfection shown by accumulation of cells in the area of the magnetic field. However, hMSCs grew homogenously distributed when no magnet was applied which is in agreement with our previous results (Figure 21). Therefore, our non-viral magnetic vector allows specific control of stem cell properties by efficient miR delivery combined with precise magnetic targeting of transfected cells *in vivo*. Thus, it might provide a basis for innovative therapies to regenerate the injured heart.

## 5 Conclusion

In conclusion, we successfully developed a novel non-viral magnetic miR delivery vector for both efficient modification of freshly isolated hMSCs using miR/PEI/MNP complexes and specific targeting of transfected hMSCs by an external magnetic field *in vitro*. Initially, we established a standardized protocol for optimal miR/PEI/MNP complex formation in expanded hMSCs with respect to their physicochemical properties as well as highest uptake rates and lowest cytotoxicity. Moreover, our MNP-containing complexes provided efficient release and processing as well as prolonged functionality of delivered miR in cultured hMSCs compared to polyplex transfection, which might be beneficial for successful stem cell-based gene therapy. Furthermore, we successfully transferred our non-viral approach for efficient miR delivery to freshly isolated CD105<sup>+</sup> hMSCs with uptake rates equaling those of miR transfection in expanded cells. Compared to commercially available magnetic transfection reagents, transfection performance of our MNP-containing complexes yielded similar values. Therefore, we were the first to approve these magnetic transfection reagents for efficient miR delivery in freshly isolated hMSCs. Additionally, both freshly isolated and expanded hMSCs could be specifically targeted by an externally applied magnetic field after transfection with the corresponding miR/PEI/MNP complexes, facilitating retention and engraftment of transplanted cells *in vivo*. Finally, this thesis provides the basis for efficient miR delivery into freshly isolated hMSCs using our novel magnetic carriers. In the future, further pre-clinical tests have to be performed to investigate magnetic targeting of modified hMSCs under *in vivo* conditions. Pharmacokinetics and pharmacodynamics of magnetically modified cells as well as of excreted transfection complexes have to be investigated before applying it to humans. In addition, *in vitro*, our MNP-containing complexes can be further applied for magselectofection, being a combination of magnetically activated cell isolation and simultaneous transfection. Subsequently, this approach could be further transferred to fully automated and closed magnetic cell separation systems (e.g. CliniMACS Prodigy<sup>®</sup> from Miltenyi Biotec) to provide safe and standardized cell products which are in line with current good manufacturing practices guidelines. Thus, autologous freshly isolated and transfected cells could be immediately transplanted during the same surgery. Therefore, we expect that our magnetic non-viral carrier will serve as a solid basis for innovative strategies in heart regeneration.

## 6 References

1. Mathers, C.D.; Loncar, D. Projections of global mortality and burden of disease from 2002 to 2030. *PLoS Med* **2006**, *3*, e442.
2. Global status report on noncommunicable diseases 2010. Available online: <http://www.who.int/mediacentre/factsheets/fs317/en/> (01.07.2014).
3. Rosenstrauch, D.; Poglajen, G.; Zidar, N.; Gregoric, I.D. Stem celltherapy for ischemic heart failure. *Tex Heart Inst J* **2005**, *32*, 339-347.
4. Boateng, S.; Sanborn, T. Acute myocardial infarction. *Dis Mon* **2013**, *59*, 83-96.
5. Yusuf, S.; Sleight, P.; Held, P.; McMahon, S. Routine medical management of acute myocardial infarction. Lessons from overviews of recent randomized controlled trials. *Circulation* **1990**, *82*, II117-134.
6. Seki, A.; Fishbein, M.C. Predicting the development of cardiac allograft vasculopathy. *Cardiovasc Pathol* **2014**.
7. Annual Report 2013 - Eurotransplant International Foundation. Available online: <http://www.eurotransplant.org/cms/mediaobject.php?file=AR20135.pdf> (01.07.2014).
8. Thomson, J.A.; Itskovitz-Eldor, J.; Shapiro, S.S.; Waknitz, M.A.; Swiergiel, J.J.; Marshall, V.S.; Jones, J.M. Embryonic stem cell lines derived from human blastocysts. *Science* **1998**, *282*, 1145-1147.
9. Kehat, I.; Kenyagin-Karsenti, D.; Snir, M.; Segev, H.; Amit, M.; Gepstein, A.; Livne, E.; Binah, O.; Itskovitz-Eldor, J.; Gepstein, L. Human embryonic stem cells can differentiate into myocytes with structural and functional properties of cardiomyocytes. *J Clin Invest* **2001**, *108*, 407-414.
10. de Peppo, G.M.; Marolt, D. State of the art in stem cell research: human embryonic stem cells, induced pluripotent stem cells, and transdifferentiation. *J Blood Transfus* **2012**, *2012*, 317632.
11. Guan, K.; Hasenfuss, G. Do stem cells in the heart truly differentiate into cardiomyocytes? *Journal of molecular and cellular cardiology* **2007**, *43*, 377-387.
12. Kaushal, S.; Jacobs, J.P.; Gossett, J.G.; Steele, A.; Steele, P.; Davis, C.R.; Pahl, E.; Vijayan, K.; Asante-Korang, A.; Boucek, R.J.; Backer, C.L.; Wold, L.E. Innovation in basic science: stem cells and their role in the treatment of paediatric cardiac failure--opportunities and challenges. *Cardiol Young* **2009**, *19 Suppl 2*, 74-84.
13. Takahashi, K.; Yamanaka, S. Induction of pluripotent stem cells from mouse embryonic and adult fibroblast cultures by defined factors. *Cell* **2006**, *126*, 663-676.
14. Takahashi, K.; Tanabe, K.; Ohnuki, M.; Narita, M.; Ichisaka, T.; Tomoda, K.; Yamanaka, S. Induction of pluripotent stem cells from adult human fibroblasts by defined factors. *Cell* **2007**, *131*, 861-872.
15. Al-Shamekh, S.; Goldberg, J.L. Retinal repair with induced pluripotent stem cells. *Transl Res* **2014**, *163*, 377-386.
16. Schenke-Layland, K.; Rhodes, K.E.; Angelis, E.; Butylkova, Y.; Heydarkhan-Hagvall, S.; Gekas, C.; Zhang, R.; Goldhaber, J.I.; Mikkola, H.K.; Plath, K.; MacLellan, W.R. Reprogrammed mouse fibroblasts differentiate into cells of the cardiovascular and hematopoietic lineages. *Stem Cells* **2008**, *26*, 1537-1546.
17. Zhang, J.; Wilson, G.F.; Soerens, A.G.; Koonce, C.H.; Yu, J.; Palecek, S.P.; Thomson, J.A.; Kamp, T.J. Functional cardiomyocytes derived from human induced pluripotent stem cells. *Circulation research* **2009**, *104*, e30-41.

18. Kempf, H.; Olmer, R.; Kropp, C.; Ruckert, M.; Jara-Avaca, M.; Robles-Diaz, D.; Franke, A.; Elliott, D.A.; Wojciechowski, D.; Fischer, M.; Roa Lara, A.; Kensah, G.; Gruh, I.; Haverich, A.; Martin, U.; Zweigerdt, R. Controlling expansion and cardiomyogenic differentiation of human pluripotent stem cells in scalable suspension culture. *Stem Cell Reports* **2014**, *3*, 1132-1146.
19. Yang, X.; Pabon, L.; Murry, C.E. Engineering adolescence: maturation of human pluripotent stem cell-derived cardiomyocytes. *Circulation research* **2014**, *114*, 511-523.
20. Chong, J.J.; Yang, X.; Don, C.W.; Minami, E.; Liu, Y.W.; Weyers, J.J.; Mahoney, W.M.; Van Biber, B.; Cook, S.M.; Palpant, N.J.; Gantz, J.A.; Fugate, J.A.; Muskheli, V.; Gough, G.M.; Vogel, K.W.; Astley, C.A.; Hotchkiss, C.E.; Baldessari, A.; Pabon, L.; Reinecke, H.; Gill, E.A.; Nelson, V.; Kiem, H.P.; Laflamme, M.A.; Murry, C.E. Human embryonic-stem-cell-derived cardiomyocytes regenerate non-human primate hearts. *Nature* **2014**, *510*, 273-277.
21. Friedenstein, A.J.; Petrakova, K.V.; Kurolesova, A.I.; Frolova, G.P. Heterotopic of bone marrow. Analysis of precursor cells for osteogenic and hematopoietic tissues. *Transplantation* **1968**, *6*, 230-247.
22. Dominici, M.; Le Blanc, K.; Mueller, I.; Slaper-Cortenbach, I.; Marini, F.; Krause, D.; Deans, R.; Keating, A.; Prockop, D.; Horwitz, E. Minimal criteria for defining multipotent mesenchymal stromal cells. The International Society for Cellular Therapy position statement. *Cytotherapy* **2006**, *8*, 315-317.
23. Zuk, P.A.; Zhu, M.; Ashjian, P.; De Ugarte, D.A.; Huang, J.I.; Mizuno, H.; Alfonso, Z.C.; Fraser, J.K.; Benhaim, P.; Hedrick, M.H. Human adipose tissue is a source of multipotent stem cells. *Mol Biol Cell* **2002**, *13*, 4279-4295.
24. In 't Anker, P.S.; Scherjon, S.A.; Kleijburg-van der Keur, C.; de Groot-Swings, G.M.; Claas, F.H.; Fibbe, W.E.; Kanhai, H.H. Isolation of mesenchymal stem cells of fetal or maternal origin from human placenta. *Stem Cells* **2004**, *22*, 1338-1345.
25. Kern, S.; Eichler, H.; Stoeve, J.; Kluter, H.; Bieback, K. Comparative analysis of mesenchymal stem cells from bone marrow, umbilical cord blood, or adipose tissue. *Stem Cells* **2006**, *24*, 1294-1301.
26. da Silva Meirelles, L.; Chagastelles, P.C.; Nardi, N.B. Mesenchymal stem cells reside in virtually all post-natal organs and tissues. *J Cell Sci* **2006**, *119*, 2204-2213.
27. Boyle, A.J.; McNiece, I.K.; Hare, J.M. Mesenchymal stem cell therapy for cardiac repair. *Methods Mol Biol* **2010**, *660*, 65-84.
28. Aslan, H.; Zilberman, Y.; Kandel, L.; Liebergall, M.; Oskouian, R.J.; Gazit, D.; Gazit, Z. Osteogenic differentiation of noncultured immunoisolated bone marrow-derived CD105+ cells. *Stem Cells* **2006**, *24*, 1728-1737.
29. Dallas, N.A.; Samuel, S.; Xia, L.; Fan, F.; Gray, M.J.; Lim, S.J.; Ellis, L.M. Endoglin (CD105): a marker of tumor vasculature and potential target for therapy. *Clin Cancer Res* **2008**, *14*, 1931-1937.
30. Gougos, A.; Letarte, M. Primary structure of endoglin, an RGD-containing glycoprotein of human endothelial cells. *The Journal of biological chemistry* **1990**, *265*, 8361-8364.
31. Barbara, N.P.; Wrana, J.L.; Letarte, M. Endoglin is an accessory protein that interacts with the signaling receptor complex of multiple members of the transforming growth factor-beta superfamily. *The Journal of biological chemistry* **1999**, *274*, 584-594.
32. Lopez-Novoa, J.M.; Bernabeu, C. The physiological role of endoglin in the cardiovascular system. *Am J Physiol Heart Circ Physiol* **2010**, *299*, H959-974.
33. ten Dijke, P.; Goumans, M.J.; Pardali, E. Endoglin in angiogenesis and vascular diseases. *Angiogenesis* **2008**, *11*, 79-89.
34. Pittenger, M.F.; Martin, B.J. Mesenchymal stem cells and their potential as cardiac therapeutics. *Circulation research* **2004**, *95*, 9-20.

35. Rombouts, W.J.; Ploemacher, R.E. Primary murine MSC show highly efficient homing to the bone marrow but lose homing ability following culture. *Leukemia* **2003**, *17*, 160-170.
36. Laflamme, M.A.; Murry, C.E. Regenerating the heart. *Nat Biotechnol* **2005**, *23*, 845-856.
37. Psaltis, P.J.; Zannettino, A.C.; Worthley, S.G.; Gronthos, S. Concise review: mesenchymal stromal cells: potential for cardiovascular repair. *Stem Cells* **2008**, *26*, 2201-2210.
38. Cao, L.; Liu, G.; Gan, Y.; Fan, Q.; Yang, F.; Zhang, X.; Tang, T.; Dai, K. The use of autologous enriched bone marrow MSCs to enhance osteoporotic bone defect repair in long-term estrogen deficient goats. *Biomaterials* **2012**, *33*, 5076-5084.
39. Dominguez-Bendala, J.; Lanzoni, G.; Inverardi, L.; Ricordi, C. Concise review: mesenchymal stem cells for diabetes. *Stem Cells Transl Med* **2012**, *1*, 59-63.
40. Ishikawa, T.; Banas, A.; Hagiwara, K.; Iwaguro, H.; Ochiya, T. Stem cells for hepatic regeneration: the role of adipose tissue derived mesenchymal stem cells. *Curr Stem Cell Res Ther* **2010**, *5*, 182-189.
41. Ringden, O.; Uzunel, M.; Rasmusson, I.; Remberger, M.; Sundberg, B.; Lonnies, H.; Marschall, H.U.; Dlugosz, A.; Szakos, A.; Hassan, Z.; Omazic, B.; Aschan, J.; Barkholt, L.; Le Blanc, K. Mesenchymal stem cells for treatment of therapy-resistant graft-versus-host disease. *Transplantation* **2006**, *81*, 1390-1397.
42. Karussis, D.; Karageorgiou, C.; Vaknin-Dembinsky, A.; Gowda-Kurkalli, B.; Gomori, J.M.; Kassis, I.; Bulte, J.W.; Petrou, P.; Ben-Hur, T.; Abramsky, O.; Slavin, S. Safety and immunological effects of mesenchymal stem cell transplantation in patients with multiple sclerosis and amyotrophic lateral sclerosis. *Arch Neurol* **2010**, *67*, 1187-1194.
43. Clinical Trials using mesenchymal stem cells. Available online: <https://clinicaltrials.gov/ct2/results?term=mesenchymal+stem+cells&recr=Open>
44. Yagi, H.; Soto-Gutierrez, A.; Parekkadan, B.; Kitagawa, Y.; Tompkins, R.G.; Kobayashi, N.; Yarmush, M.L. Mesenchymal stem cells: Mechanisms of immunomodulation and homing. *Cell Transplant* **2010**, *19*, 667-679.
45. Pittenger, M.F.; Mackay, A.M.; Beck, S.C.; Jaiswal, R.K.; Douglas, R.; Mosca, J.D.; Moorman, M.A.; Simonetti, D.W.; Craig, S.; Marshak, D.R. Multilineage potential of adult human mesenchymal stem cells. *Science* **1999**, *284*, 143-147.
46. Caplan, A.I. Mesenchymal stem cells. *J Orthop Res* **1991**, *9*, 641-650.
47. Silva, G.V.; Litovsky, S.; Assad, J.A.; Sousa, A.L.; Martin, B.J.; Vela, D.; Coulter, S.C.; Lin, J.; Ober, J.; Vaughn, W.K.; Branco, R.V.; Oliveira, E.M.; He, R.; Geng, Y.J.; Willerson, J.T.; Perin, E.C. Mesenchymal stem cells differentiate into an endothelial phenotype, enhance vascular density, and improve heart function in a canine chronic ischemia model. *Circulation* **2005**, *111*, 150-156.
48. Makino, S.; Fukuda, K.; Miyoshi, S.; Konishi, F.; Kodama, H.; Pan, J.; Sano, M.; Takahashi, T.; Hori, S.; Abe, H.; Hata, J.; Umezawa, A.; Ogawa, S. Cardiomyocytes can be generated from marrow stromal cells in vitro. *J Clin Invest* **1999**, *103*, 697-705.
49. Toma, C.; Pittenger, M.F.; Cahill, K.S.; Byrne, B.J.; Kessler, P.D. Human mesenchymal stem cells differentiate to a cardiomyocyte phenotype in the adult murine heart. *Circulation* **2002**, *105*, 93-98.
50. Siegel, G.; Krause, P.; Wohrle, S.; Nowak, P.; Ayturan, M.; Kluba, T.; Brehm, B.R.; Neumeister, B.; Kohler, D.; Rosenberger, P.; Just, L.; Northoff, H.; Schafer, R. Bone marrow-derived human mesenchymal stem cells express cardiomyogenic proteins but do not exhibit functional cardiomyogenic differentiation potential. *Stem cells and development* **2012**, *21*, 2457-2470.



51. Ankrum, J.; Karp, J.M. Mesenchymal stem cell therapy: Two steps forward, one step back. *Trends in molecular medicine* **2010**, *16*, 203-209.
52. Di Nicola, M.; Carlo-Stella, C.; Magni, M.; Milanese, M.; Longoni, P.D.; Matteucci, P.; Grisanti, S.; Gianni, A.M. Human bone marrow stromal cells suppress T-lymphocyte proliferation induced by cellular or nonspecific mitogenic stimuli. *Blood* **2002**, *99*, 3838-3843.
53. Zhang, W.; Ge, W.; Li, C.; You, S.; Liao, L.; Han, Q.; Deng, W.; Zhao, R.C. Effects of mesenchymal stem cells on differentiation, maturation, and function of human monocyte-derived dendritic cells. *Stem cells and development* **2004**, *13*, 263-271.
54. Zhang, B.; Liu, R.; Shi, D.; Liu, X.; Chen, Y.; Dou, X.; Zhu, X.; Lu, C.; Liang, W.; Liao, L.; Zenke, M.; Zhao, R.C. Mesenchymal stem cells induce mature dendritic cells into a novel Jagged-2-dependent regulatory dendritic cell population. *Blood* **2009**, *113*, 46-57.
55. Corcione, A.; Benvenuto, F.; Ferretti, E.; Giunti, D.; Cappiello, V.; Cazzanti, F.; Risso, M.; Gualandi, F.; Mancardi, G.L.; Pistoia, V.; Uccelli, A. Human mesenchymal stem cells modulate B-cell functions. *Blood* **2006**, *107*, 367-372.
56. Asari, S.; Itakura, S.; Ferreri, K.; Liu, C.P.; Kuroda, Y.; Kandeel, F.; Mullen, Y. Mesenchymal stem cells suppress B-cell terminal differentiation. *Exp Hematol* **2009**, *37*, 604-615.
57. Spaggiari, G.M.; Capobianco, A.; Becchetti, S.; Mingari, M.C.; Moretta, L. Mesenchymal stem cell-natural killer cell interactions: evidence that activated NK cells are capable of killing MSCs, whereas MSCs can inhibit IL-2-induced NK-cell proliferation. *Blood* **2006**, *107*, 1484-1490.
58. English, K.; Ryan, J.M.; Tobin, L.; Murphy, M.J.; Barry, F.P.; Mahon, B.P. Cell contact, prostaglandin E(2) and transforming growth factor beta 1 play non-redundant roles in human mesenchymal stem cell induction of CD4+CD25(High) forkhead box P3+ regulatory T cells. *Clin Exp Immunol* **2009**, *156*, 149-160.
59. Matthay, M.A.; Thompson, B.T.; Read, E.J.; McKenna, D.H., Jr.; Liu, K.D.; Calfee, C.S.; Lee, J.W. Therapeutic potential of mesenchymal stem cells for severe acute lung injury. *Chest* **2010**, *138*, 965-972.
60. Otto, W.R.; Wright, N.A. Mesenchymal stem cells: from experiment to clinic. *Fibrogenesis Tissue Repair* **2011**, *4*, 20.
61. Song, H.; Song, B.W.; Cha, M.J.; Choi, I.G.; Hwang, K.C. Modification of mesenchymal stem cells for cardiac regeneration. *Expert opinion on biological therapy* **2010**, *10*, 309-319.
62. Kofidis, T.; de Bruin, J.L.; Yamane, T.; Balsam, L.B.; Lebl, D.R.; Swijnenburg, R.J.; Tanaka, M.; Weissman, I.L.; Robbins, R.C. Insulin-like growth factor promotes engraftment, differentiation, and functional improvement after transfer of embryonic stem cells for myocardial restoration. *Stem Cells* **2004**, *22*, 1239-1245.
63. Hahn, J.Y.; Cho, H.J.; Kang, H.J.; Kim, T.S.; Kim, M.H.; Chung, J.H.; Bae, J.W.; Oh, B.H.; Park, Y.B.; Kim, H.S. Pre-treatment of mesenchymal stem cells with a combination of growth factors enhances gap junction formation, cytoprotective effect on cardiomyocytes, and therapeutic efficacy for myocardial infarction. *J Am Coll Cardiol* **2008**, *51*, 933-943.
64. Pasha, Z.; Wang, Y.; Sheikh, R.; Zhang, D.; Zhao, T.; Ashraf, M. Preconditioning enhances cell survival and differentiation of stem cells during transplantation in infarcted myocardium. *Cardiovascular research* **2008**, *77*, 134-142.
65. Herrmann, J.L.; Wang, Y.; Abarbanell, A.M.; Weil, B.R.; Tan, J.; Meldrum, D.R. Preconditioning mesenchymal stem cells with transforming growth factor-alpha improves mesenchymal stem cell-mediated cardioprotection. *Shock* **2010**, *33*, 24-30.

66. Yang, Y.J.; Qian, H.Y.; Huang, J.; Geng, Y.J.; Gao, R.L.; Dou, K.F.; Yang, G.S.; Li, J.J.; Shen, R.; He, Z.X.; Lu, M.J.; Zhao, S.H. Atorvastatin treatment improves survival and effects of implanted mesenchymal stem cells in post-infarct swine hearts. *Eur Heart J* **2008**, *29*, 1578-1590.
67. Song, L.; Yang, Y.J.; Dong, Q.T.; Qian, H.Y.; Gao, R.L.; Qiao, S.B.; Shen, R.; He, Z.X.; Lu, M.J.; Zhao, S.H.; Geng, Y.J.; Gersh, B.J. Atorvastatin enhance efficacy of mesenchymal stem cells treatment for swine myocardial infarction via activation of nitric oxide synthase. *PloS one* **2013**, *8*, e65702.
68. Erwin, G.S.; Crisostomo, P.R.; Wang, Y.; Wang, M.; Markel, T.A.; Guzman, M.; Sando, I.C.; Sharma, R.; Meldrum, D.R. Estradiol-treated mesenchymal stem cells improve myocardial recovery after ischemia. *The Journal of surgical research* **2009**, *152*, 319-324.
69. Liu, X.; Hou, J.; Shi, L.; Chen, J.; Sang, J.; Hu, S.; Cong, X.; Chen, X. Lysophosphatidic acid protects mesenchymal stem cells against ischemia-induced apoptosis in vivo. *Stem cells and development* **2009**, *18*, 947-954.
70. Choudhery, M.S.; Badowski, M.; Muise, A.; Harris, D.T. Effect of mild heat stress on the proliferative and differentiative ability of human mesenchymal stromal cells. *Cytotherapy* **2014**.
71. Hu, X.; Yu, S.P.; Fraser, J.L.; Lu, Z.; Ogle, M.E.; Wang, J.A.; Wei, L. Transplantation of hypoxia-preconditioned mesenchymal stem cells improves infarcted heart function via enhanced survival of implanted cells and angiogenesis. *J Thorac Cardiovasc Surg* **2008**, *135*, 799-808.
72. Lu, H.H.; Li, Y.F.; Sheng, Z.Q.; Wang, Y. Preconditioning of stem cells for the treatment of myocardial infarction. *Chinese medical journal* **2012**, *125*, 378-384.
73. Beegle, J.; Lakatos, K.; Kalomoiris, S.; Stewart, H.; Isseroff, R.R.; Nolta, J.A.; Fierro, F.A. Hypoxic Preconditioning of Mesenchymal Stromal Cells Induces Metabolic Changes, Enhances Survival and Promotes Cell Retention in Vivo. *Stem Cells* **2015**.
74. Samper, E.; Diez-Juan, A.; Montero, J.A.; Sepulveda, P. Cardiac cell therapy: boosting mesenchymal stem cells effects. *Stem Cell Rev* **2013**, *9*, 266-280.
75. Karvinen, H.; Yla-Herttuala, S. New aspects in vascular gene therapy. *Curr Opin Pharmacol* **2010**, *10*, 208-211.
76. Sluijter, J.P.; Condorelli, G.; Davidson, S.M.; Engel, F.B.; Ferdinandy, P.; Hausenloy, D.J.; Lecour, S.; Madonna, R.; Ovize, M.; Ruiz-Meana, M.; Schulz, R.; Van Laake, L.W. Novel therapeutic strategies for cardioprotection. *Pharmacol Ther* **2014**, *144*, 60-70.
77. Wang, X.; Zhao, T.; Huang, W.; Wang, T.; Qian, J.; Xu, M.; Kranias, E.G.; Wang, Y.; Fan, G.C. Hsp20-engineered mesenchymal stem cells are resistant to oxidative stress via enhanced activation of Akt and increased secretion of growth factors. *Stem Cells* **2009**, *27*, 3021-3031.
78. Li, W.; Ma, N.; Ong, L.L.; Nesselmann, C.; Klopsch, C.; Ladilov, Y.; Furlani, D.; Piechaczek, C.; Moebius, J.M.; Lutzow, K.; Lendlein, A.; Stamm, C.; Li, R.K.; Steinhoff, G. Bcl-2 engineered MSCs inhibited apoptosis and improved heart function. *Stem Cells* **2007**, *25*, 2118-2127.
79. Gneocchi, M.; He, H.; Liang, O.D.; Melo, L.G.; Morello, F.; Mu, H.; Noiseux, N.; Zhang, L.; Pratt, R.E.; Ingwall, J.S.; Dzau, V.J. Paracrine action accounts for marked protection of ischemic heart by Akt-modified mesenchymal stem cells. *Nat Med* **2005**, *11*, 367-368.

80. Gneccchi, M.; He, H.; Noiseux, N.; Liang, O.D.; Zhang, L.; Morello, F.; Mu, H.; Melo, L.G.; Pratt, R.E.; Ingwall, J.S.; Dzau, V.J. Evidence supporting paracrine hypothesis for Akt-modified mesenchymal stem cell-mediated cardiac protection and functional improvement. *FASEB journal : official publication of the Federation of American Societies for Experimental Biology* **2006**, *20*, 661-669.
81. Jiang, Y.; Chen, L.; Tang, Y.; Ma, G.; Shen, C.; Qi, C.; Zhu, Q.; Yao, Y.; Liu, N. HO-1 gene overexpression enhances the beneficial effects of superparamagnetic iron oxide labeled bone marrow stromal cells transplantation in swine hearts underwent ischemia/reperfusion: an MRI study. *Basic Res Cardiol* **2010**, *105*, 431-442.
82. Grauss, R.W.; van Tuyn, J.; Steendijk, P.; Winter, E.M.; Pijnappels, D.A.; Hogers, B.; Gittenberger-De Groot, A.C.; van der Geest, R.; van der Laarse, A.; de Vries, A.A.; Schalij, M.J.; Atsma, D.E. Forced myocardin expression enhances the therapeutic effect of human mesenchymal stem cells after transplantation in ischemic mouse hearts. *Stem Cells* **2008**, *26*, 1083-1093.
83. Penn, M.S. Cell-based gene therapy for the prevention and treatment of cardiac dysfunction. *Nat Clin Pract Cardiovasc Med* **2007**, *4 Suppl 1*, S83-88.
84. Douglas, M.R. Gene therapy for Parkinson's disease: state-of-the-art treatments for neurodegenerative disease. *Expert Rev Neurother* **2013**, *13*, 695-705.
85. Duarte, S.; Carle, G.; Faneca, H.; de Lima, M.C.; Pierrefite-Carle, V. Suicide gene therapy in cancer: where do we stand now? *Cancer Lett* **2012**, *324*, 160-170.
86. Olowoyeye, A.; Okwundu, C.I. Gene therapy for sickle cell disease. *Cochrane Database Syst Rev* **2014**, *10*, CD007652.
87. Sharma, A.; Easow Mathew, M.; Sriganesh, V.; Neely, J.A.; Kalipatnapu, S. Gene therapy for haemophilia. *Cochrane Database Syst Rev* **2014**, *11*, CD010822.
88. Vile, R.G.; Russell, S.J.; Lemoine, N.R. Cancer gene therapy: hard lessons and new courses. *Gene therapy* **2000**, *7*, 2-8.
89. Ulrich, H.; Trujillo, C.A.; Nery, A.A.; Alves, J.M.; Majumder, P.; Resende, R.R.; Martins, A.H. DNA and RNA aptamers: from tools for basic research towards therapeutic applications. *Comb Chem High Throughput Screen* **2006**, *9*, 619-632.
90. Spiel, A.O.; Mayr, F.B.; Ladani, N.; Wagner, P.G.; Schaub, R.G.; Gilbert, J.C.; Jilma, B. The aptamer ARC1779 is a potent and specific inhibitor of von Willebrand Factor mediated ex vivo platelet function in acute myocardial infarction. *Platelets* **2009**, *20*, 334-340.
91. Akhtar, S.; Hughes, M.D.; Khan, A.; Bibby, M.; Hussain, M.; Nawaz, Q.; Double, J.; Sayyed, P. The delivery of antisense therapeutics. *Adv Drug Deliv Rev* **2000**, *44*, 3-21.
92. Rayner, B.S.; Figtree, G.A.; Sabaretnam, T.; Shang, P.; Mazhar, J.; Weaver, J.C.; Lay, W.N.; Witting, P.K.; Hunyor, S.N.; Grieve, S.M.; Khachigian, L.M.; Bhindi, R. Selective inhibition of the master regulator transcription factor Egr-1 with catalytic oligonucleotides reduces myocardial injury and improves left ventricular systolic function in a preclinical model of myocardial infarction. *J Am Heart Assoc* **2013**, *2*, e000023.
93. Fechner, H.; Wang, X.; Srouf, M.; Siemetzki, U.; Seltsmann, H.; Sutter, A.P.; Scherubl, H.; Zouboulis, C.C.; Schwaab, R.; Hillen, W.; Schultheiss, H.P.; Poller, W. A novel tetracycline-controlled transactivator-transrepressor system enables external control of oncolytic adenovirus replication. *Gene therapy* **2003**, *10*, 1680-1690.
94. Zhang, H.; Takayama, K.; Zhang, L.; Uchino, J.; Harada, A.; Harada, T.; Hisasue, J.; Nakagaki, N.; Zhou, C.; Nakanishi, Y. Tetracycline-inducible promoter-based conditionally replicative adenoviruses for the control of viral replication. *Cancer gene therapy* **2009**, *16*, 415-422.

95. Binley, K.; Askham, Z.; Iqball, S.; Spearman, H.; Martin, L.; de Alwis, M.; Thrasher, A.J.; Ali, R.R.; Maxwell, P.H.; Kingsman, S.; Naylor, S. Long-term reversal of chronic anemia using a hypoxia-regulated erythropoietin gene therapy. *Blood* **2002**, *100*, 2406-2413.
96. Binley, K.; Iqball, S.; Kingsman, A.; Kingsman, S.; Naylor, S. An adenoviral vector regulated by hypoxia for the treatment of ischaemic disease and cancer. *Gene therapy* **1999**, *6*, 1721-1727.
97. Glover, D.J.; Leyton, D.L.; Moseley, G.W.; Jans, D.A. The efficiency of nuclear plasmid DNA delivery is a critical determinant of transgene expression at the single cell level. *The journal of gene medicine* **2010**, *12*, 77-85.
98. Moore, P.S.; Chang, Y. Why do viruses cause cancer? Highlights of the first century of human tumour virology. *Nat Rev Cancer* **2010**, *10*, 878-889.
99. Yakubov, E.; Rechavi, G.; Rozenblatt, S.; Givol, D. Reprogramming of human fibroblasts to pluripotent stem cells using mRNA of four transcription factors. *Biochemical and biophysical research communications* **2010**, *394*, 189-193.
100. Hausburg, F.; Na, S.; Voronina, N.; Skorska, A.; Muller, P.; Steinhoff, G.; David, R. Defining Optimized Properties of Modified mRNA to Enhance Virus- and DNA-Independent Protein Expression in Adult Stem Cells and Fibroblasts. *Cell Physiol Biochem* **2015**, *35*, 1360-1371.
101. Dunham, I.; Kundaje, A.; Aldred, S.; Collins, P.; Davis, C.; Doyle, F.; Epstein, C. An integrated encyclopedia of DNA elements in the human genome. *Nature* **2012**, *489*, 57-74.
102. Ounzain, S.; Micheletti, R.; Beckmann, T.; Schroen, B.; Alexanian, M.; Pezzuto, I.; Crippa, S.; Nemir, M.; Sarre, A.; Johnson, R.; Dauvillier, J.; Burdet, F.; Ibberson, M.; Guigo, R.; Xenarios, I.; Heymans, S.; Pedrazzini, T. Genome-wide profiling of the cardiac transcriptome after myocardial infarction identifies novel heart-specific long non-coding RNAs. *Eur Heart J* **2015**, *36*, 353-368.
103. Ounzain, S.; Crippa, S.; Pedrazzini, T. Small and long non-coding RNAs in cardiac homeostasis and regeneration. *Biochimica et biophysica acta* **2013**, *1833*, 923-933.
104. Zhao, J.; Sun, B.K.; Erwin, J.A.; Song, J.J.; Lee, J.T. Polycomb proteins targeted by a short repeat RNA to the mouse X chromosome. *Science* **2008**, *322*, 750-756.
105. Latos, P.A.; Pauler, F.M.; Koerner, M.V.; Senergin, H.B.; Hudson, Q.J.; Stocsits, R.R.; Allhoff, W.; Stricker, S.H.; Klement, R.M.; Warczok, K.E.; Aumayr, K.; Pasierbek, P.; Barlow, D.P. Airn transcriptional overlap, but not its lncRNA products, induces imprinted Igf2r silencing. *Science* **2012**, *338*, 1469-1472.
106. Tripathi, V.; Ellis, J.D.; Shen, Z.; Song, D.Y.; Pan, Q.; Watt, A.T.; Freier, S.M.; Bennett, C.F.; Sharma, A.; Bubulya, P.A.; Blencowe, B.J.; Prasanth, S.G.; Prasanth, K.V. The nuclear-retained noncoding RNA MALAT1 regulates alternative splicing by modulating SR splicing factor phosphorylation. *Mol Cell* **2010**, *39*, 925-938.
107. Tsai, M.C.; Manor, O.; Wan, Y.; Mosammaparast, N.; Wang, J.K.; Lan, F.; Shi, Y.; Segal, E.; Chang, H.Y. Long noncoding RNA as modular scaffold of histone modification complexes. *Science* **2010**, *329*, 689-693.
108. Klattenhoff, C.A.; Scheuermann, J.C.; Surface, L.E.; Bradley, R.K.; Fields, P.A.; Steinhäuser, M.L.; Ding, H.; Butty, V.L.; Torrey, L.; Haas, S.; Abo, R.; Tabeboardbar, M.; Lee, R.T.; Burge, C.B.; Boyer, L.A. Braveheart, a long noncoding RNA required for cardiovascular lineage commitment. *Cell* **2013**, *152*, 570-583.

109. Loewer, S.; Cabili, M.N.; Guttman, M.; Loh, Y.H.; Thomas, K.; Park, I.H.; Garber, M.; Curran, M.; Onder, T.; Agarwal, S.; Manos, P.D.; Datta, S.; Lander, E.S.; Schlaeger, T.M.; Daley, G.Q.; Rinn, J.L. Large intergenic non-coding RNA-RoR modulates reprogramming of human induced pluripotent stem cells. *Nat Genet* **2010**, *42*, 1113-1117.
110. Carthew, R.W.; Sontheimer, E.J. Origins and Mechanisms of miRNAs and siRNAs. *Cell* **2009**, *136*, 642-655.
111. Golden, D.E.; Gerbasi, V.R.; Sontheimer, E.J. An inside job for siRNAs. *Mol Cell* **2008**, *31*, 309-312.
112. Hannon, G.J. RNA interference. *Nature* **2002**, *418*, 244-251.
113. Tu, S.; Liu, Z.Q.; Fu, J.J.; Zhu, W.F.; Luo, D.Y.; Wan, F.S. Inhibitory effect of p53 upregulated modulator of apoptosis targeting siRNA on hypoxia/reoxygenation-induced cardiomyocyte apoptosis in rats. *Cardiology* **2012**, *122*, 93-100.
114. Kim, D.; Hong, J.; Moon, H.H.; Nam, H.Y.; Mok, H.; Jeong, J.H.; Kim, S.W.; Choi, D.; Kim, S.H. Anti-apoptotic cardioprotective effects of SHP-1 gene silencing against ischemia-reperfusion injury: use of deoxycholic acid-modified low molecular weight polyethyleneimine as a cardiac siRNA-carrier. *Journal of controlled release : official journal of the Controlled Release Society* **2013**, *168*, 125-134.
115. Kumarswamy, R.; Thum, T. Non-coding RNAs in cardiac remodeling and heart failure. *Circulation research* **2013**, *113*, 676-689.
116. Liu, N.; Olson, E.N. MicroRNA regulatory networks in cardiovascular development. *Dev Cell* **2010**, *18*, 510-525.
117. Jakob, P.; Landmesser, U. Role of microRNAs in stem/progenitor cells and cardiovascular repair. *Cardiovascular research* **2012**, *93*, 614-622.
118. Eulalio, A.; Mano, M.; Dal Ferro, M.; Zentilin, L.; Sinagra, G.; Zacchigna, S.; Giacca, M. Functional screening identifies miRNAs inducing cardiac regeneration. *Nature* **2012**, *492*, 376-381.
119. Yau, W.W.; Rujitanaroj, P.O.; Lam, L.; Chew, S.Y. Directing stem cell fate by controlled RNA interference. *Biomaterials* **2012**, *33*, 2608-2628.
120. Ozcan, G.; Ozpolat, B.; Coleman, R.L.; Sood, A.K.; Lopez-Berestein, G. Preclinical and clinical development of siRNA-based therapeutics. *Adv Drug Deliv Rev* **2015**.
121. Hwang, H.W.; Mendell, J.T. MicroRNAs in cell proliferation, cell death, and tumorigenesis. *Br J Cancer* **2007**, *96 Suppl*, R40-44.
122. Ambros, V. The functions of animal microRNAs. *Nature* **2004**, *431*, 350-355.
123. Guo, L.; Zhao, R.C.; Wu, Y. The role of microRNAs in self-renewal and differentiation of mesenchymal stem cells. *Exp Hematol* **2011**, *39*, 608-616.
124. Small, E.M.; Olson, E.N. Pervasive roles of microRNAs in cardiovascular biology. *Nature* **2011**, *469*, 336-342.
125. Cordes, K.R.; Srivastava, D. MicroRNA regulation of cardiovascular development. *Circulation research* **2009**, *104*, 724-732.
126. Yang, W.J.; Yang, D.D.; Na, S.; Sandusky, G.E.; Zhang, Q.; Zhao, G. Dicer is required for embryonic angiogenesis during mouse development. *The Journal of biological chemistry* **2005**, *280*, 9330-9335.
127. van Rooij, E.; Sutherland, L.B.; Thatcher, J.E.; DiMaio, J.M.; Naseem, R.H.; Marshall, W.S.; Hill, J.A.; Olson, E.N. Dysregulation of microRNAs after myocardial infarction reveals a role of miR-29 in cardiac fibrosis. *Proceedings of the National Academy of Sciences of the United States of America* **2008**, *105*, 13027-13032.

128. Shan, Z.X.; Lin, Q.X.; Fu, Y.H.; Deng, C.Y.; Zhou, Z.L.; Zhu, J.N.; Liu, X.Y.; Zhang, Y.Y.; Li, Y.; Lin, S.G.; Yu, X.Y. Upregulated expression of miR-1/miR-206 in a rat model of myocardial infarction. *Biochemical and biophysical research communications* **2009**, *381*, 597-601.
129. van Rooij, E.; Olson, E.N. MicroRNA therapeutics for cardiovascular disease: opportunities and obstacles. *Nat Rev Drug Discov* **2012**, *11*, 860-872.
130. Hullinger, T.G.; Montgomery, R.L.; Seto, A.G.; Dickinson, B.A.; Semus, H.M.; Lynch, J.M.; Dalby, C.M.; Robinson, K.; Stack, C.; Latimer, P.A.; Hare, J.M.; Olson, E.N.; van Rooij, E. Inhibition of miR-15 protects against cardiac ischemic injury. *Circulation research* **2012**, *110*, 71-81.
131. Porrello, E.R.; Mahmoud, A.I.; Simpson, E.; Johnson, B.A.; Grinsfelder, D.; Canseco, D.; Mammen, P.P.; Rothmel, B.A.; Olson, E.N.; Sadek, H.A. Regulation of neonatal and adult mammalian heart regeneration by the miR-15 family. *Proceedings of the National Academy of Sciences of the United States of America* **2013**, *110*, 187-192.
132. Bonauer, A.; Carmona, G.; Iwasaki, M.; Mione, M.; Koyanagi, M.; Fischer, A.; Burchfield, J.; Fox, H.; Doebele, C.; Ohtani, K.; Chavakis, E.; Potente, M.; Tjwa, M.; Urbich, C.; Zeiher, A.M.; Dimmeler, S. MicroRNA-92a controls angiogenesis and functional recovery of ischemic tissues in mice. *Science* **2009**, *324*, 1710-1713.
133. Boon, R.A.; Iekushi, K.; Lechner, S.; Seeger, T.; Fischer, A.; Heydt, S.; Kaluza, D.; Treguer, K.; Carmona, G.; Bonauer, A.; Horrevoets, A.J.; Didier, N.; Girmatsion, Z.; Biliczki, P.; Ehrlich, J.R.; Katus, H.A.; Muller, O.J.; Potente, M.; Zeiher, A.M.; Hermeking, H.; Dimmeler, S. MicroRNA-34a regulates cardiac ageing and function. *Nature* **2013**, *495*, 107-110.
134. Hu, S.; Huang, M.; Li, Z.; Jia, F.; Ghosh, Z.; Lijkwan, M.A.; Fasanaro, P.; Sun, N.; Wang, X.; Martelli, F.; Robbins, R.C.; Wu, J.C. MicroRNA-210 as a novel therapy for treatment of ischemic heart disease. *Circulation* **2010**, *122*, S124-131.
135. Zhang, L.L.; Liu, J.J.; Liu, F.; Liu, W.H.; Wang, Y.S.; Zhu, B.; Yu, B. MiR-499 induces cardiac differentiation of rat mesenchymal stem cells through wnt/beta-catenin signaling pathway. *Biochemical and biophysical research communications* **2012**, *420*, 875-881.
136. Huang, F.; Li, M.L.; Fang, Z.F.; Hu, X.Q.; Liu, Q.M.; Liu, Z.J.; Tang, L.; Zhao, Y.S.; Zhou, S.H. Overexpression of MicroRNA-1 improves the efficacy of mesenchymal stem cell transplantation after myocardial infarction. *Cardiology* **2013**, *125*, 18-30.
137. Dakhllallah, D.; Zhang, J.; Yu, L.; Marsh, C.B.; Angelos, M.G.; Khan, M. MicroRNA-133a Engineered Mesenchymal Stem Cells Augment Cardiac Function and Cell Survival in the Infarct Heart. *J Cardiovasc Pharmacol* **2015**, *65*, 241-251.
138. Wen, Z.; Huang, W.; Feng, Y.; Cai, W.; Wang, Y.; Wang, X.; Liang, J.; Wani, M.; Chen, J.; Zhu, P.; Chen, J.M.; Millard, R.W.; Fan, G.C. MicroRNA-377 regulates mesenchymal stem cell-induced angiogenesis in ischemic hearts by targeting VEGF. *PLoS One* **2014**, *9*, e104666.
139. Xing, Y.; Hou, J.; Guo, T.; Zheng, S.; Zhou, C.; Huang, H.; Chen, Y.; Sun, K.; Zhong, T.; Wang, J.; Li, H.; Wang, T. MicroRNA-378 promotes mesenchymal stem cells survival and vascularization under hypoxic-ischemic condition in vitro. *Stem Cell Res Ther* **2014**, *5*, 130.
140. Xu, J.; Ren, D.; Fu, M.; Gao, Y.; Lou, Y.; Cai, S.; Qian, J.; Ge, J. [MicroRNA-210 mediates the protective effect of rosuvastatin on human mesenchymal stem cells apoptosis induced by tumor necrosis factor-alpha]. *Zhonghua Xin Xue Guan Bing Za Zhi* **2014**, *42*, 932-937.

141. Huang, F.; Zhu, X.; Hu, X.Q.; Fang, Z.F.; Tang, L.; Lu, X.L.; Zhou, S.H. Mesenchymal stem cells modified with miR-126 release angiogenic factors and activate Notch ligand Delta-like-4, enhancing ischemic angiogenesis and cell survival. *International journal of molecular medicine* **2013**, *31*, 484-492.
142. Iekushi, K.; Seeger, F.; Assmus, B.; Zeiher, A.M.; Dimmeler, S. Regulation of cardiac microRNAs by bone marrow mononuclear cell therapy in myocardial infarction. *Circulation* **2012**, *125*, 1765-1773, S1761-1767.
143. Suzuki, Y.; Kim, H.W.; Ashraf, M.; Haider, H. Diazoxide potentiates mesenchymal stem cell survival via NF-kappaB-dependent miR-146a expression by targeting Fas. *Am J Physiol Heart Circ Physiol* **2010**, *299*, H1077-1082.
144. Tome, M.; Lopez-Romero, P.; Albo, C.; Sepulveda, J.C.; Fernandez-Gutierrez, B.; Dopazo, A.; Bernad, A.; Gonzalez, M.A. miR-335 orchestrates cell proliferation, migration and differentiation in human mesenchymal stem cells. *Cell death and differentiation* **2011**, *18*, 985-995.
145. Wen, Z.; Zheng, S.; Zhou, C.; Yuan, W.; Wang, J.; Wang, T. Bone marrow mesenchymal stem cells for post-myocardial infarction cardiac repair: microRNAs as novel regulators. *Journal of cellular and molecular medicine* **2012**, *16*, 657-671.
146. Zhang, Y.; Wang, Z.; Gemeinhart, R.A. Progress in microRNA delivery. *Journal of controlled release : official journal of the Controlled Release Society* **2013**, *172*, 962-974.
147. Boulaiz, H.; Marchal, J.A.; Prados, J.; Melguizo, C.; Aranega, A. Non-viral and viral vectors for gene therapy. *Cellular and molecular biology* **2005**, *51*, 3-22.
148. Ramamoorth, M.; Narvekar, A. Non viral vectors in gene therapy- an overview. *J Clin Diagn Res* **2015**, *9*, GE01-06.
149. Thomas, C.E.; Ehrhardt, A.; Kay, M.A. Progress and problems with the use of viral vectors for gene therapy. *Nat Rev Genet* **2003**, *4*, 346-358.
150. Al-Dosari, M.S.; Gao, X. Nonviral gene delivery: principle, limitations, and recent progress. *The AAPS journal* **2009**, *11*, 671-681.
151. Caporali, A.; Meloni, M.; Vollenkle, C.; Bonci, D.; Sala-Newby, G.B.; Addis, R.; Spinetti, G.; Losa, S.; Masson, R.; Baker, A.H.; Agami, R.; le Sage, C.; Condorelli, G.; Madeddu, P.; Martelli, F.; Emanuelli, C. Deregulation of microRNA-503 contributes to diabetes mellitus-induced impairment of endothelial function and reparative angiogenesis after limb ischemia. *Circulation* **2011**, *123*, 282-291.
152. Chen, J.J.; Zhou, S.H. Mesenchymal stem cells overexpressing MiR-126 enhance ischemic angiogenesis via the AKT/ERK-related pathway. *Cardiology journal* **2011**, *18*, 675-681.
153. Fish, J.E.; Santoro, M.M.; Morton, S.U.; Yu, S.; Yeh, R.F.; Wythe, J.D.; Ivey, K.N.; Bruneau, B.G.; Stainier, D.Y.; Srivastava, D. miR-126 regulates angiogenic signaling and vascular integrity. *Dev Cell* **2008**, *15*, 272-284.
154. Mutharasan, R.K.; Nagpal, V.; Ichikawa, Y.; Ardehali, H. microRNA-210 is upregulated in hypoxic cardiomyocytes through Akt- and p53-dependent pathways and exerts cytoprotective effects. *Am J Physiol Heart Circ Physiol* **2011**, *301*, H1519-1530.
155. Wang, S.; Aurora, A.B.; Johnson, B.A.; Qi, X.; McAnally, J.; Hill, J.A.; Richardson, J.A.; Bassel-Duby, R.; Olson, E.N. The endothelial-specific microRNA miR-126 governs vascular integrity and angiogenesis. *Dev Cell* **2008**, *15*, 261-271.
156. Li, Z.; Rana, T.M. Therapeutic targeting of microRNAs: current status and future challenges. *Nat Rev Drug Discov* **2014**, *13*, 622-638.
157. Scholz, C.; Wagner, E. Therapeutic plasmid DNA versus siRNA delivery: common and different tasks for synthetic carriers. *Journal of controlled release : official journal of the Controlled Release Society* **2012**, *161*, 554-565.

158. Reischl, D.; Zimmer, A. Drug delivery of siRNA therapeutics: potentials and limits of nanosystems. *Nanomedicine* **2009**, *5*, 8-20.
159. Fan, Y.; Xin, X.Y.; Chen, B.L.; Ma, X. Knockdown of RAB25 expression by RNAi inhibits growth of human epithelial ovarian cancer cells in vitro and in vivo. *Pathology* **2006**, *38*, 561-567.
160. Hagemann, C.; Meyer, C.; Stojic, J.; Eicker, S.; Gerngras, S.; Kuhnel, S.; Roosen, K.; Vince, G.H. High efficiency transfection of glioma cell lines and primary cells for overexpression and RNAi experiments. *J Neurosci Methods* **2006**, *156*, 194-202.
161. Tano, N.; Kim, H.W.; Ashraf, M. microRNA-150 regulates mobilization and migration of bone marrow-derived mononuclear cells by targeting Cxcr4. *PloS one* **2011**, *6*, e23114.
162. Gao, X.; Kim, K.S.; Liu, D. Nonviral gene delivery: what we know and what is next. *The AAPS journal* **2007**, *9*, E92-104.
163. Khatri, N.; Rath, M.; Baradia, D.; Trehan, S.; Misra, A. In vivo delivery aspects of miRNA, shRNA and siRNA. *Critical reviews in therapeutic drug carrier systems* **2012**, *29*, 487-527.
164. Pereira, D.M.; Rodrigues, P.M.; Borralho, P.M.; Rodrigues, C.M. Delivering the promise of miRNA cancer therapeutics. *Drug Discov Today* **2013**, *18*, 282-289.
165. Park, T.G.; Jeong, J.H.; Kim, S.W. Current status of polymeric gene delivery systems. *Adv Drug Deliv Rev* **2006**, *58*, 467-486.
166. Felgner, P.L.; Gadek, T.R.; Holm, M.; Roman, R.; Chan, H.W.; Wenz, M.; Northrop, J.P.; Ringold, G.M.; Danielsen, M. Lipofection: a highly efficient, lipid-mediated DNA-transfection procedure. *Proceedings of the National Academy of Sciences of the United States of America* **1987**, *84*, 7413-7417.
167. Xu, Y.; Szoka, F.C., Jr. Mechanism of DNA release from cationic liposome/DNA complexes used in cell transfection. *Biochemistry* **1996**, *35*, 5616-5623.
168. Alaiti, M.A.; Ishikawa, M.; Masuda, H.; Simon, D.I.; Jain, M.K.; Asahara, T.; Costa, M.A. Up-regulation of miR-210 by vascular endothelial growth factor in ex vivo expanded CD34+ cells enhances cell-mediated angiogenesis. *J Cell Mol Med* **2012**, *16*, 2413-2421.
169. O'Mahony, A.M.; Godinho, B.M.; Cryan, J.F.; O'Driscoll, C.M. Non-viral nanosystems for gene and small interfering RNA delivery to the central nervous system: formulating the solution. *J Pharm Sci* **2013**, *102*, 3469-3484.
170. Lv, H.; Zhang, S.; Wang, B.; Cui, S.; Yan, J. Toxicity of cationic lipids and cationic polymers in gene delivery. *Journal of controlled release : official journal of the Controlled Release Society* **2006**, *114*, 100-109.
171. Pathak, A.; Patnaik, S.; Gupta, K.C. Recent trends in non-viral vector-mediated gene delivery. *Biotechnology journal* **2009**, *4*, 1559-1572.
172. Urban-Klein, B.; Werth, S.; Abuharbeid, S.; Czubayko, F.; Aigner, A. RNAi-mediated gene-targeting through systemic application of polyethylenimine (PEI)-complexed siRNA in vivo. *Gene therapy* **2005**, *12*, 461-466.
173. de Fougerolles, A.R. Delivery vehicles for small interfering RNA in vivo. *Human gene therapy* **2008**, *19*, 125-132.
174. Boussif, O.; Lezoualc'h, F.; Zanta, M.A.; Mergny, M.D.; Scherman, D.; Demeneix, B.; Behr, J.P. A versatile vector for gene and oligonucleotide transfer into cells in culture and in vivo: polyethylenimine. *Proceedings of the National Academy of Sciences of the United States of America* **1995**, *92*, 7297-7301.
175. Pack, D.W.; Hoffman, A.S.; Pun, S.; Stayton, P.S. Design and development of polymers for gene delivery. *Nat Rev Drug Discov* **2005**, *4*, 581-593.



176. Ibrahim, A.F.; Weirauch, U.; Thomas, M.; Grunweller, A.; Hartmann, R.K.; Aigner, A. MicroRNA replacement therapy for miR-145 and miR-33a is efficacious in a model of colon carcinoma. *Cancer research* **2011**, *71*, 5214-5224.
177. Kafil, V.; Omid, Y. Cytotoxic impacts of linear and branched polyethylenimine nanostructures in a431 cells. *Bioimpacts* **2011**, *1*, 23-30.
178. Grayson, A.C.; Doody, A.M.; Putnam, D. Biophysical and structural characterization of polyethylenimine-mediated siRNA delivery in vitro. *Pharmaceutical research* **2006**, *23*, 1868-1876.
179. Liu, B. Exploring cell type-specific internalizing antibodies for targeted delivery of siRNA. *Brief Funct Genomic Proteomic* **2007**, *6*, 112-119.
180. Sioud, M. RNAi therapy: antibodies guide the way. *Gene therapy* **2006**, *13*, 194-195.
181. Ikeda, Y.; Taira, K. Ligand-targeted delivery of therapeutic siRNA. *Pharmaceutical research* **2006**, *23*, 1631-1640.
182. Cardoso, A.L.; Simoes, S.; de Almeida, L.P.; Pelisek, J.; Culmsee, C.; Wagner, E.; Pedroso de Lima, M.C. siRNA delivery by a transferrin-associated lipid-based vector: a non-viral strategy to mediate gene silencing. *The journal of gene medicine* **2007**, *9*, 170-183.
183. Dobson, J. Gene therapy progress and prospects: magnetic nanoparticle-based gene delivery. *Gene therapy* **2006**, *13*, 283-287.
184. Schillinger, U.; Brill, T.; Rudolph, C.; Huth, S.; Gersting, S.; Krötz, F.; Hirschberger, J.; Bergemann, C.; Plank, C. Advances in magnetofection-magnetically guided nucleic acid delivery. *Journal of Magnetism and Magnetic Materials* **2005**, *293*, 501-508.
185. Peng, X.H.; Qian, X.; Mao, H.; Wang, A.Y.; Chen, Z.G.; Nie, S.; Shin, D.M. Targeted magnetic iron oxide nanoparticles for tumor imaging and therapy. *Int J Nanomedicine* **2008**, *3*, 311-321.
186. Marek, R.; Caruso, M.; Rostami, A.; Grinspan, J.B.; Das Sarma, J. Magnetic cell sorting: a fast and effective method of concurrent isolation of high purity viable astrocytes and microglia from neonatal mouse brain tissue. *J Neurosci Methods* **2008**, *175*, 108-118.
187. Lin, C.T.; Moore, P.A.; Kery, V. Automated 96-well purification of hexahistidine-tagged recombinant proteins on MagneHis Ni(2)+-particles. *Methods Mol Biol* **2009**, *498*, 129-141.
188. Ahrens, E.T.; Bulte, J.W. Tracking immune cells in vivo using magnetic resonance imaging. *Nat Rev Immunol* **2013**, *13*, 755-763.
189. McBain, S.C.; Griesenbach, U.; Xenariou, S.; Keramane, A.; Batich, C.D.; Alton, E.W.; Dobson, J. Magnetic nanoparticles as gene delivery agents: enhanced transfection in the presence of oscillating magnet arrays. *Nanotechnology* **2008**, *19*, 405102.
190. Herranz, F.; Almaraz, E.; Rodriguez, I.; Salinas, B.; Rosell, Y.; Desco, M.; Bulte, J.W.; Ruiz-Cabello, J. The application of nanoparticles in gene therapy and magnetic resonance imaging. *Microsc Res Tech* **2011**, *74*, 577-591.
191. Muthana, M.; Scott, S.D.; Farrow, N.; Morrow, F.; Murdoch, C.; Grubb, S.; Brown, N.; Dobson, J.; Lewis, C.E. A novel magnetic approach to enhance the efficacy of cell-based gene therapies. *Gene therapy* **2008**, *15*, 902-910.
192. Scherer, F.; Anton, M.; Schillinger, U.; Henke, J.; Bergemann, C.; Kruger, A.; Gansbacher, B.; Plank, C. Magnetofection: enhancing and targeting gene delivery by magnetic force in vitro and in vivo. *Gene therapy* **2002**, *9*, 102-109.
193. Huth, S.; Lausier, J.; Gersting, S.W.; Rudolph, C.; Plank, C.; Welsch, U.; Rosenecker, J. Insights into the mechanism of magnetofection using PEI-based magnetofectins for gene transfer. *The journal of gene medicine* **2004**, *6*, 923-936.

194. Plank, C.; Zelphati, O.; Mykhaylyk, O. Magnetically enhanced nucleic acid delivery. Ten years of magnetofection-progress and prospects. *Adv Drug Deliv Rev* **2011**, *63*, 1300-1331.
195. Mykhaylyk, O.; Sanchez-Antequera, Y.; Vlaskou, D.; Cerda, M.B.; Bokharaei, M.; Hammerschmid, E.; Anton, M.; Plank, C. Magnetic nanoparticle and magnetic field assisted siRNA delivery in vitro. *Methods Mol Biol* **2015**, *1218*, 53-106.
196. del Pino, P.; Munoz-Javier, A.; Vlaskou, D.; Rivera Gil, P.; Plank, C.; Parak, W.J. Gene silencing mediated by magnetic lipospheres tagged with small interfering RNA. *Nano Lett* **2010**, *10*, 3914-3921.
197. Lim, J.; Clements, M.A.; Dobson, J. Delivery of short interfering ribonucleic acid-complexed magnetic nanoparticles in an oscillating field occurs via caveolae-mediated endocytosis. *PloS one* **2012**, *7*, e51350.
198. Yiu, H.H.; McBain, S.C.; Lethbridge, Z.A.; Lees, M.R.; Dobson, J. Preparation and characterization of polyethylenimine-coated Fe<sub>3</sub>O<sub>4</sub>-MCM-48 nanocomposite particles as a novel agent for magnet-assisted transfection. *Journal of biomedical materials research. Part A* **2008**, *92*, 386-392.
199. Tan, Z.; Sun, X.; Hou, F.S.; Oh, H.W.; Hilgenberg, L.G.; Hol, E.M.; van Leeuwen, F.W.; Smith, M.A.; O'Dowd, D.K.; Schreiber, S.S. Mutant ubiquitin found in Alzheimer's disease causes neuritic beading of mitochondria in association with neuronal degeneration. *Cell death and differentiation* **2007**, *14*, 1721-1732.
200. Li, W.; Ma, N.; Ong, L.L.; Kaminski, A.; Skrabal, C.; Ugurlucan, M.; Lorenz, P.; Gatzert, H.H.; Lutzow, K.; Lendlein, A.; Putzer, B.M.; Li, R.K.; Steinhoff, G. Enhanced thoracic gene delivery by magnetic nanobead-mediated vector. *The journal of gene medicine* **2008**, *10*, 897-909.
201. Schade, A.; Delyagina, E.; Scharfenberg, D.; Skorska, A.; Lux, C.; David, R.; Steinhoff, G. Innovative Strategy for MicroRNA Delivery in Human Mesenchymal Stem Cells via Magnetic Nanoparticles. *Int J Mol Sci* **2013**, *14*, 10710-10726.
202. Delyagina, E.; Schade, A.; Scharfenberg, D.; Skorska, A.; Lux, C.; Li, W.; Steinhoff, G. Improved transfection in human mesenchymal stem cells: effective intracellular release of pDNA by magnetic polyplexes. *Nanomedicine* **2013**.
203. Delyagina, E.; Li, W.; Ma, N.; Steinhoff, G. Magnetic targeting strategies in gene delivery. *Nanomedicine* **2011**, *6*, 1593-1604.
204. Gaebel, R.; Furlani, D.; Sorg, H.; Polchow, B.; Frank, J.; Bieback, K.; Wang, W.; Klopsch, C.; Ong, L.L.; Li, W.; Ma, N.; Steinhoff, G. Cell origin of human mesenchymal stem cells determines a different healing performance in cardiac regeneration. *PloS one* **2011**, *6*, e15652.
205. Livak, K.J.; Schmittgen, T.D. Analysis of relative gene expression data using real-time quantitative PCR and the 2(-Delta Delta C(T)) Method. *Methods* **2001**, *25*, 402-408.
206. Schade, A.; Muller, P.; Delyagina, E.; Voronina, N.; Skorska, A.; Lux, C.; Steinhoff, G.; David, R. Magnetic Nanoparticle Based Nonviral MicroRNA Delivery into Freshly Isolated CD105(+) hMSCs. *Stem Cells Int* **2014**, *2014*, 197154.
207. Mueller, P. Comparative analysis of different non-viral miR transfection methods in primary hMSCs. Master Thesis; University of Rostock, 2013.
208. Scharfenberg, D. Magnetic nanoparticle-based delivery of microRNA-335 into human mesenchymal stem cells. Master Thesis; University of Rostock, 2012.
209. Dong, W.; Jin, G.H.; Li, S.F.; Sun, Q.M.; Ma, D.Y.; Hua, Z.C. Cross-linked polyethylenimine as potential DNA vector for gene delivery with high efficiency and low cytotoxicity. *Acta Biochim Biophys Sin (Shanghai)* **2006**, *38*, 780-787.

210. Wang, Y.; Su, J.; Cai, W.; Lu, P.; Yuan, L.; Jin, T.; Chen, S.; Sheng, J. Hepatocyte-targeting gene transfer mediated by galactosylated poly(ethylene glycol)-graft-polyethylenimine derivative. *Drug design, development and therapy* **2013**, *7*, 211-221.
211. Przybyt, E.; Harmsen, M.C. Mesenchymal stem cells: promising for myocardial regeneration? *Curr Stem Cell Res Ther* **2013**, *8*, 270-277.
212. Caplan, A.I.; Dennis, J.E. Mesenchymal stem cells as trophic mediators. *Journal of cellular biochemistry* **2006**, *98*, 1076-1084.
213. Boiret, N.; Rapatel, C.; Veyrat-Masson, R.; Guillouard, L.; Guerin, J.J.; Pigeon, P.; Descamps, S.; Boisgard, S.; Berger, M.G. Characterization of nonexpanded mesenchymal progenitor cells from normal adult human bone marrow. *Exp Hematol* **2005**, *33*, 219-225.
214. Boquest, A.C.; Shahdadfar, A.; Fronsdal, K.; Sigurjonsson, O.; Tunheim, S.H.; Collas, P.; Brinchmann, J.E. Isolation and transcription profiling of purified uncultured human stromal stem cells: alteration of gene expression after in vitro cell culture. *Mol Biol Cell* **2005**, *16*, 1131-1141.
215. Alves, H.; Munoz-Najar, U.; De Wit, J.; Renard, A.J.; Hoeijmakers, J.H.; Sedivy, J.M.; Van Blitterswijk, C.; De Boer, J. A link between the accumulation of DNA damage and loss of multi-potency of human mesenchymal stromal cells. *Journal of cellular and molecular medicine* **2010**, *14*, 2729-2738.
216. Wise, J.K.; Alford, A.I.; Goldstein, S.A.; Stegemann, J.P. Comparison of uncultured marrow mononuclear cells and culture-expanded mesenchymal stem cells in 3D collagen-chitosan microbeads for orthopedic tissue engineering. *Tissue Eng Part A* **2014**, *20*, 210-224.
217. Herschkoviz, R.; Miron, S.; Cahalon, L.; Lider, O. The beta 1-integrin (CD29) receptors: mediators of T lymphocyte--extracellular matrix recognition that affect adhesion, activation and lymphokine secretion. *Isr J Med Sci* **1993**, *29*, 321-325.
218. Fink, T.; Zachar, V. Adipogenic differentiation of human mesenchymal stem cells. *Methods Mol Biol* **2011**, *698*, 243-251.
219. Jaiswal, N.; Haynesworth, S.E.; Caplan, A.I.; Bruder, S.P. Osteogenic differentiation of purified, culture-expanded human mesenchymal stem cells in vitro. *Journal of cellular biochemistry* **1997**, *64*, 295-312.
220. Delyagina, E.; Schade, A.; Scharfenberg, D.; Skorska, A.; Lux, C.; Li, W.; Steinhoff, G. Improved transfection in human mesenchymal stem cells: effective intracellular release of pDNA by magnetic polyplexes. *Nanomedicine* **2014**.
221. Evans, C.W.; Fitzgerald, M.; Clemons, T.D.; House, M.J.; Padman, B.S.; Shaw, J.A.; Saunders, M.; Harvey, A.R.; Zdyrko, B.; Luzinov, I.; Silva, G.A.; Dunlop, S.A.; Iyer, K.S. Multimodal analysis of PEI-mediated endocytosis of nanoparticles in neural cells. *ACS Nano* **2011**, *5*, 8640-8648.
222. Silva, A.K.; Wilhelm, C.; Kolosnjaj-Tabi, J.; Luciani, N.; Gazeau, F. Cellular transfer of magnetic nanoparticles via cell microvesicles: impact on cell tracking by magnetic resonance imaging. *Pharmaceutical research* **2012**, *29*, 1392-1403.
223. Guzman-Villanueva, D.; El-Sherbiny, I.M.; Herrera-Ruiz, D.; Vlassov, A.V.; Smyth, H.D. Formulation approaches to short interfering RNA and MicroRNA: challenges and implications. *J Pharm Sci* **2012**, *101*, 4046-4066.
224. Hobel, S.; Koburger, I.; John, M.; Czubyko, F.; Hadwiger, P.; Vornlocher, H.P.; Aigner, A. Polyethylenimine/small interfering RNA-mediated knockdown of vascular endothelial growth factor in vivo exerts anti-tumor effects synergistically with Bevacizumab. *The journal of gene medicine* **2010**, *12*, 287-300.

225. Chen, Y.; Zhu, X.; Zhang, X.; Liu, B.; Huang, L. Nanoparticles modified with tumor-targeting scFv deliver siRNA and miRNA for cancer therapy. *Molecular therapy : the journal of the American Society of Gene Therapy* **2010**, *18*, 1650-1656.
226. Godbey, W.T.; Wu, K.K.; Mikos, A.G. Poly(ethylenimine) and its role in gene delivery. *Journal of controlled release : official journal of the Controlled Release Society* **1999**, *60*, 149-160.
227. Thomas, M.; Lu, J.J.; Ge, Q.; Zhang, C.; Chen, J.; Klibanov, A.M. Full deacylation of polyethylenimine dramatically boosts its gene delivery efficiency and specificity to mouse lung. *Proceedings of the National Academy of Sciences of the United States of America* **2005**, *102*, 5679-5684.
228. Kwok, A.; Hart, S.L. Comparative structural and functional studies of nanoparticle formulations for DNA and siRNA delivery. *Nanomedicine* **2011**, *7*, 210-219.
229. Grzelinski, M.; Urban-Klein, B.; Martens, T.; Lamszus, K.; Bakowsky, U.; Hobel, S.; Czubayko, F.; Aigner, A. RNA interference-mediated gene silencing of pleiotrophin through polyethylenimine-complexed small interfering RNAs in vivo exerts antitumoral effects in glioblastoma xenografts. *Human gene therapy* **2006**, *17*, 751-766.
230. Breunig, M.; Lungwitz, U.; Liebl, R.; Goepferich, A. Breaking up the correlation between efficacy and toxicity for nonviral gene delivery. *Proceedings of the National Academy of Sciences of the United States of America* **2007**, *104*, 14454-14459.
231. Florea, B.I.; Meaney, C.; Junginger, H.E.; Borchard, G. Transfection efficiency and toxicity of polyethylenimine in differentiated Calu-3 and nondifferentiated COS-1 cell cultures. *AAPS PharmSci* **2002**, *4*, E12.
232. Moghimi, S.M.; Symonds, P.; Murray, J.C.; Hunter, A.C.; Debska, G.; Szewczyk, A. A two-stage poly(ethylenimine)-mediated cytotoxicity: implications for gene transfer/therapy. *Molecular therapy : the journal of the American Society of Gene Therapy* **2005**, *11*, 990-995.
233. Kong, W.H.; Bae, K.H.; Hong, C.A.; Lee, Y.; Hahn, S.K.; Park, T.G. Multimerized siRNA cross-linked by gold nanoparticles. *Bioconjug Chem* **2011**, *22*, 1962-1969.
234. Chen, C.B.; Chen, J.Y.; Lee, W.C. Fast transfection of mammalian cells using superparamagnetic nanoparticles under strong magnetic field. *J Nanosci Nanotechnol* **2009**, *9*, 2651-2659.
235. Giouroudi, I.; Kosel, J. Recent progress in biomedical applications of magnetic nanoparticles. *Recent Pat Nanotechnol* **2010**, *4*, 111-118.
236. Boeckle, S.; Wagner, E. Optimizing targeted gene delivery: chemical modification of viral vectors and synthesis of artificial virus vector systems. *The AAPS journal* **2006**, *8*, E731-742.
237. Cheng, K.; Malliaras, K.; Li, T.S.; Sun, B.; Houde, C.; Galang, G.; Smith, J.; Matsushita, N.; Marban, E. Magnetic enhancement of cell retention, engraftment, and functional benefit after intracoronary delivery of cardiac-derived stem cells in a rat model of ischemia/reperfusion. *Cell Transplant* **2012**, *21*, 1121-1135.
238. von Gersdorff, K.; Sanders, N.N.; Vandenbroucke, R.; De Smedt, S.C.; Wagner, E.; Ogris, M. The internalization route resulting in successful gene expression depends on both cell line and polyethylenimine polyplex type. *Molecular therapy : the journal of the American Society of Gene Therapy* **2006**, *14*, 745-753.
239. Sioud, M. Overcoming the challenges of siRNA activation of innate immunity: design better therapeutic siRNAs. *Methods Mol Biol* **2015**, *1218*, 301-319.
240. Wang, Y.X.; Xuan, S.; Port, M.; Idee, J.M. Recent advances in superparamagnetic iron oxide nanoparticles for cellular imaging and targeted therapy research. *Curr Pharm Des* **2013**, *19*, 6575-6593.

241. Prabha, S.; Zhou, W.Z.; Panyam, J.; Labhasetwar, V. Size-dependency of nanoparticle-mediated gene transfection: studies with fractionated nanoparticles. *International journal of pharmaceutics* **2002**, *244*, 105-115.
242. Rejman, J.; Oberle, V.; Zuhorn, I.S.; Hoekstra, D. Size-dependent internalization of particles via the pathways of clathrin- and caveolae-mediated endocytosis. *Biochem J* **2004**, *377*, 159-169.
243. Kim, W.J.; Kim, S.W. Efficient siRNA delivery with non-viral polymeric vehicles. *Pharmaceutical research* **2009**, *26*, 657-666.
244. Duman, O.; Tunç, S. Electrokinetic and rheological properties of Na-bentonite in some electrolyte solutions. *Microporous and Mesoporous Materials* **2009**, *117*, 331-338.
245. Mekhamer, W.K. The colloidal stability of raw bentonite deformed mechanically by ultrasound. *Journal of Saudi Chemical Society* **2010**, *14*, 301-306.
246. Tavazoie, S.F.; Alarcon, C.; Oskarsson, T.; Padua, D.; Wang, Q.; Bos, P.D.; Gerald, W.L.; Massague, J. Endogenous human microRNAs that suppress breast cancer metastasis. *Nature* **2008**, *451*, 147-152.
247. Vandesompele, J.; De Preter, K.; Pattyn, F.; Poppe, B.; Van Roy, N.; De Paepe, A.; Speleman, F. Accurate normalization of real-time quantitative RT-PCR data by geometric averaging of multiple internal control genes. *Genome Biol* **2002**, *3*, RESEARCH0034.
248. Choong, M.L.; Yang, H.H.; McNiece, I. MicroRNA expression profiling during human cord blood-derived CD34 cell erythropoiesis. *Exp Hematol* **2007**, *35*, 551-564.
249. Corney, D.C.; Flesken-Nikitin, A.; Godwin, A.K.; Wang, W.; Nikitin, A.Y. MicroRNA-34b and MicroRNA-34c are targets of p53 and cooperate in control of cell proliferation and adhesion-independent growth. *Cancer research* **2007**, *67*, 8433-8438.
250. Mattie, M.D.; Benz, C.C.; Bowers, J.; Sensinger, K.; Wong, L.; Scott, G.K.; Fedele, V.; Ginzinger, D.; Getts, R.; Haqq, C. Optimized high-throughput microRNA expression profiling provides novel biomarker assessment of clinical prostate and breast cancer biopsies. *Mol Cancer* **2006**, *5*, 24.
251. Peltier, H.J.; Latham, G.J. Normalization of microRNA expression levels in quantitative RT-PCR assays: identification of suitable reference RNA targets in normal and cancerous human solid tissues. *RNA* **2008**, *14*, 844-852.
252. Clamme, J.P.; Krishnamoorthy, G.; Mely, Y. Intracellular dynamics of the gene delivery vehicle polyethylenimine during transfection: investigation by two-photon fluorescence correlation spectroscopy. *Biochimica et biophysica acta* **2003**, *1617*, 52-61.
253. Ishigaki, T.; Imanaka-Yoshida, K.; Shimojo, N.; Matsushima, S.; Taki, W.; Yoshida, T. Tenascin-C enhances crosstalk signaling of integrin  $\alpha$ v $\beta$ 3/PDGFR- $\beta$  complex by SRC recruitment promoting PDGF-induced proliferation and migration in smooth muscle cells. *J Cell Physiol* **2011**, *226*, 2617-2624.
254. Tucker, R.P.; Ferralli, J.; Schittny, J.C.; Chiquet-Ehrismann, R. Tenascin-C and tenascin-W in whisker follicle stem cell niches: possible roles in regulating stem cell proliferation and migration. *J Cell Sci* **2013**, *126*, 5111-5115.
255. Vimalraj, S.; Arumugam, B.; Miranda, P.J.; Selvamurugan, N. Runx2: Structure, Function, and Phosphorylation in Osteoblast Differentiation. *International journal of biological macromolecules* **2015**.
256. Larsen, H.O.; Roug, A.S.; Nielsen, K.; Sondergaard, C.S.; Hokland, P. Nonviral transfection of leukemic primary cells and cells lines by siRNA-a direct comparison between Nucleofection and Accell delivery. *Exp Hematol* **2011**, *39*, 1081-1089.

257. He, W.; Bennett, M.J.; Luistro, L.; Carvajal, D.; Nevins, T.; Smith, M.; Tyagi, G.; Cai, J.; Wei, X.; Lin, T.A.; Heimbrook, D.C.; Packman, K.; Boylan, J.F. Discovery of siRNA lipid nanoparticles to transfect suspension leukemia cells and provide in vivo delivery capability. *Molecular therapy : the journal of the American Society of Gene Therapy* **2014**, *22*, 359-370.
258. Plank, C.; Schillinger, U.; Scherer, F.; Bergemann, C.; Remy, J.S.; Krotz, F.; Anton, M.; Lausier, J.; Rosenecker, J. The magnetofection method: using magnetic force to enhance gene delivery. *Biological chemistry* **2003**, *384*, 737-747.
259. Fischer, S.; Wagner, A.; Kos, A.; Aschrafi, A.; Handrick, R.; Hannemann, J.; Otte, K. Breaking limitations of complex culture media: functional non-viral miRNA delivery into pharmaceutical production cell lines. *J Biotechnol* **2013**, *168*, 589-600.
260. Elouahabi, A.; Ruysschaert, J.M. Formation and intracellular trafficking of lipoplexes and polyplexes. *Molecular therapy : the journal of the American Society of Gene Therapy* **2005**, *11*, 336-347.
261. Billiet, L.; Gomez, J.P.; Berchel, M.; Jaffres, P.A.; Le Gall, T.; Montier, T.; Bertrand, E.; Cheradame, H.; Guegan, P.; Mevel, M.; Pitard, B.; Benvegna, T.; Lehn, P.; Pichon, C.; Midoux, P. Gene transfer by chemical vectors, and endocytosis routes of polyplexes, lipoplexes and lipopolyplexes in a myoblast cell line. *Biomaterials* **2012**, *33*, 2980-2990.
262. Lang, C.; Lehner, S.; Todica, A.; Boening, G.; Zacherl, M.; Franz, W.M.; Krause, B.J.; Bartenstein, P.; Hacker, M.; David, R. In-vivo comparison of the acute retention of stem cell derivatives and fibroblasts after intramyocardial transplantation in the mouse model. *Eur J Nucl Med Mol Imaging* **2014**, *41*, 2325-2336.
263. Vandergriff, A.C.; Hensley, T.M.; Henry, E.T.; Shen, D.; Anthony, S.; Zhang, J.; Cheng, K. Magnetic targeting of cardiosphere-derived stem cells with ferumoxytol nanoparticles for treating rats with myocardial infarction. *Biomaterials* **2014**, *35*, 8528-8539.

## 7 Appendix

### List of Abbreviations

°C	degree Celsius
μ	micro (10 <sup>-6</sup> )
Δ	difference
AF 488	Alexa Fluor 488
Akt	serine/threonine-specific protein kinase
AmCyan	Anemonia majano cyan fluorescent protein
APC	allophycocyanin
Bax	Bcl-2-associated X protein
Bcl-2	B-cell lymphoma-2
BGBI	Bundesgesetzblatt
BMP	bone morphogenetic protein
BSA	bovine serum albumin
CCR2	C-C chemokine receptor type 2
CCR3	C-C chemokine receptor type 3
CCR4	C-C chemokine receptor type 4
CD	cluster of differentiation
cDNA	copy DNA
cm <sup>2</sup>	square centimeter
CO <sub>2</sub>	carbon dioxide
C <sub>T</sub>	threshold cycle
CVDs	cardiovascular diseases
CXCR4	C-X-C chemokine receptor type 4
Cy3	cyanine 3
Cy5	cyanine 5
Da	Dalton
DAPI	4',6-diamidino-2-phenylindole
dH <sub>2</sub> O	distilled water
DLS	dynamic light scattering
DMSO	dimethyl sulfoxide
DNA	deoxyribonucleic acid

---

DOPE	dioleoyl phosphatidylethanolamine
DOSPA	2,3-dioleoyloxy-N-[2-(spermine-carboxamido)ethyl]-N,N-dimethyl-1-propanaminium trifluoroacetate
dsRNA	double stranded RNAs
e.g.	for example
EDTA	ethylenediaminetetraacetic acid
Egr-1	early growth response protein-1
eNOS	endothelial nitric oxide synthase
ESchG	Embryonenschutzgesetz
FABP-4	fatty acid binding protein-4
FBS	fetal bovine serum
FGF-2	fibroblast growth factor-2
Flk-1	fetal liver kinase-1
g	gram
<i>g</i>	standard gravity
GAPDH	glyceraldehyde-3-phosphate dehydrogenase
HER-2	human epidermal growth factor receptor-2
hESCs	human embryonic stem cells
HGF	hepatocyte growth factor
HIF-1 $\alpha$	hypoxia-inducible factor-1 $\alpha$
HLA	human leukocyte antigen
HMG-CoA	3-hydroxy-3-methylglutaryl-coenzyme A
hMSCs	human mesenchymal stem cells
hMSZ	humane mesenchymale Stammzellen
HO-1	heme oxygenase-1
Hsp-20	heat shock protein-20
IGF-1	insulin-like growth factor-1
IgG	immunoglobulin G
IL	interleukin
iPSCs	induced pluripotent stem cells
k	kilo
Klf4	Kruppel-like factor 4
l	liter
lncRNA	long non-coding RNA
LSM	laser scanning microscopy



m	milli ( $10^{-3}$ )
M	molar
MACS	magnetic activated cell sorting
MCGS	mesenchymal cell growth supplement
MEF	myocyte enhancer factor
miR	microRNA
miR-Cy5	microRNA labeled with cyanine 5
MNCs	mononuclear cells
MNP	magnetic nanoparticles
MNP-565	magnetic nanoparticles labeled with Atto 565
Mol	mole
MRI	magnetic resonance imaging
mRNA	messenger RNA
MSCBM	Mesenchymal Stem Cell Basal Medium
MSCGM™	Mesenchymal Stem Cell Growth Medium
MSCs	mesenchymal stem cells
n	amount of substance
n	nano ( $10^{-9}$ )
n	statistical sample size
N	nitrogen
NaCl	sodium chloride
ncRNA	non-coding RNA
Nkx2.5	NK2 homeobox 5
NP ratio	molar ratio of PEI nitrogen and miR phosphate
n.s.	no significant difference
Oct3/4	octamer-binding transcription factor-3/4
P	phosphate
PALS	phase analysis light scattering
PBS	phosphate buffered saline
PCR	polymerase chain reaction
PE	phycoerythrin
PEI	polyethylenimine
PEI-488	polyethylenimine labeled with Alexa Fluor 488
PerCP	peridinin-chlorophyll proteins
PFA	paraformaldehyde

---

pH	negative logarithm of the hydrogen ion concentration
PUMA	p53 upregulated modulator of apoptosis
R	relative expression ratio
RISC	RNA-induced silencing complex
RNA	ribonucleic acid
RNAi	RNA interference
RT	reverse transcription
RUNX2	runt-related transcription factor 2
SD	standard deviation
SDF-1	stromal-derived factor-1
SEM	standard error of the mean
SIM	structured illumination microscopy
siRNA	small interfering RNA
Sox2	SRY-related high-mobility-group-box protein 2
T	tesla
TBE	TRIS-borate-EDTA buffer
TGF	transforming growth factor
TNC	tenascin C
TRIS	2-amino-2-hydroxymethyl-propane-1,3-diol
T $\beta$ RI	type I transforming growth factor-beta receptor
T $\beta$ RII	type II transforming growth factor-beta receptor
T $\beta$ RIII	type III transforming growth factor-beta receptor
U	unit
V	volt
V	volume
VEGF	vascular endothelial growth factor
vs	versus
w/w	weight to weight ratio
WHO	World Health Organization
$\alpha$ -MEM	minimum essential medium alpha

## List of Figures

<b>Figure 1:</b>	Biogenesis and Function of miR and siRNA .....	11
<b>Figure 2:</b>	<i>Ex Vivo</i> Genetic Modifications of hMSCs using miRs.....	13
<b>Figure 3:</b>	Construction of Magnetic Transfection Complexes. ....	18
<b>Figure 4:</b>	Cell Morphology of Freshly Isolated and Expanded hMSCs .....	39
<b>Figure 5:</b>	Differentiation Capacity of hMSCs .....	40
<b>Figure 6:</b>	Immunophenotyping of hMSCs.....	43
<b>Figure 7:</b>	Transfection Optimization of miR Amounts in Cultured hMSCs .....	44
<b>Figure 8:</b>	Transfection Optimization of PEI Amounts in Cultured hMSCs .....	45
<b>Figure 9:</b>	Transfection Optimization of MNP Amounts in Cultured hMSCs .....	46
<b>Figure 10:</b>	Classification of Transfection Complexes .....	48
<b>Figure 11:</b>	Monitoring of pre-miR-335 Processing in Cultured hMSCs.....	50
<b>Figure 12:</b>	Visualization of Transfection Complexes.....	51
<b>Figure 13:</b>	Intracellular Visualization of Transfection Complexes in Cultured hMSCs ....	52
<b>Figure 14:</b>	Gene Knockdown of TNC and RUNX2 after miR-335 Transfection in Cultured hMSCs.....	53
<b>Figure 15:</b>	Inhibition of the Migratory Ability of Cultured hMSCs after miR-335 Transfection .....	54
<b>Figure 16:</b>	Transfection Optimization of miR Amounts in Freshly Isolated hMSCs.....	56
<b>Figure 17:</b>	Transfection Optimization of PEI Amounts in Freshly Isolated hMSCs .....	58
<b>Figure 18:</b>	Transfection Optimization of MNP Amounts in Freshly Isolated hMSCs with and without the Application of a Magnetic Field .....	59
<b>Figure 19:</b>	Processing of pre-miR-335 in Freshly Isolated hMSCs .....	60
<b>Figure 20:</b>	Transfection Performances of Optimized miR/PEI/MNP Complexes in Comparison with Commercially Available Magnetic Transfection Carriers in Freshly Isolated hMSCs.....	62
<b>Figure 21:</b>	Paramagnetic Properties of MNPs .....	63
<b>Figure 22:</b>	<i>In Vitro</i> Magnetic Targeting of Cultured hMSCs .....	64

## List of Tables

<b>Table 1:</b>	List of Chemicals Used in this Thesis.....	20
<b>Table 2:</b>	List of Solutions Used in this Thesis .....	22
<b>Table 3:</b>	Immunofluorescent Labeling of hMSCs.....	25
<b>Table 4:</b>	Transfection Protocol for Cultured hMSCs .....	28
<b>Table 5:</b>	Transfection Protocol for Freshly Isolated hMSCs .....	28
<b>Table 6:</b>	Preparation of RT Master Mix for RT of miRs .....	34
<b>Table 7:</b>	Program for RT of miRs .....	34
<b>Table 8:</b>	Real-Time PCR Pipetting Scheme for miR Quantification .....	35
<b>Table 9:</b>	Program for Real-Time PCR .....	35
<b>Table 10:</b>	Preparation of 2x RT Master Mix for RT of Target Genes .....	36
<b>Table 11:</b>	Program for RT of Target Genes .....	36
<b>Table 12:</b>	Real-Time PCR Pipetting Scheme for Target Gene Quantification .....	37

## List of Equations

<b>Equation 1:</b>	Calculation of the NP Ratio Referring to the Number of Nitrogen Atoms (N) in PEI per Phosphate Group (P) of miR.....	27
<b>Equation 2:</b>	Calculation of the Relative Expression Ratio (R) using the $\Delta\Delta C_T$ Method .....	35

## Curriculum Vitae

### PERSÖNLICHE DATEN

<b>Name</b>	Anna Schade (geb. Sponholz)
<b>Anschrift</b>	Glockengießerhof 5 18055 Rostock
<b>Geburtsdatum</b>	17.02.1987
<b>Geburtsort</b>	Rostock
<b>Staatsangehörigkeit</b>	deutsch
<b>Familienstand</b>	verheiratet, 2 Kinder (2008, 2014)



### SPRACHEN

Deutsch	Muttersprache
Englisch	fließend in Wort und Schrift

### BERUFLICHER WERDEGANG

#### Schulausbildung

06/2005	<b>CJD Jugendorf-Christophorusschule Rostock</b> Abschluss: Abitur Leistungskurse: Mathematik, Biologie, Chemie
---------	---

#### Universitäre Ausbildung

10/2005 – 07/2009	<b>Universität Rostock, Medizinische Fakultät</b> Studium: Medizinische Biotechnologie Abschluss: Bachelor of Science Thema der Bachelorarbeit: „Influence of Tetradecylthioacetic Acid for the Deposition of Amyloid in an Alzheimer’s Disease Mouse Model“, am NRL in Rostock
10/2009 – 09/2011	<b>Universität Rostock, Medizinische Fakultät</b> Studium: Medizinische Biotechnologie Abschluss: Master of Science Thema der Masterarbeit: „Intracellular Visualization of Nanoparticle-based Gene Delivery via Selective Fluorescent Labeling“, am FKGO in Rostock

**Berufliche Erfahrungen**

10/2008 -12/2009	<b>Neurodegeneration Research Laboratory (NRL), Universitätsmedizin Rostock</b> Anstellung: studentische Hilfskraft
06/2009 – 09/2011	<b>Forschungslabor für kardialen Gewebe- und Organersatz (FKGO)/ Klinik für Herzchirurgie, Universitätsmedizin Rostock</b> Anstellung: studentische Hilfskraft
10/2011 – laufend	<b>Forschungslabor für kardialen Gewebe- und Organersatz (FKGO)/ Klinik für Herzchirurgie, Universitätsmedizin Rostock</b> Beginn der Arbeiten zur Erlangung des Doktorgrades Thema: "MicroRNA-based Stem Cell Modifications using Magnetic Transfection Complexes - A Non-Viral Approach towards Cardiac Regeneration." Anstellung: wissenschaftliche Mitarbeiterin
10/2011 - laufend	<b>Mitglied im strukturierten Promotionsstudiengang „Molekulare Mechanismen Regenerativer Prozesse“ &amp; Mitglied in der Graduiertenakademie Rostock</b>

**KONFERENZEN**

12/2012	<b>3rd EACTS Meeting on Cardiac and Pulmonary Regeneration, Berlin/ Deutschland,</b> „An innovative non-viral strategy for efficient microRNA delivery in human mesenchymal stem cells for regenerative medicine“, Posterpräsentation
06/2013	<b>Rostock's Eleven 2013, Rostock/ Deutschland,</b> „Neuartiger Genträger für die Modifikation von Stammzellen“, Vortrag
03/2014	<b>BioNanoMed 2014, 5th International Conference of Nanotechnology, Medicine &amp; Biology, Krems/ Österreich,</b> „Nonviral gene carriers for efficient modifications of human mesenchymal stem cells for cardiac regeneration“, Vortrag

## PUBLIKATIONEN

**Schade, A.**; Müller, P.; Delyagina, E. et al. Magnetic Nanoparticle Based Nonviral MicroRNA Delivery into Freshly Isolated CD105+ hMSCs. Stem Cells Int., 1-11 (2014).

**Schade, A.**; Delyagina, E.; Scharfenberg, D. et al. Innovative strategy for microRNA delivery in human mesenchymal stem cells via magnetic nanoparticles. IJMS 14 (6), 10710–10726 (2013).

Delyagina, E.; **Schade, A.**; Scharfenberg, D. et al. Improved transfection in human mesenchymal stem cells: Effective intracellular release of pDNA by magnetic polyplexes. Nanomedicine (Lond) 0(0), 1-18 (2013).

Delyagina, E., Li, W., **Schade, A.** et al. Low Molecular Weight Polyethyleimine conjugated to magnetic nanoparticles as a vector for gene delivery. AIP Conference Proceedings, CP1311, 479-484 (2010).

## BETREUUNG

- |         |  |
|---------|--|
| 08/2012 | “Magnetic nanoparticle-based delivery of microRNA-335 into human mesenchymal stem cells”,<br>Masterarbeit Dorothee Scharfenberg (Medizinische Biotechnologie), Note: 1,0 |
| 08/2013 | “Comparative analysis of different non-viral miR transfection methods in primary hMSCs“,<br>Masterarbeit Paula Müller (Biologie), Note: 1,0                              |

## Acknowledgement

First of all, I would like to thank my principal supervisor Prof. Gustav Steinhoff for giving me the opportunity to work on this interesting topic. Thanks for inspiring scientific discussions, motivation and support which have been majorly influencing my last four years.

I would like to express my gratitude to Prof. Robert David for his kind supervision and evaluation of my work as well as critical revision of my dissertation. His continuous support essentially contributed to the successful completion.

I am grateful for the persistent critical evaluation of my results by Prof. Michael Glocker and the members of the structured PhD program “Molecular Mechanisms of Regenerative Processes”.

Special thanks are directed to my colleague and friend Evgenya Delyagina for her outstanding support, her good advice, fruitful discussions, joy and the good times spent together. Her devotion to science has always impressed and motivated me.

I sincerely thank Anna Skorska and Madeleine Bartsch for their practical support, friendly advice and optimism.

Additionally, I want to extend my thanks to the whole FKGO research group: Dr. Ralf Gäbel, Dr. Christian Rimbach, Dr. Cajetan Lang, Dr. Nan Ma, Dr. Wenzhong Li, Dr. Weiwei Wang, Dr. Yue Zhang, Natalia Voronina, Frauke Hausburg, Paula Müller, Julia Jung, Marion Ludwig, Peter Mark, Erik Pittermann, Dorothee Scharfenberg, Margit Schwarz, Anita Tölk, Margit Fritsche. Thank you for a pleasant working atmosphere, profound discussions and a great time.

Moreover, I would like to express my gratitude to the team of the Reference and Translation Center for Cardiac Stem Cell Therapy: Dr. Gudrun Tiedemann, Dr. Ulrike Ruch, Dr. Jana Große, Dr. Sandra Kurzawski, Dr. Frauke Stähler, Jana Gabriel and Katrin Höfer. Thanks for helpful advice and suggestions.

I give warm thanks to my husband and my daughters, Nico, Greta and Klara, for their everlasting love, their support, patience and motivation.

I am also very grateful to my family, especially my parents, Dr. Marion and Dr. Frank Sponholz, for their love, moral support and encouraging words during the past years.

Finally, I would like to thank my friends for their patience and ongoing help during this exciting time.



## Selbständigkeitserklärung

Ich versichere, die vorliegende Arbeit zum Thema „ *MicroRNA-based Stem Cell Modifications using Magnetic Transfection Complexes - A Non-Viral Approach towards Cardiac Regeneration*“ selbstständig verfasst und keine anderen Hilfsmittel als die angegebenen benutzt zu haben. Stellen, die anderen Werken dem Wortlaut oder dem Sinn nach entnommen sind, habe ich in jedem einzelnen Fall durch Angabe der Quelle kenntlich gemacht.

Ich erkläre, meine wissenschaftliche Arbeit nach den Prinzipien der guten wissenschaftlichen Praxis gemäß der gültigen „Satzung der Universität Rostock zur Sicherung guter wissenschaftlicher Praxis“ angefertigt zu haben.

Rostock, 18. Juni 2015